**Univerzita Karlova v Praze**
**Přírodovědecká fakulta**

Studijní program: Anorganická chemie

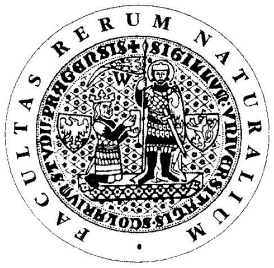


**Mgr. Michaela Fridrichová**

# Crystal engineering of novel materials for nonlinear optics

# Krystalové inženýrství nových materiálů pro nelineární optiku

Disertační práce

Školitel: Doc. RNDr. Ivan Němec, PhD.

Praha 2012

**Charles University in Prague**
**Faculty of Science**

PhD study programme: Inorganic Chemistry

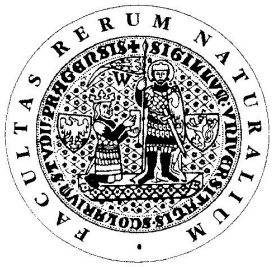

**Mgr. Michaela Fridrichová**

# Crystal engineering of novel materials for nonlinear optics

# Krystalové inženýrství nových materiálů pro nelineární optiku

PhD thesis

Supervisor: Doc. RNDr. Ivan Němec, PhD.

Prague 2012

Prohlašuji, že jsem tuto disertační práci zpracovala samostatně a že jsem uvedla všechny použité informační zdroje a literaturu. Tato práce ani její podstatná část nebyla předložena k získání jiného nebo stejného akademického titulu.
Jsem si vědoma toho, že případné využití výsledků získaných v této práci mimo Univerzitu Karlovu v Praze je možné pouze po písemném souhlasu této univerzity.

V Praze dne 15. 8. 2012

This PhD thesis was elaborated at the Charles University in Prague, Faculty of Science, Department of Inorganic chemistry in years 2007-2012 under the supervision of Doc. RNDr. Ivan Němec, PhD. This work was funded by the Grant Agency of Charles University in Prague (Grant No. 58608), Czech Science Foundation (Grant No. 203/09/0878), and it is a part of the long term Research Plan of the Ministry of Education of the Czech Republic (No. MSM0021620857).

The author states that the PhD thesis is an original work and that the results contained in this thesis were not used to obtain any other academic degree. All the used literature is cited in the reference list.

The author is aware that the results obtained in this thesis can be utilized outside the Charles University in Prague solely with the previously issued written consent of this University.

**Acknowledgements**

I am obliged to my supervisor Doc. RNDr. Ivan Němec, Ph.D. for his kind help, wise advice and patience during the preparation of this thesis. I am grateful to RNDr. Ivana Císařová, CSc. and to RNDr. Jan Fábry, CSc. for determinations of single crystal structures and for their help with the crystallographic issues. I would like to thank Doc. RNDr. Petr Němec, CSc. and Mgr. Naďa Tesařová from Faculty of Mathematics and Physics, Department of Chemical Physics and Optics for enabling the measurements of SHG. I am obliged to RNDr. Jan Kroupa, CSc. from Institute of Physics of the ASCR for advanced NLO characterizations and for his kind advice concerning the optical issues. I am grateful to Prof. Dr. Ladislav Bohatý for preparations of the large crystals of GUHP, for enabling my research stays at the University of Cologne and for sharing with me his rich experience with the crystal breeding issues. I would like to thank RNDr. Přemysl Vaněk, CSc. from Institute of Physics of the ASCR for the DSC measurements. I am very grateful to RNDr. Irena Matulková, PhD. for her friendly support and wise advice. I would like to thank my colleagues from laboratory Nr. 239 for a friendly working atmosphere.

Above all, special thanks belong to my family for their support, help and patience during my long work on the PhD thesis.

The Grant Agency of Charles University in Prague (Grant No. 58608), Czech Science Foundation (Grant No. 203/09/0878) and the long term Research Plan of the Ministry of Education of the Czech Republic (No. MSM0021620857) are acknowledged for the financial support of the work.

**Contents**

**Abstract**

This thesis focuses on preparation of novel compounds suitable for nonlinear optics (NLO). In particular, the target property is the second harmonic generation (SHG) and the group of interest are salts of the cations with delocalized π electrons which can serve as carriers of the NLO properties. In particular, four derivatives of the highly interesting molecule of guanidine were selected and their NLO potential was proven by quantum chemical computations.

In total, twenty new structures were described and those with the noncentrosymmetric structure assembly were examined for the SHG efficiency. Four of the prepared compounds exhibited a noticeable SHG efficiency, two of them even comparable to urea. The most promising compound, the guanylurea hydrogen phosphite (GUHP), was examined in more detail while many interesting NLO properties were revealed. The results of this work are presented also in 10 attached publications which are an integral part of the thesis.

Keywords: nonlinear optics, second harmonic generation, guanidine derivatives, guanylurea, *N*-phenylbiguanide, *N*,*N*-dimethylbiguanide, *N*,*N*′,*N*″-triphenylguanidine

# 1. **INTRODUCTION**

## 1. 1 **Crystal engineering**

A crystal is any solid object in which an orderly three-dimensional arrangement of the atoms, ions, or molecules is repeated throughout the entire volume [1]. Although this classical definition is still commonly used in popular texts, after the discovery of quasicrystals [2] the term has been provisionally redefined by the International Union of Crystallography ("By 'crystal' we mean any solid having an essentially discrete diffraction diagram" [3]) and the discussion about the definition of a crystal continues [4, 5]. Nevertheless, the old definition, actually describing what is nowadays called 'a periodic crystal' [6] is fully sufficient for the purposes of this work.

From the chemical point of view, a crystal can be considered 'a supramolecule par excellence' [7]. Moreover, crystallization from a solution containing several solutes is a self-organization process, necessarily involving also specific molecular recognition at an amazing level of precision [7]. Such processes, results of various intermolecular interactions, are studied by supramolecular chemistry, 'a chemistry beyond the molecule' [8, 9].

The popular name for the targeted preparation of crystals with desired properties is a sligthly vague term crystal engineering, that has first appeared more than forty years ago [10]. The term 'crystal engineering' can be defined as the design and construction of crystal structures from molecular components [11] or, in other words, the supramolecular synthesis of new solid phases with predictable stoichiometry and architecture [12]. In practice, such efforts consist of a reasonable choice of particular building blocks (and alternatively also their targeted modifications), understanding and use of their assembling tendencies (*e.g.*, formation of hydrogen-bonded supramolecular synthons) and combination of these blocks in order to form a desired structure. Definitely, crystal engineering is not primarily focused on a precise prediction of a new crystal structure, but deals with understanding and design of a certain blueprint or structure network [12] exhibiting desirable properties.

Properties of a crystal cannot be considered only as a sum of properties of its individual building blocks. Their prediction is very complicated due to many variables more or less influencing the packing of the structure. The factors of major importance in packing are the geometry of the building blocks (especially hard to predict with flexible molecules), the type and behaviour of the supramolecular synthons [13] formed in the particular case, and various intermolecular interactions (covalent bonds, ionic

interactions, ion-dipole, dipole-dipole, cation-π, π-π and van der Waals interactions [14]). Especially the hydrogen bonds (belonging actually to the dipole-dipole interactions) are of great importance for the final assembly of the building blocks in the structure.

A hydrogen bond can be described as an interaction of a hydrogen-bond donor center D-H containing covalently bonded hydrogen atom with an H-bond acceptor center. During the interaction, the system D-H...A is formed while the electrons are redistributed so that the covalent D-H is lengthened and the distance of H...A is shortened so that its length is shorter than the sum of van der Waals radii of the participating atoms [15]. A hydrogen bond involves contributions from electrostatic interactions, charge transfer and dispersion forces and it effects only in the direction connecting the H-bond donor and the H-bond acceptor centers [16]. The properties of hydrogen bonds vary according to the particular H-bond type and energy. Their variety can be roughly visualised in a diagram situating every H-bond type in a field among three extremes, the fully covalent bond, fully ionic interaction and an interaction of a van der Waals type (Fig. 1 taken from [16]).

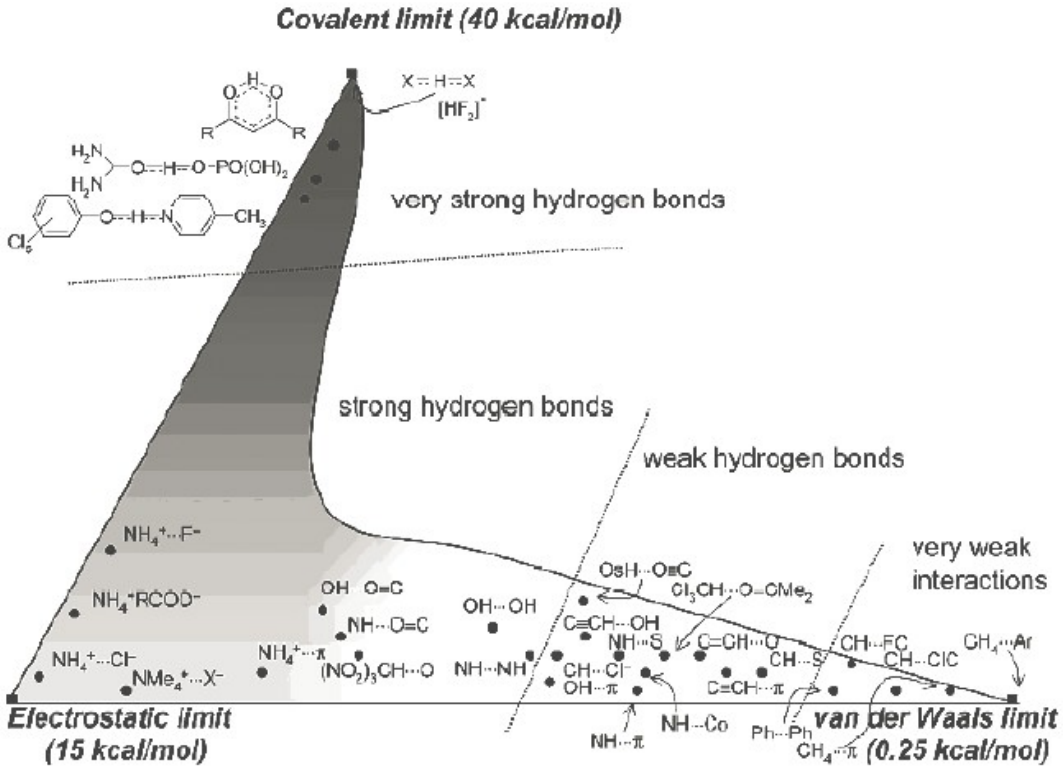


Fig. 1 Scheme of hydrogen bonds classification, taken from [16]

Especially the strong hydrogen bonds and those of average strength can serve as useful means of the crystal design. They can be introduced by targeted embodying

of the typical H-bond donor or acceptor groups into the building blocks. On the contrary, the weak ones often form unexpected, undesired and hardly predictable systems which might complicate the results of the self-assembly and that might even act synergically [16]. The intense study of the formation of H-bonds led to the stating of the set of general rules known as the Etter's rules: **1.** All good proton donors and acceptors are used in hydrogen bonding. **2.** Six-membered-ring intramolecular hydrogen bonds form in preference to intermolecular hydrogen bonds. **3.** The best proton donors and acceptors remaining after an intramolecular hydrogen-bond formation form intermolecular hydrogen bonds to one another [17]. The system of classification of hydrogen bond types in the structure is called graph set analysis [18].

In recent years efforts were given to find computational methods enabling a realistic approach of all of these influences and to predict at least the general features of novel structures. Efforts to solve this problem by a computation of the energetically advantageous state of the system (*e.g.* the 'lattice energy minimization' [19]) are complicated by the ocurrence of more states with similar energies at the level of individual molecules, synthons or even whole structures (sometimes realized in existence of polymorphs [20]). The extent of understanding of all of the influencing factors and their proportions is still not sufficient to distinguish which one of the theoretically considerable polymorphic structures is the most likely one to occur [21]. Although there are some promising results even in the computational prediction of crystal structures only from the knowledge of their components and stoichiometry, including the famous *blind tests* [21] being carried out from the late 1990s in the community of crystallographers, the practical use of such computations for design of new structures is still limited.

While the prediction of a particular structure is still a complicated task, another more general approach to the planning of new materials is being intensely used. It is the targeted search for compounds exhibiting a desirable property. This is based on stating the conditions which should be fulfilled so as to enable the property to occur at all. Then a 'translation' of the conditions expressed by means of mathematics and physics to the 'language' of chemistry must be carried out – *i.e.* stating a symmetry, electron distribution, charge, bonding or other qualities that should be reached. This is followed by searching for the motifs or moieties which can fulfil these conditions and finally, by the investigation of a wide spectrum of assemblies of these motifs in order to find a structure that would exhibit the target behaviour. Such approach can principally lead to finding of a chemically diverse moieties which do not have much in common except the target property.

1.2 **Nonlinear optical properties**

The origin of the NLO processes is the nonlinear response of the dielectric medium to an applied oscillating electric field. Generally, the field applied on a crystalline material induces the oscillation of the electron distribution. The induced dielectric polarization $\boldsymbol{P}$ depends on the applied field $\boldsymbol{E}$ and can be expressed in power series of $\boldsymbol{E}$ according to the Equation 1, where $\chi^{(1)}$ is the linear dielectric susceptibility pertinent to linear optics and $\chi^{(2)}$, $\chi^{(3)}$, ... are the nonlinear susceptibilities of the second, third and higher orders, respectively.

$$\boldsymbol{P}(E) = \varepsilon_0 (\chi^{(1)}\boldsymbol{E}^1 + \chi^{(2)}\boldsymbol{E}^2 + \chi^{(3)}\boldsymbol{E}^3 + ...) \quad (1)$$

For small fields (as, *e.g.*, the daylight) just the linear term is relevant. However, for higher fields (*i.e.* energies in order of $10^6$ V/m) the higher order terms become important and the Maxwell equations then include interactions of electromagnetic waves of different frequencies. As a result a radiation corresponding to a combination of the original frequency (-ies) and its (their) harmonics occurs. The NLO interactions belong to the energy conserving processes. The most important examples of nonlinear optical effects are listed in Table 1 together with their relevant terms of $\chi^{(n)}$ [22]. It should be noted that a non-zero second order nonlinear susceptibility can occur only in non-centrosymmetric compounds.

The efficiency of many NLO processes as the second harmonic generation (SHG) is generally low, but in case that the condition for phase matching (or momentum conservation, Equation 2) is fulfilled, the efficiency significantly increases. The Equation 2 expresses the relationship between the wavevectors $\boldsymbol{k}_i$ ($i$ = 1 - 4) corresponding to waves with frequencies $\omega_i$ and the refractive index $n$ and the phase velocity $\upsilon$ at the given frequency.

$$\boldsymbol{k}_3 = \boldsymbol{k}_2 + \boldsymbol{k}_1 \text{ or } \boldsymbol{k}_4 = \boldsymbol{k}_2 - \boldsymbol{k}_1, \text{ where } |\boldsymbol{k}_i| = \frac{\omega_i n(\omega_i)}{c} = \frac{\omega_i}{\upsilon(\omega_i)} \quad (2)$$

For the SHG ($\omega_1 = \omega_2$, $\omega_3 = 2\omega_1$), this condition can be fulfilled either if $\boldsymbol{k}_3 = 2\boldsymbol{k}_1$ or $n_3 = n_1$, but this can never be reached with normal dispersion in isotropic materials ($n_1 < n_3$). This problem can be overcome either by use of the anomalous dispersion (which has only a very limited range of applications) or by using the natural birefringence of uniaxial or biaxial crystals. Then, with an appropriate orientation of the crystal of a convenient symmetry, the phase matching condition can be fulfilled.

Still, it is necessary to stress that only a minority of chemical compounds possesses the noncentrosymmetric assembly (22% of all entries in Cambridge Structure Database [23] and 18% of entries in the Inorganic Crystal Structure Database [24]), which is a basic condition for the second harmonic generation, and only some of these compounds are phase-matchable. A classification of the material types in relation to SHG has been done by Kurtz and Perry [25] and the phase matching was further classified and discussed by Hobden [26].

Table 1 Selected NLO processes and their relevant terms – after [22]

| NLO process | Relevant terms |
|---|---|
| *Second order* | |
| Second harmonic generation | $\chi^{(2)}(-\omega_3; \omega_1, \omega_1), \omega_3 = 2\omega_1$ |
| Sum/Difference frequency generation | $\chi^{(2)}(-\omega_3; \omega_1, \pm\omega_2), \omega_3 = \omega_1 + \omega_2$ |
| Pockels effect (linear electrooptic effect) | $\chi^{(2)}(-\omega; 0, \omega)$ |
| *Third order* | |
| Third harmonic generation | $\chi^{(3)}(-\omega_4; \omega_1, \omega_1, \omega_1), \omega_4 = 3\omega_1$ |
| General four wave mixing | $\chi^{(3)}(-\omega_4; \omega_1, \omega_2, \omega_3)$ |
| Kerr effect (quadratic electrooptic effect) | $\chi^{(3)}(-\omega; 0, 0, \omega)$ |

### 1.3 **Second harmonic generation – an important nonlinear optical property**

The second harmonic generation, also called frequency doubling, is actually a special case of the sum frequency generation, in which a pair of photons of frequency $\omega_1$ give origin to one photon of frequency $2\omega_1$. The necessary condition for existence of this effect, similarly as for the other $\chi^{(2)}$ effects, is a noncentrosymmetric assembly of the considered compound [27]. The efficiency of the SHG process differs by the particular compound structure. It is dependent on the refractive indices and phase matchability, on the quality and orientation of the compound's crystal.

The SHG is utilized in numerous applications in physics (laser wavelength conversions [28], optical signalization [29], signal processing [27]), information technologies (reading, processing, storage and transfer of data [30]) and in biology and medicine (special confocal microscopy [31], endoscopy techniques [32]). Although the material requirements on a compound capable of SHG vary according to the particular application, some general requirements can be pointed out: large NLO coefficients,

possibility of the (preferably noncritical) phase matching, good transmission for the given wavelength, sufficient resistivity to the optical damage and the possibility of preparation of the compound's crystals in optical quality, chemically stable and of good mechanical properties [33].

Similarly as the above mentioned macroscopic polarization, the microscopic (molecular) polarization can be expressed by Equation 3,

$$\boldsymbol{P} = \alpha \boldsymbol{E} + \beta \boldsymbol{E}^2 + \gamma \boldsymbol{E}^3 + \ldots \quad (3)$$

where $\boldsymbol{P}$ symbolizes the polarization vector, $\boldsymbol{E}$ corresponds to the vector of the electric filed intensity and the coefficients $\alpha$, $\beta$ and $\gamma$ are the molecular polarizability, the first molecular hyperpolarizability and the second molecular hyperpolarizability, respectively. As $\beta$ represents the nonlinear effects of the second order, its calculation can be used to indicate whether a molecule would be capable of SHG or not. The problem is that the molecular $\beta$ describes only the properties of a single molecule, not the resulting (hyper)polarizability of the whole structure, which depends on the assembly of the individual building blocks.

### 1.4 **Methods of investigation of the NLO properties**

There are several techniques for measurement of the microscopic and macroscopic NLO properties. Concerning the microscopic NLO properties, one of the widespread methods is the EFISH (electric field-induced second harmonic generation) that is the measurement of second harmonic response in solution of the sample on which the static electric field is applied [34]. This method enables to find the macroscopic second order polarizabilities of molecules. Its advantage is the large amount of data available for comparison as it is a widely used method, its limitations rise from the principle of this method – there can be problems with the insufficiency of solubility of some samples and, above all, this method is not usable for the salts, as the solutions of the charged moieties would be electrolyzed during the measurements.

An alternative technique of measurements of the second order polarizabilities is the solvatochromism method [35]. It is based on comparing the UV-Vis spectra of a compound in solution and in the gas phase, utilizing the solvatochromic effect. Its main advantage is the available and simple measurement technique, but it is a subjective method of measurement and it requires, similarly as EFISH, determining of the dipole moments.

The measurement of the hyper-Rayleigh scattering [36] in solutions enables direct determination of the first hyperpolarizabilities. It requires very good quality of the applied laser beam. This method does not use the electric filed and so it is suitable also for

the ionic compounds. On the contrary, the Langmuir-Blodgett film method [37] is suitable for compounds with long aliphatic chains and the measurement is carried out rapidly in the aqueous solution.

As a method of first choice for measurement of the SHG efficiency of new crystalline compounds directly in the solid state serves the powder technique [25]. It is based on interaction of a laser beam with a powderized sample with particles much smaller than is the diameter of the beam. The recorded SHG response of the sample is an average of responses obtained from many different randomly oriented individual crystallites, but still it bears a qualitative and also a rough quantitative information about the SHG efficiency of the sample. Moreover, by measurement of fractions with different crystallite size it is possible to determine whether the compound is phase-matchable or not [25], Fig. 2.

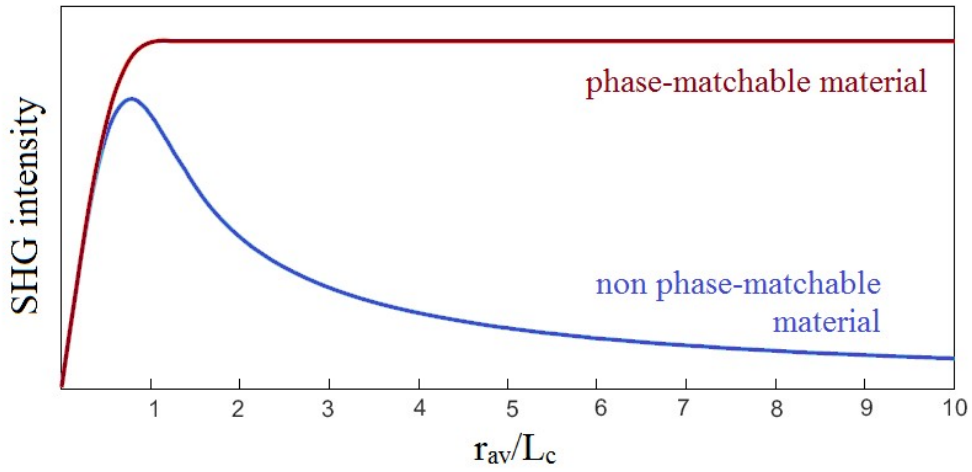


Fig. 2 Typical phase-matching curves for the phase-matchable and the non phase-matchable powder samples. The $r_{av}$ symbolizes the average particle size and the coherence length $L_c$ can be expressed as $L_c = \lambda_\omega/4(n_{2\omega}-n_\omega)$ where the $\lambda_\omega$ is fundamental wavelength and $n_\omega$ and $n_{2\omega}$ are refractive indices for the fundamental and SHG wavelength, respectively. Drawn after [25].

A more advanced technique, the study of SHG on an oriented monocrystal, allows precise determination of the individual nonlinear coefficients of the compound but, in addition, it requires determination of the material's refractive indices for the fundamental and the second harmonic wavelengths. A widespread method for SHG measurements of crystals is the Maker-fringe method [38] based on analysis of periodic oscillations of the SHG response while a planar sample is rotated in a defined way (Fig. 3). This is a standard method for investigation of organic or semiorganic crystals. A variation of this measurement is the wedge method [39] especially suitable for the non-phase

matchable samples (Fig. 3). The observed values of the SHG efficiency are usually presented in comparison with standards as KDP, urea or $\alpha$-quartz.

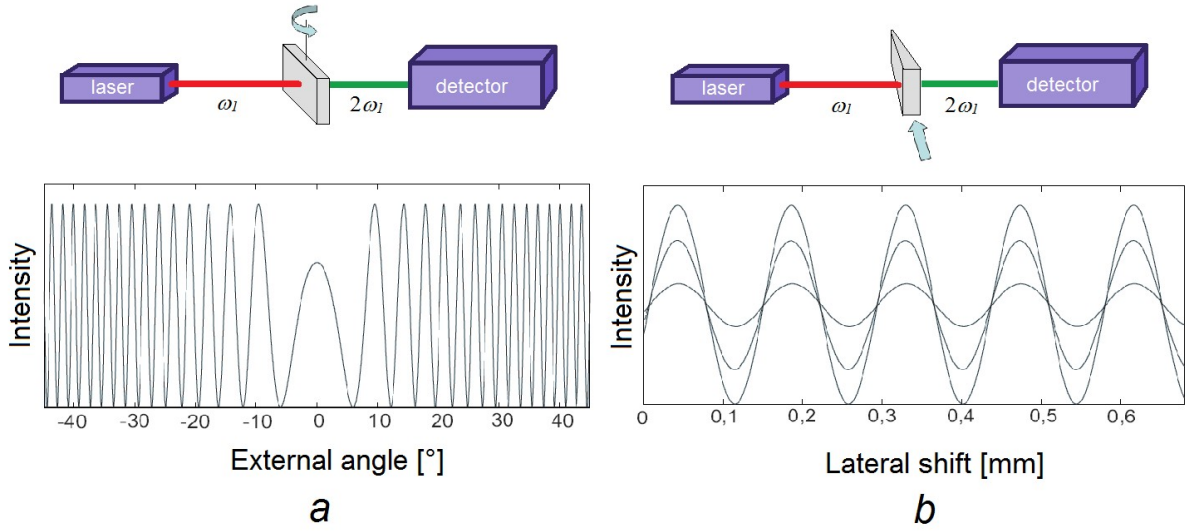


Fig. 3 Methods of investigation of the SHG efficiency of single crystal samples, a – Maker fringe method, b – wedge method, adjusted after [40]

### 1.5 **Materials for second harmonic generation**

Materials for SHG are very diverse, but they still can be roughly divided into three groups: ***I***. *inorganic salts and oxides*, ***II***. *organic and organometallic compounds* and ***III***. *organic salts and cocrystals* [41].

To the group ***I*** belong the classical materials like $\alpha$-quartz or the water soluble KDP and ADP ($KH_2PO_4$ and $NH_4H_2PO_4$, respectively) utilized also for their piezoelectric properties [41]. The non-hygroscopic borates with a high resistence to optical damage like BBO ($\beta$-$BaB_2O_4$), LBO ($LiB_3O_5$) or BIBO ($BiB_3O_6$) are prepared from melts [22, 42]. The $LiNbO_3$ and $NaBaNb_5O_{15}$ serve also as piezoelectrics and in case of a damage, their structure can be restored at an elevated temperature [43]. The mineral proustit, $Ag_3AsS_3$, is also an interesting material with a high SHG efficiency and a high birefringence [44].

The common advantageous features of the group ***I*** are the high melting points and the thermal stability, hardness and a relative wide transparency window in the Vis and UV region [45]. On the other hand, the general disadvantages of this group are a limited transparency in IR region, often only a limited birefringence and resistivity to optical damage and also low nonlinear coefficients [27].

***II.*** *Organic and organometallic compounds* often possess a large hyperpolarizability $\beta$. Their main advantage is the possibility of tuning their properties

by means of molecular design. Unfortunately, the high $\beta$ often occurs together with a high dipole moment which leads to an undesirable tendency of the molecules to form a centrosymmetric assembly [46].

A large group of organic compounds for SHG are materials containing an aromatic group and/or a system of conjugated double bonds, often along with substituent(s) of electron donor/acceptor nature. Examples of such assembly are the p-nitroaniline, MNA (2-methyl-4-nitroaniline) [47], POM (3-methyl-4-nitropyridine-1-oxide) [48], DAST (4´-dimethylamino-*N*-methyl-4-stilbazoliumtosylate) [49] or even the "push-pull" polyenes [50]. An important NLO active compound is also the simple molecule of urea [51].

The NLO active organometallic compounds are, *e.g.*, the sandwich structures as (tetraaryl-$\eta^4$-cyclobutadien)cobalt [52] or complexes utilizing the nitrilotriacetato (NTA) ligand like $M^I_2[Zr(NTA)_2].2H_2O$ where $M^I$ are the cations of alcali metals [53].

***III.*** Formation of the *organic salts and cocrystals* with a rich network of hydrogen bonds can assist the efforts against the centrosymmetric assembly of the promising molecules with a high $\beta$ [54]. This group of compounds can combine the advantages of the both previously mentioned groups. According to their nature, the counterions of the NLO properties bearers can form chains or networks functioning as a framework for the structure or they can even direct the noncentrosymmetric assembly [46].

An interesting example of a commercially used compound belonging to this group is LAP (argininium(1+) dihydrogen phosphate monohydrate) with the SHG efficiency about 3 times higher than KDP and better material properties [55]. Similarly, many other salts of argininium(1+) exhibit a fair SHG efficiency [56, 57]. The molecule of arginine can be theoretically divided into two motifs – ornitine, which exhibits no NLO properties and guanidine, which was found to be an extremely interesting building block for NLO active compounds [58]. This finding led to an intense investigation of the hydrogen-bonded salts of guanidine and its derivatives and some of the salts with inorganic oxy-acids [59, 60], dicarboxylic acids [61] or chiral organic acids [58] exhibited noticeable NLO properties.

This concept of functional salts consists of anions serving as important means of the structure assembly (forming chains or networks *via* hydrogen bonds; in case of chiral organic anions even directing the noncentrosymmetric structure assembly) and of cations responsible for the NLO properties. Acyclic cations with delocalized π electrons,

forming so called Y-aromatic systems as many guanidine derivatives [62], are especially appropriate [30].

## 1.6 **From the promising building blocks to novel materials**

At the beginning of a planning of a new structure, the reasonable choice of a building block capable of the desired property [63] and its rational modification (loftly called 'molecular design' [64, 65]) can be aided by quantum chemical computations with good results [66]. So can be computed, *e.g.* the polarizability and hyperpolarizability [66] of a molecule or its dipole moment. Changes of these values with addition of a substituent or a charge on the molecule can be estimated as well.

The next step in designing a structure is putting the building blocks together [67]. Some molecules tend to form certain layout. Some of these layouts, assisted mostly by hydrogen bonds, especially those appearing in many structures, are called supramolecular synthons [67]. Such entities strongly influence the structure assembly. For example, a robust centrosymmetric synthon [68, 69] formed by hydrogen-bond aided dimerization of two molecules of monocarboxylic acids [12] belongs to the most typical ones. It is necessary to add that there is also another common way of monocarboxylic acids arrangement, namely the head-to-tail assembly forming an infinite polar chain [70, 69].

When a moiety, intended to form a crystal, tends to assemble in an unwanted way (and therefore loses or limits the functionality it was prepared for), it can be useful to supplement such a carrier of a desired property with moieties that can assist (or prevent) certain assembly [46]. A typical example of such a strategy is embodying the polarizable organic cations with the tendency to form head-to-tail pairs in a dense anionic network in order to prevent their centrosymmetric arrangement [46]. Although there are many sophisticated strategies to obtain a desired assembly, we have to admit that the results do not always correspond to the original intention [54].

The product of the targeted preparation is usually first characterized by the single crystal X-ray diffraction [71] and the study of phase homogenity of the product as a whole is also important. Assuring that the bulk material is identical with the monocrystal used in the structure determination is vital in this stage. A preliminary examination of the expected properties, *e.g.* the SHG efficiency measurement of powderized samples, can be consecutively carried out.

If the behaviour of the prepared crystalline or microcrystalline solid complies with the requirements, it is time to attempt to grow some large monocrystals. This includes the preparation of a sufficient amount of the novel compound, experimenting in search

for the general method suitable for the given group of compounds, and finally also tuning of the conditions necessary for the proper crystal growth of the particular material. Although there is a large amount of knowledge on this issue, the successful 'crystal breeding' [72] has also much to do with one's personal experience and sense for the art [72].

The last stage after the obtaining of large crystals of a material is the detailed investigation of its properties. Finally comes the critical assessment of all known facts in order to contribute to the understanding of the relationship between the structure and the properties and also to consider the perspective of applications of the prepared entity [27]. Naturally, only a few of the syntheses attempted lead to the compounds capable of going successfully through all of the stages described.

### 1.7 **Selected systems with delocalized π electrons**

Guanidine (Fig. 4) is a well known compound [73] that has been already successfully used as a building block in the molecular design [59, 74]. Its protonated form, a guanidinium(1+) cation, is a typical example of a Y-aromatic moiety, exhibiting also a trigonal symmetry suitable for preparation of octupolar materials [73, 75]. There are generally two ways of modification of this successful motif. The first one is a formation of longitudinal molecules with high hyperpolarizability and the second one is a symmetric substitution on all the amino groups leading to sustaining of the trigonal symmetry in cations (see Fig. 5).

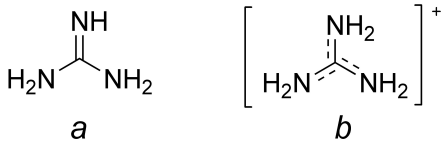


Fig. 4: Guanidine (*a*) and guanidinium(1+) cation (*b*).

A simple molecule of guanylguanidine, usually called biguanide, has been thoroughly studied by Matulková (PhD Thesis in 2007 [76] and [59, 61]). Biguanide is a strong base with exceptional exothermicity of the neutralization [77]. Its derivative *N*-phenylbiguanide is even more prospective for our purposes due to high hyperpolarizability of its cations (Table 2) and according to the Matulková's results [76] it is worth being further investigated. Another biguanide derivative, *N*,*N*-dimethylbiguanide, known under the common name Metformin, has been thoroughly studied from the medical point of view [78, 79] and its cations also exhibit a remarkable hyperpolarizability (Table 2).

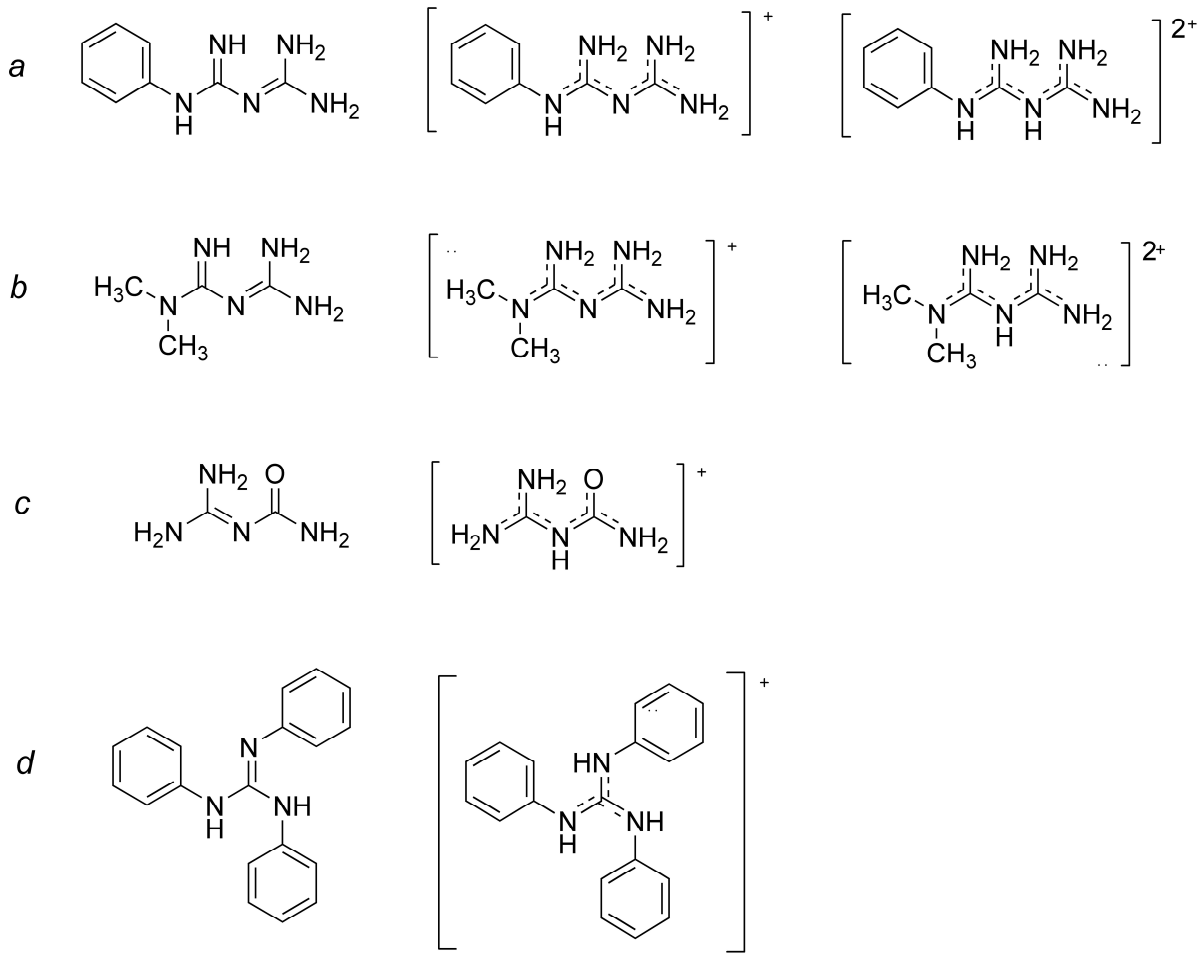


Fig. 5: Selected guanidine derivatives: *a* – *N*-phenylbiguanide and its 1+ and 2+ charged cations, *b* – *N*,*N*-dimethylbiguanide and its 1+ and 2+ charged cations, *c* – *N*-carbamoylguanidine (guanylurea) and its 1+ charged cation, *d* – *N*,*N*′,*N*″-triphenylguanidine and its 1+ charged cation.

A molecule of *N*-carbamoylguanidine, commonly known as guanylurea, combines the motif of guanidine with urea, a molecule with many interesting properties, used also as a SHG standard. Although the first report of a guanylurea salt occured more than a century ago [80], a novel salt of this compound was found interesting for NLO in recent research [81] and the theme of guanylurea deserves a deeper study.

A modality of development of the guanidinium motif without losing the capability of the trigonal symmetry (*i.e.* with a perspective of preparation of octupolar materials [58]) is a symmetric substitution on all of its three amino groups. Such an idea can be represented by *N*,*N*′,*N*″-triphenylguanidine, by its cation in particular [82].

The static hyperpolarizabilities of all of the mentioned guanidine derivatives and their cations are listed in the Table 2 together with the $\beta$ computed for urea for comparison. All of them reach values of the total $\beta$ which can be considered reasonable for the building blocks for NLO compounds. In some of them, especially in case of the *N*-phenylbiguanide,

the protonization to a higher grade would be advantageous. The protonization may be influenced by selection of the acids of appropriate strength as the sources of the counterions.

The common features of all of the enumerated guanidine derivatives are the so-called Y-aromaticity of their cations, their relative stability, synthetical or commercial availability of the bases and a reasonable solubility in common polar solvents. These properties are necessary prerequisities for preparation of salts.

Table 2: Calculated values of the total first static hyperpolarizability ($\times 10^{-30}$ esu) for guanidine, its selected derivatives and urea at B3LYP level with 6-311G(d,p) basis set. Abbreviations: ***gua*** - guanidine, ***bigua*** - biguanide, ***phbigua*** – *N*-phenylbiguanide, ***dmbigua*** – *N*,*N*-dimethylbiguanide, ***gu*** - guanylurea, ***tphgua*** – *N*,*N*′,*N*″-triphenylguanidine, $\boldsymbol{\beta_{tot}}$ – total first molecular hyperpolarizability, computed as $\beta_{tot} = [(\beta_{xxx} + \beta_{xyy} + \beta_{xzz})^2 + (\beta_{yyy} + \beta_{yzz} + \beta_{yxx})^2 + (\beta_{zzz} + \beta_{zxx} + \beta_{zyy})^2]^{1/2}$; *see Appendix II. †The $\beta_{tot}$ value for ***tphgua*** was not computed for the ideal trigonal symmetry of the cation but for a distorted one known from the structures (see Fig. 25).

| Compound | ***gua*** | | ***bigua*** | | | ***phbigua*** | | |
|---|---|---|---|---|---|---|---|---|
| Charge | 0 | 1+ | 0 | 1+ | 2+ | 0 | 1+ | 2+ |
| $\beta_{tot}$ | 0.99 | 0.64 | 10.4 | 0.98[61] | 0.52[61] | 4.47 | 8.62[83] | 11.23[83] |
| Compound | ***dmbigua*** | | | ***gu*** | | ***tphgua*** | | ***urea*** |
| Charge | 0 | 1+ | 2+ | 0 | 1+ | 0 | 1+ | 0 |
| $\beta_{tot}$ | 1.46 | 1.61 | 1.92 | 1.04 | 1.18* | 7.22 | 1.39 | 0.78 |

### 1.7.1 *N-phenylbiguanide*

Synthesis of the *N*-phenylbiguanide was first reported by Cohn in 1912 [84] and the effects of pH on the kinetics of the same reaction (*i.e.* synthesis of the N-phenylbiguanide from aniline and dicyandiamide) have been described in detail recently [85]. This compound exhibits effects on various receptors in organisms and therefore it has been widely investigated in pharmacology [86, 87]. It is also used as an additive for pigments and resins [88].

Currently, there are only six entries in the Cambidge Structure Database (CSD) concerning the *N*-phenylbiguanide. Two of them and other seven structures were recently described by Matulková in her PhD thesis [76] and publications [89, 90]. All of the known structures are listed in Table 3. Although there have only been records of structures containing (1+) charged cations, there are strong indices that also a (2+) charged cation might occur and form reasonably stable compounds [76].

Table 3: Known structures containing the *N*-phenylbiguanide

| CCDC code | Compound name | Space group |
|---|---|---|
| DIHSUI01 | *N*-phenylbiguanidium(1+) chloride | $P2_1/c$ |
| HIJCUY | *N*-phenylbiguanide | $P2_1/c$ |
| PEYPUF | *N*-phenylbiguanidium(1+) diliturate monohydrate | *P*-1 |
| QAKCUC | *N*-phenylbiguanidium(1+) adipate monohydrate | *P*-1 |
| WADTEC | *N*-phenylbiguanidium(1+) succinate methanol monosolvate | $P2_1/c$ |
| - | *N*-phenylbiguanidium(1+) nitrate | *C*2/c |
| - | *N*-phenylbiguanidium(1+) perchlorate | *P*-1 |
| - | *N*-phenylbiguanidium(1+) sulphate | *C*2 |
| - | *N*-phenylbiguanidium(1+) hydrogen phosphite dihydrate | $P2_1/n$ |
| - | *N*-phenylbiguanidium(1+) hydrogen phosphate sesquihydrate | *P*-1 |
| - | *N*-phenylbiguanidium(1+) oxalate | *C*c |
| - | *N*-phenylbiguanidium(1+) oxalate | $P2_1/c$ |

### 1.7.2 ***N,N-dimethylbiguanide***

The *N*,*N*-dimethylbiguanide was first studied for its antiviral and analgesic activity [91], but its main application in the last fifty years lies in the diabetes treatment [92]. It exhibits also interesting vasculoprotective effects [93] and antitumor properties [94].

There are many structures containing *N*,*N*-dimethylbiguanide in CSD (selected structures listed in Table 4). Most of them are complex compounds with *N*,*N*-dimethylbiguanide in form of an uncharged or even a (1-) charged ligand [95].

Table 4: Known structures containing *N*,*N*-dimethylbiguanidium(1+) or (2+) cations (* published in the framework of this thesis, see Appendix I)

| CCDC code | Compound name | Space group |
|---|---|---|
| ELUJUR | *N*,*N*-dimethylbiguanidium(2+) hexafluorosilane | $P2_1/c$ |
| ETIVUY | *N*,*N*-dimethylbiguanidium(1+) bromide | $P2_1/c$ |
| HULBUL | *N*,*N*-dimethylbiguanidium(1+) tetrabromothallate | $P2_1/n$ |
| HUZLUJ | *N*,*N*-dimethylbiguanidium(1+) nitrate | *P*-1 |
| JAMRIY | *N*,*N*-dimethylbiguanidium(1+) chloride (polymorph A) | $P2_1/a$ |
| JAMRIY02 | *N*,*N*-dimethylbiguanidium(1+) chloride (polymorph B) | $P2_1/c$ |
| OJOSUC | *N*,*N*-dimethylbiguanidium(1+) acetate | $P2_1/n$ |
| ODEZOO | *N*,*N*-dimethylbiguanidium(2+) hydrogensquarate | *P*-1 |
| PAJBUY | *N*,*N*-dimethylbiguanidium(2+) oxalate monohydrate | $P2_1/c$ |
| PAJCAF | *N*,*N*-dimethylbiguanidium(2+) sulphate monohydrate | *P*-1 |
| VOPLAO | *N*,*N*-dimethylbiguanidium(1+) (ethoxycarbonyl)(p-tosyl)azanide | *P*-1 |
| WIBSIJ | *N*,*N*-dimethylbiguanidium(2+) tetrachlorocuprate | $P2_1/a$ |
| SAFQIB* | *N*,*N*-dimethylbiguanidium(2+) dinitrate | $P2_1/c$ |

In salts the *N*,*N*-dimethylbiguanide occurs as a mono- or dication and the occurence of (1+) and (2+) charged cations is roughly equal in the known structures (see Table 4).

### 1.7.3 ***N-carbamoylguanidine (guanylurea)***

Synthesis of the guanylurea was first described by Haag in 1862 [96] and descriptions of guanylurea salts followed – *e.g.* [80]. The guanylurea exhibits certain biological activity as it can interfere with action of some enzymes [97]. Compounds of guanylurea (Table 5) have a wide range of technical applications – some of them are used as corrosion inhibitors [98] and take part in a composition of specialized fertilizers [99], others were examined for explosivity [100], some are patented for use in fuel cells [101] or in compositions for gas development in airbags [102].

Table 5: Known structures containing guanylurea (* published in the framework of this thesis, see Appendix II)

| CCDC code | Compound name | Space group |
|---|---|---|
| AGUSAX | guanylurea(1+) chloride | $P2_1/c$ |
| AGUSEB | guanylurea(1+) azide monohydrate | $P2_1/c$ |
| AGUSIF | guanylurea(1+) 5-aminotetrazolate | $P2_1$ |
| DAWDAH | guanylurea(1+) dicyanamide | $C2/c$ |
| DIVVAF | guanylurea ethanol monosolvate | $P2_12_12_1$ |
| DIVVEJ | guanylurea(1+) perchlorate | $P2_1/c$ |
| DOKLIY | bis(guanylurea)-copper(II) nitrate | $P2_1/n$ |
| DUNHID | guanylurea(1+) dihydrogen phosphate | $P$-1 |
| EKIBAB | guanylurea(1+) hydrogen selenite | $P$-1 |
| GADQAE | guanylurea(1+) methylphosphonate monohydrate | $P2_1/c$ |
| GADWUD | bis(guanylurea(1+)) diaqua-tetrachloro-copper(II) | $P2_1/c$ |
| JIRKIF | bis(guanylurea(1+)) aqua-bis(oxalato)-dioxo-uranium(VI) | $Pn$ |
| JODZOR | guanylurea(1+) chloride hemihydrate | $P2_1/n$ |
| KAGLUA | bis(guanylurea(1+)) diaqua-tetrachloro-cobalt(II) | $P2_1/n$ |
| LOXROF | guanylurea(1+) tetravanadium(V)-hexaarsenate | $P$-1 |
| MECSOD | catena-(guanylurea(1+)-($\mu^4$-phosphato)-chloro-zinc) | $Cc$ |
| MECSUJ | catena-(bis(guanylurea(1+))-bis($\mu^3$-phosphito)-bis($\mu^2$-phosphito)-aqua-tri-zinc) | $P$-1 |
| NAZBOG | guanylurea(1+) sulphate dihydrate | $C2/c$ |
| NOJKIH | guanylurea(1+) hydrogen sulphate | $P$-1 |
| QELSUW | catena-(bis(guanylurea(1+))-bis($\mu^2$-hydroxo)-oxalato-bis(formato-O)-tetraoxo-di-uranium(VI)) | $P$-1 |
| QIRGIH | guanylurea(1+) dinitramide | $Pna2_1$ |
| TAKZOV | bis(guanylurea(1+)) trans-diaqua-tetrachloro-manganate(II) | $P2_1/n$ |
| VUZVAN | catena-(guanylurea(1+))-$\mu^4$-phosphato-zinc | $P2_1/c$ |
| WEGXAI | catena-(bis(guanylurea(1+))-bis($\mu^3$-sulfato)-bis($\mu^2$-hydroxo)-tetraoxo-di-uranium monohydrate | $P2_1/c$ |
| CUYZEC* | guaylurea(1+) hydrogen phosphite | $Cc$ |

Concerning optical properties, only a spectroscopic study of guanylurea(1+) chloride hemihydrate was carried out more than twenty years ago [103]. A recent preliminary investigation of some guanylurea compounds with respect to their nonlinear optical properties led to interesting results (Fridrichová, Diploma thesis 2007 [81]).

Nowadays there are more than twenty records of structures containing guanylurea in CSD (see Table 5), most of them are salts of a (1+) charged cation. An interesting point of guanylurea is that the molecule or its cation in all of the known structures occur as a more or less planar moiety (see Table 8 and 9 in the Results and discussion chapter) and this noticeable fact contrasts with the variety of layouts found, *e.g.* in the comparable molecule of biguanide.

### 1.7.4 ***N,N′,N″-triphenylguanidine***

One of the first reports on *N*,*N′*,*N″*-triphenylguanidine synthesis was published by Merz & Weith in 1869 [104]. The *N*,*N′*,*N″*-triphenylguanidine is used as an auxilliary compound in some analytical methods [105] and as a sensitizer of photodegradation of plastics [106]. It exhibits quite a versatile behaviour, complexing as an uncharged ligand [107] or in form of *N*,*N′*,*N″*-triphenylguanidinate(1-) or even (2-) anions [108, 109]. There is also quite a large number of structures of its salts in CSD (see Table 6).

Table 6: Known structures of *N*,*N′*,*N″*-triphenylguanidine and its salts (numerous structures of complexes with *N*,*N′*,*N″*-triphenylguanidine in role of a ligand not listed)

| CCDC code | Compound name | Space group |
|---|---|---|
| ADEHUN | *N*,*N′*,*N″*-triphenylguanidinium(1+) nitrate | *P*-1 |
| PEZCUT | *N*,*N′*,*N″*-triphenylguanidinium(1+) choride | $P2_1/c$ |
| PODTIM | bis(*N*,*N′*,*N″*-triphenylguanidinium(1+)) tetrachloro-copper(II) | $P2_1/c$ |
| PONHAC | *N*,*N′*,*N″*-triphenylguanidinium(1+) tetraphenylborate ethanol solvate | $P2_1/c$ |
| VEKSOT02 | *N*,*N′*,*N″*-triphenylguanidine (monoclinic polymorph) | $P2_1/c$ |
| VEKSOT03 | *N*,*N′*,*N″*-triphenylguanidine (orthorhombic polymorph) | $Pna2_1$ |
| VEKSUZ | *N*,*N′*,*N″*-triphenylguanidine acetic acid monosolvate | $P2_1/c$ |
| VEKTAG | *N*,*N′*,*N″*-triphenylguanidine trichloroacetic acid monosolvate | $P2_1/c$ |
| WIZXAF | *N*,*N′*,*N″*triphenylguanidinium(1+) 5-nitrouracilate | $P2_1/c$ |
| XIBZUE | *N*,*N′*,*N″*-triphenylguanidinium(1+) hydrogen sulphate | $P2_1/c$ |
| YICMIH | *N*,*N′*,*N″*-triphenylguanidinium(1+) bromide | $P2_1/c$ |
| ZATSOC | *N*,*N′*,*N″*-triphenylguanidinium(1+) nitrate acetone hemisolvate | $P\text{-}42_1c$ |
| EWODOK | *N*,*N′*,*N″*-triphenylguanidinium(1+) formate | $P2_12_12_1$ |
| EWODUQ | *N*,*N′*,*N″*-triphenylguanidinium(1+) benzoate | *C*c |
| EWOFAY | *N*,*N′*,*N″*-triphenylguanidinium(1+) 3-methoxybenzoate | $P2_12_12_1$ |

Some of the known salts exhibit a reasonable SHG efficiency [110]. Several studies of NLO properties of some prospective new *N*,*N*′,*N*″-triphenylguanidine salts have been carried out [82, 110]. Also studies of vibrational spectra of the uncharged molecule [111, 82] and the monocation [82] have been carried out.

The (1+) charged cation, exhibiting the Y-delocalization similarly as guanidinium(1+) cation, can theoretically maintain the trigonal symmetry and therefore it can be also considered as promising for the formation of the octupolar materials [73], although there is no structure with such symmetry of the **tphgua**(1+) cation known.

### 1.8 **Selected acids**

The choice of counterions to the selected bases is oriented to several groups. The *strong inorganic acids* enable the protonization of a base even to a higher grade, which would be, *e.g.* in case of the *N*-phenylbiguanide an effective way to reach the state of the maximal hyperpolarizability of the cationic moiety. Additionally, many of the anions of strong inorganic acids tend to form chains that could significantly influence the structure. The more or less tetrahedral hydrogenated anions of the phosphorous and the phosphoric acid and also of the sulphuric acid have a tendency to form chains or networks as they can simultaneously act as hydrogen bond donors and acceptors.

The sulphate or phosphate anions can act only as hydrogen bond acceptors and, although they do not form chains, they are ideal as counterparts to the cations of nature of hydrogen bond donors enabling a rich network of hydrogen bonds in the resulting structure. The nitric acid supplies a planar trigonal anion that acts only as a hydrogen bond acceptor. The use of the hydrochloric acid as an anion source is advantageous for study of the vibrational spectra of the given cations.

Concerning the *weak inorganic acids*, the carbonic acid forms two kinds of salts from which the hydrogen carbonate acts both as a hydrogen bond donor and acceptor. Both of its anions are planar and the carbonate exhibits a trigonal symmetry. The amidosulphuric acid has similar advantages as the sulphuric acid and its amino group improves its chaining capability as it serves as the hydrogen bond donor, while the oxygens appear in the role of a hydrogen bond acceptor. Additionally, the amidosulphuric acid is known for numerous noncentrosymmetric salts [112, 113, 114].

The anions of the short-chained *dicarboxylic organic acids* can take part in the dense network of hydrogen bonds, acting there as hydrogen bond donors and acceptors at the same time [76]. For example, the planar anions of oxalic acid can contribute

to a layered structure assembly. The dicarboxylic acids with longer chains can be utilized also for the steric effects.

Utilizing the individual enantiomers of the *chiral organic acids* enables the noncetrosymmetric assembly of the resulting structure. Moreover, many of the chiral organic acids anions can contribute to the NLO properties of the salt as they exhibit their own NLO activity. An example of such an advantageous anion is the L-tartrate. Unfortunately, in cases that the noncentrosymmetry of the crystal structure is enforced by such an anion, but the cations still assemble so that their hyperpolarizabilities counteract, a high SHG efficiency or other desired NLO properties cannot be expected (Appendix X).

## 1.9 **Aim of the thesis**

The aim of the thesis is to prepare and characterize a wide spectrum of new salts of selected guanidine derivatives. The first stage of this research is the "scanning" of a large scale of systems in search for novel compounds. The next step is the selection of compounds with interesting optical properties, especially NLO properties with accent to SHG. Next follow their detailed investigation and efforts to prepare large monocrystals of the most promising ones. The preparation of oriented slices of the large monocrystals enables the detailed study of the material properties of the particular compound and the realistic assessment of its potential for material applications can follow.

In particular, there are four compounds to be used as sources of cations for the target salts, namely the *N*-phenylbiguanide, the *N*,*N*-dimethylbiguanide, the *N*-carbamoylguanidine (guanylurea) and the *N*,*N*′,*N*″-triphenylguanidine which all possess a hyperpolarizability that signals a reasonable potential of them as building blocks for NLO active compounds. The sources of anions will be both inorganic acids (strong acids as $H_2SO_4$ or $H_3PO_4$ or weaker acids as $H_3PO_3$ and $HSO_3NH_2$) and organic acids (selected dicarboxylic acids or, above all, the chiral acids which direct the noncentrosymmetric assembly of the resulting compound, *e.g.* the tartaric acid).

This work develops the promising theme of the salts of Y-aromatic compounds and continues the works carried out on biguanides and phenylbiguanides [76] and on substituted phenylbiguanides [81] in order to obtain detailed information about further interesting members of the guanidine derivatives family.

## 2. **EXPERIMENTAL**

### 2.1 **Preparation of selected bases and the target crystalline materials**

#### 2.1.1 ***N-phenylbiguanide***

Although the *N*-phenylbiguanide was commercially available, efforts were given to its synthesis. The reason for this was that the compound was relatively expensive and the amount of the base necessary for a large scale preparation of interesting salts was high.

The synthesis of the *N*-phenylbiguanide was carried out in two steps according to the method described by Cohn [84], using the findings of Guo et al. [85] (see Scheme 1).

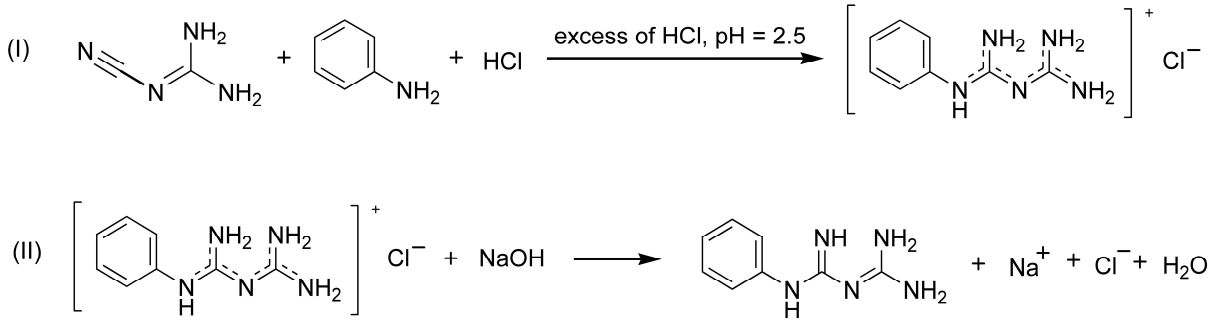


Scheme 1: Synthesis of the *N*-phenylbiguanide

During the study of substituted phenylbiguanides, also two salts of an interesting heterocyclic compound, the 2,4-diaminoquinazoline, were prepared. This digression from the main topic of the work is described in a publication in Appendix X.

#### 2.1.2 ***N,N-dimethylbiguanide***

The *N*,*N*-dimethylbiguanide was commercially available in form of a hydrochloride. The free base was released by an exchange reaction on an anex. Salts were prepared by neutralization of the base with the aqueous solution of a stoichiometric amount of a corresponding acid.

#### 2.1.3 ***N-carbamoylguanidine (guanylurea)***

Salts of the guanylurea with strong acids were prepared in analogy with the method described by Ostrogovich [80] from the dicyandiamide and a corresponding acid (according to the Scheme 2). Salts of the guanylurea with weak acids were prepared in two

steps. The first was a release of the guanylurea(1+) hydroxide by an exchange reaction on an anex from a guanylurea(1+) chloride prepared by the former method. The second step was the neutralization of the hydroxide with the aqueous solution of a stoichiometric amount of a corresponding acid.

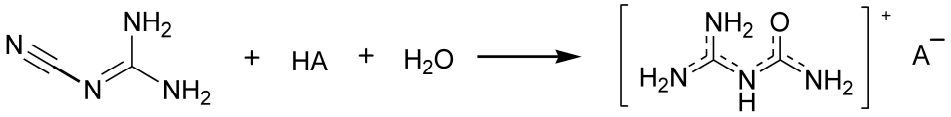


Scheme 2: Synthesis of guanylurea(1+) salts

### 2.1.4 *N,N′,N″-triphenylguanidine*

Salts of the *N*,*N*′,*N*″-triphenylguanidine were prepared directly from the commercially available base suspended in water and the stoichiometric amount of the aqueous solution of the corresponding acid. The free base was almost insoluble in water, but its protonized form was much more soluble and the salts crystallized from the dilute aqueous solutions.

In some salts, an alternative method of preparation was also applied, consisting in dissolution of the base in a small amount of acetone, followed by addition of the aqueous solution of the corresponding acid.

### 2.1.5 *Systematic preparation of salts*

The systems for crystallization of the salts were prepared in stoichiometries corresponding to all of the considerable simple molar ratios of the cations and anions in the product. *E.g.*, for reaction of a base capable of a (1+) or a (2+) charge with the phosphoric acid, both protonizations of the bases and formation of all possible (hydrogen) phosphates were considered, leading to testing of the stoichiometries (3:1), (2:1), (3:2), (1:1), and (1:2).

The general way of preparation of the crystallization solutions was dissolution (or suspension) of the solid base in water in the weight ratio (1:10) (or dissolution of the liquid base so that a similar concentration was reached) and addition of the 1 M aqueous solution of the respective acid, or the 0.4 M solution in case of less soluble acids (tartaric and oxalic acid, amidosulphuric acid) to the reaction mixture. The only exception were the salts of guanylurea and strong acids that were prepared *in situ* from dicyandiamide (Scheme 2).

The crystallizations were carried out in a desiccator over NaOH. In case that the product did not form crystals suitable for the X-ray structure analysis, efforts were given to recrystallize it from water or alcohols. All deviations from this general strategy are mentioned in the descriptions of preparation of a particular compound.

## 2.2 **Methods of characterization**

### 2.2.1 ***X-ray structure determination and X-ray powder diffraction***

Collection of the X-ray structural data was performed on a Nonius Kappa CCD diffractometer ($MoK_\alpha$ radiation, graphite monochromator). The phase problem was mostly solved by direct methods in implementation of SIR-92 [115] and the non-hydrogen atoms were refined anisotropically, using the full-matrix least-squares procedure taken from SHELXL-97 [116]. The positions of the hydrogen atoms were localised on difference Fourier maps and refined isotropically. (All differences from this procedure will be mentioned with the concrete structures.)

Crystallographic data of the new structures have been deposited with the Cambridge Crystallographic Data Centre as supplementary publications. A copy of the data can be obtained free of charge on application to CCDC, 12 Union Road, Cambridge CG21, EZ, UK (fax: +44 1223 336 033; e-mail: deposit@ccdc.cam.ac.uk) or *via* www.ccdc.cam.ac.uk.

The powder X-ray patterns were recorded at ambient temperature using a diffractometer Phillips X-pert with Cu $K_\alpha$-radiation. In order to confirm the identity of the bulk sample with a representative monocrystal selected for the X-ray structure determination, a recorded powder pattern was compared to the pattern simulated from the structural data by the programme Platon [117] in application SimPowder.

### 2.2.2 ***Vibrational spectra***

The IR spectra were recorded using nujol and fluorolube mull (AgCl windows – MID IR region, PE windows – FAR IR region) techniques (or alternatively using DRIFTS technique for MID IR) on a Nicolet 6700 FTIR spectrometer with 2 $cm^{-1}$ resolution and Happ-Genzel apodization in the 50 - 4000 $cm^{-1}$ region.

The Raman spectra of polycrystalline samples were recorded on a Nicolet 6700 FTIR spectrometer equipped with the Nicolet Nexus FT Raman module (2 $cm^{-1}$ resolution,

Happ-Genzel apodization, 1064 nm Nd:$YVO_4$ laser excitation, 200 mW power at the sample) in the 100–3700 $cm^{-1}$ region.

### 2.2.3 *UV-Vis-NIR*

The UV–Vis–NIR spectra of the diluted aqueous solutions of samples were recorded in the 190–1100 nm range using an Unicam UV 300 spectrometer.

### 2.2.4 *Thermal behaviour*

The melting points of the studied compounds were determined on a Büchi Melting Point B-540 device calibrated on two standards.

The difference scanning calorimetry (DSC) measurements were carried out on a Perkin Elmer Pyris Diamond DSC and DSC 7 instruments in the temperature region between 93 K and the melting point of the given compound (nitrogen and helium atmospheres above and below 298 K respectively – 20 ml/min). A heating rate of 10 K/min was selected to measure approximately 20 mg of the finely ground sample placed in hermetically sealed aluminium pans.

### 2.2.5 *Quantum chemical computations*

The quantum chemical computations (Gaussian 09W program package [118]) were performed using the closed-shell restricted Density Functional Theory (B3LYP) method with 6-311G(d,p) or 6-311+G(d,p) basis set, applying tight convergence criteria and an ultrafine integration grid. The geometry optimization of the isolated cation was followed by vibrational frequency calculations using the same method and basis set, while also the static hyperpolarizability was calculated. The geometry parameters of the optimized geometry of the cation were compared with those determined by the X-ray structure analysis.

### 2.2.7 *SHG efficiency measurements on powdered samples*

Measurements of SHG efficiency at 800 nm were performed by the modified powder technique [25] with 80 fs laser pulses generated at an 82 MHz repetition rate by a Ti:sapphire laser (Tsunami, Spectra Physics) with a measurement of the back-scattered laser light intensity at 400 nm by a grating spectrograph with diode array (InstaSpec II,

Oriel). This particular wavelength was selected (instead of the historically used 1064 nm) because it is typically emitted by femtosecond laser systems that are commercially available nowadays (*i.e.* Ti:sapphire and fiber lasers). For quantitative determination of the SHG efficiency, the intensity of the back-scattered laser light at 400 nm generated in the sample was measured by a grating spectrograph with diode array (InstaSpec II, Oriel) and the signal was compared with that generated in urea or KDP ($KH_2PO_4$). As a first approach, the relative efficiency of SHG was determined for the fraction of a powdered sample of 100–150 mm particle size loaded into 5 mm glass cells using a vibrator. To minimise the signal fluctuations induced by sample packing, the measurements were repeated on different areas of the same sample and the results were averaged.

Because the SHG efficiency of powders strongly depends on the particle size, the measurement of phase-matching curve was also performed for the most promising samples. The experiment was carried out for samples sieved into distinct particle size ranges: 25–45, 45–63, 63–75, 75–100, 100–125 and 125–150 mm.

### 2.3 **List of chemicals**

dicyandiamide, 99%, Sigma-Aldrich
aniline, 99%, Sigma-Aldrich
*N*-phenylbiguanide, 98%, Sigma-Aldrich
*N*,*N*′,*N*″-triphenylguanidine, 97,5%, Lach-Ner
*N*,*N*-dimethylbiguanidium(1+) hydrochloride 97%, Sigma-Aldrich
sulphuric acid, 96%, p.a., Lach-Ner
amidosulphuric acid, p.a., Chemapol
phosphorous acid, 99%, Sigma-Aldrich
phosphoric acid, >85%, Chemapol
nitric acid, 65%, p.a., Lachema
hydrochloric acid, 35%, p.a., Lach-Ner
boric acid, p.a., Lachema
tetrafluoroboric acid, 48 wt. % in $H_2O$, Sigma-Aldrich
oxalic acid, p.a., Lachema
formic acid, 87%, Lachema
acetic acid, 99%, Lachema
L-(+)-tartaric acid, p.a., Lachema
sodium hydroxide, pure, Lach-Ner
acetone, p.a., Penta
ethanol, 96%, denaturized with n-hexane, Penta
methanol, p.a., Lach-Ner
argon, 99,998%, Linde
anex Dowex Serva, type 2X8, mesh 20-50, ion exchange $OH^-/Cl^-$, Entwicklungslabor Heidelberg, Germany

## 3. RESULTS AND DISCUSSION

### 3.1 *N*-phenylbiguanide

The *N*-phenylbiguanide appears in the salts deposited in the CSD only as a (1+) charged cation. Still there was a nitrate studied by Matulková [76] found to be **phbigua**(2+), but unfortunately its structure could not be determined. As both **phbigua**(1+) and **phbigua**(2+) exhibit a remarkable hyperpolarizability (Table 2), efforts were given to prepare new salts out of them.

There are three *N*-phenylbiguanide salts to be described in this work: an amidosulphate, a carbonate and a **phbigua(2+)** sulphate dihydrate (Table 7). The **phbigua**(1+) amidosulphate (**phbiguaAMS**) was prepared by neutralization of the stoichiometric amount of **phbigua** with the 0.8 M aqueous solution of amidosulphuric acid. The **phbigua**(1+) hydrogen carbonate (**phbiguaHCO$_3$**) crystallized as a by-product in the solution of the amidosulphate during the recrystallization due to the reaction with the atmospheric $CO_2$.

The **phbigua**(2+) sulphate dihydrate (**phbiguaSO$_4$**) was prepared together with the already known **phbigua**(1+) sulphate [76] by neutralization of the free base with the 2 M aqueous solution of sulphuric acid. The much more soluble salt of the (2+) charged cation was easily separated by rinsing the product with a surplus of water and recrystallized. Noticeable is the spontaneous growth of large monocrystals of **phbigua(2+)** sulphate dihydrate from the diluted aqueous solutions and the stability of the compound – it is stable on air and non-hygroscopic. Efforts were given to synthesize the **phbigua** sulphates by the modification of the Cohn's method (Scheme 1) with the direct use of the sulphuric acid as an acidifier, but the product was contamined by guanylurea occuring in a concurrent reaction [85] and this method was given up.

Table 7: New salts of **phbigua**

| Abbreviation | Chemical name | Crystal system | Space group | Z | R factor (Temperature) | CCDC No./Code |
|---|---|---|---|---|---|---|
| **phbiguaHCO$_3$** | *N*-phenylbiguanidium(1+) hydrogen carbonate | monoclinic | $P2_1/c$ | 4 | 0.0383 (150 K) | 880720 |
| **phbiguaAMS** | *N*-phenylbiguanidium(1+) amidosulphate | monoclinic | *P*n | 4 | 0.0499 (150 K) | 880719 |
| **phbiguaSO$_4$** | *N*-phenylbiguanidium(2+) sulphate dihydrate | orthorhombic | *F*dd2 | 16 | 0.0270 (150 K) | 880721 |

The amidosulphate and the carbonate are presented in this chapter. The more detailed description of the **phbiguaSO$_4$**, the first ever described structure containing **phbigua(2+)**, is also in the article [83].

### 3.1.1 *The structure of new phbigua salts*

For the general atom numbering of the **phbigua**(1+) cation see Fig. 6. The **phbiguaHCO$_3$** crystallizes in a the $P2_1/c$ space group. The main feature of its structure are the layers parallel to the *bc* plane (Fig. 7). They are formed by hydrogen-bonded anions and cations that alternate regularly. The chains formed can be described by a graph set descriptor C(8) and the chains within a given layer are interconnected so that the large hydrogen-bonded rings $R_4^2(16)$ are formed (Fig. 8). Actually, only the biguanide parts of the cations are involved in the system of hydrogen bonds in these layers, while the phenyl rings stick out facing the phenyl rings pertinent to the neighbouring layer. There are two different orientations of the phenyl rings offset by 60°. No evidence of a π-π interaction between the phenyl rings was found.

The almost planar hydrogen carbonate anion acts as a H-bond acceptor in hydrogen bonds of N-H...O type [2.806(1) – 2.878(2) Å]. The only exception is the O-H...N3 bond [2.794(1) Å]. The **phbigua**(1+) cation contains two intramolecular hydrogen bonds of N-H...N type [both 2.849(1) Å]. There are no hydrogen bonds interconnecting the neighbouring hydrogen-bonded layers.

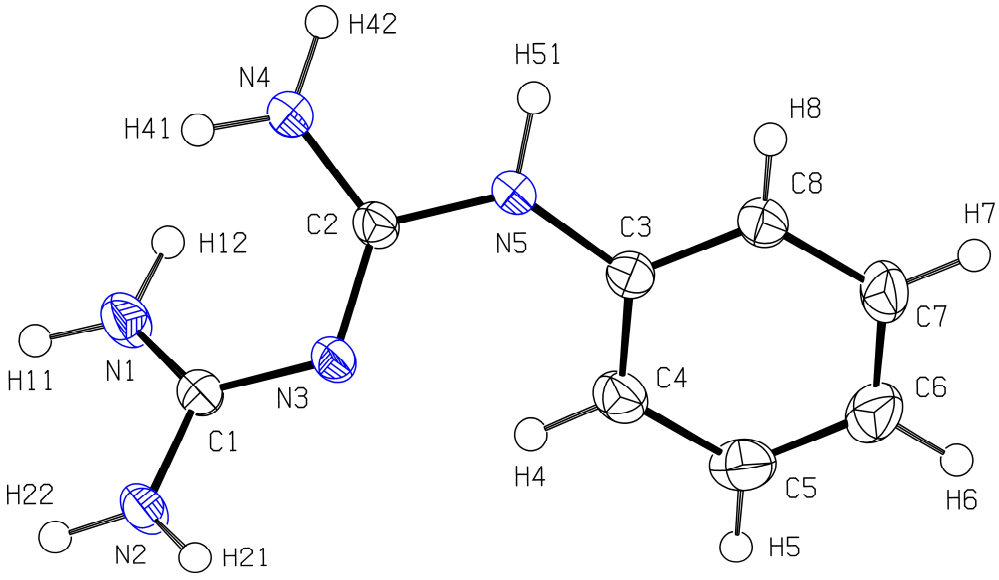


Fig. 6 Numbering of the **phbigua**(1+) cation in **phbiguaHCO$_3$**. The displacement parameters are drawn at the 50% probability level

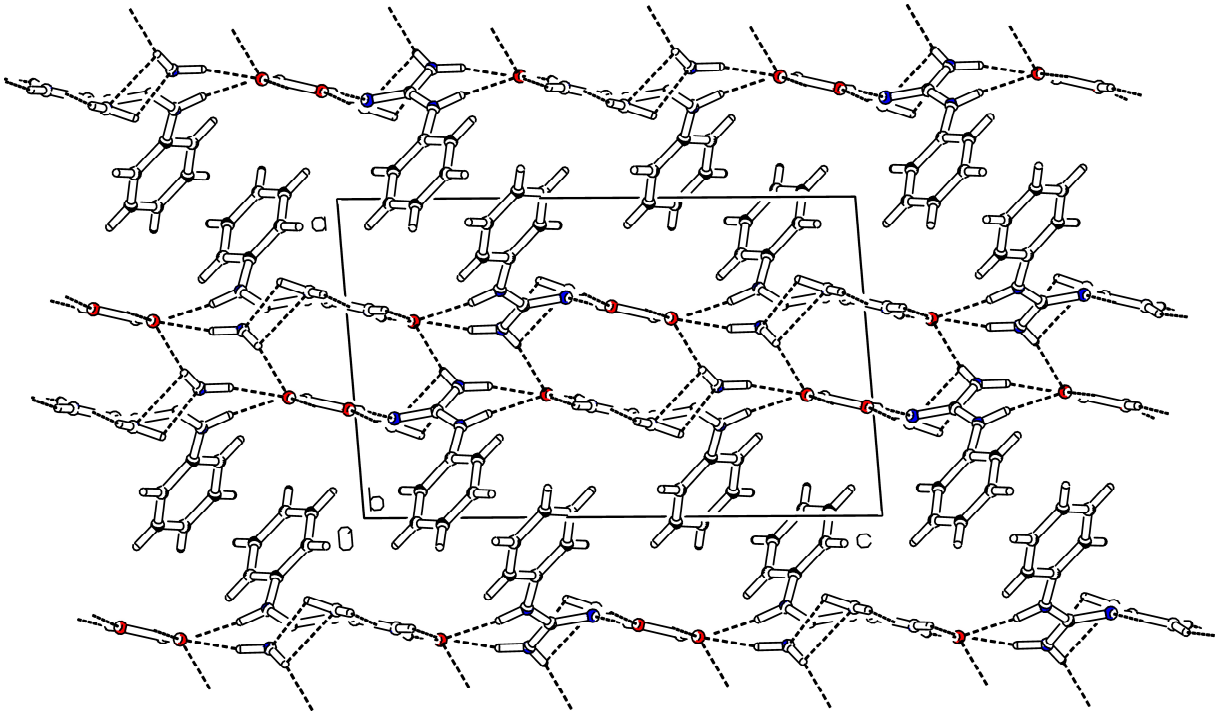


Fig. 7 The packing of the **phbiguaHCO$_3$** structure viewed down the *b* axial direction of the unit cell, hydrogen bonds symbolized by dashes. The oxygen atoms are symbolized by red circles, nitrogen blue, carbon black and hydrogen atoms are colourless.

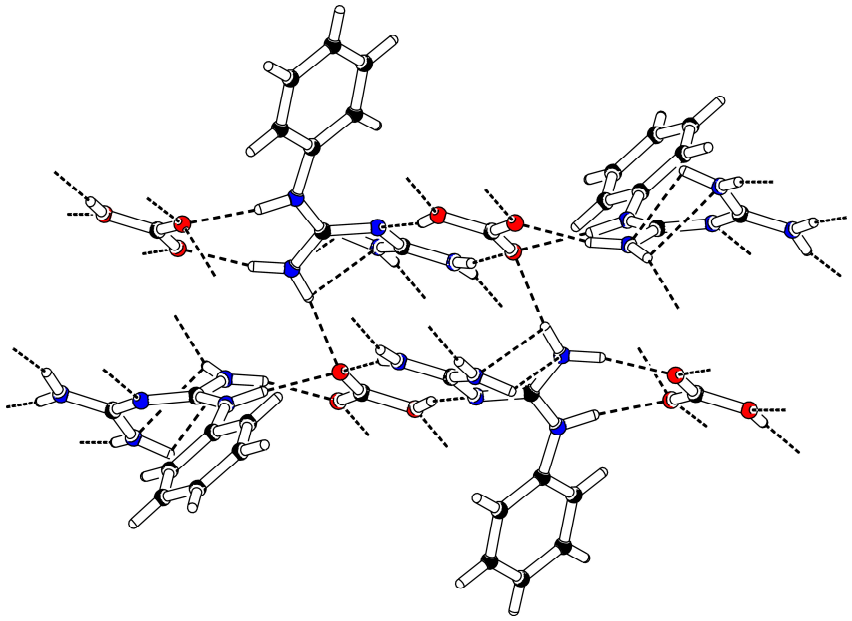

Fig. 8 The detail of the centrosymmetric **phbiguaHCO$_3$** packing. The cations and anions alternate regularly, cationic phenyl rings occur in two positions offset by 60°. A detail of the hydrogen-bonded ring $R_4^2(16)$ can be seen in the centre. The oxygen atoms are symbolized by red circles, nitrogen blue, carbon black and hydrogen atoms are colourless.

The **phbiguaAMS** crystallizes as needle-shaped colourless crystals in the noncentrosymmetric *P*n space group. The unit cell of the **phbiguaAMS** consists of two **phbigua**(1+) cations and two amidosulphate anions. Although the amidosulphate anion is not planar, the regularly alternating anions and cations form layers so that the cationic phenyl rings stick to the space between the layers similarly as in **phbiguaHCO$_3$**. In **phbiguaAMS**, these layers are parallel to the *ab* plane (Fig. 9) and their main building blocks are anionic chains corresponding to the graph set descriptor C(4). The attachment of the cations to this chain can be described by the $R_3^3(10)$ graph set descriptors. The neighbouring phenyl rings are not parallel and there is no evidence of any π-π interactions between the rings.

Functioning the amidosulphate anions as H-bond donors and H-bond acceptors, they are involved in following hydrogen bonds: the anion-anion interactions of N-H...O type [2.961(5) –2.981(4) Å], the numerous cation-anion hydrogen bonds of N-H...O type [2.817(4) – 3.221(4) Å] and also in interactions of N-H...N type with the anion in the H-bond acceptor [3.035(4) – 3.174(5) Å] or the H-bond donor [3.466(5) Å] role.

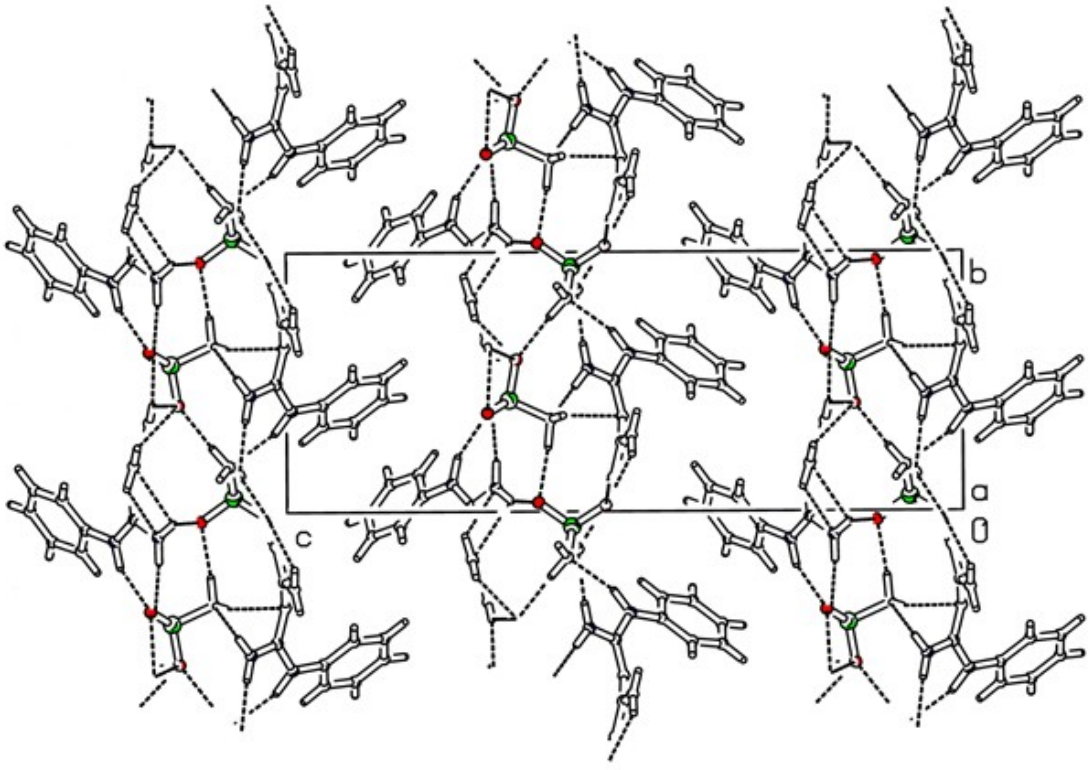


Fig. 9 The packing of the **phbiguaAMS** structure viewed down the *a* axial direction of the unit cell, hydrogen bonds symbolized by dashes. The oxygen atoms are symbolized by red circles, nitrogen blue, carbon black, atoms of sulphur are green and hydrogens are colourless.

The **phbiguaSO$_4$** crystallizes in form of colourless bars in the orthorhombic system in the *F*dd2 space group. The unit cell of **phbiguaSO$_4$** consists of one **phbigua**(2+) cation, one sulphate anion and two water molecules of solvation. The anions and the biguanide parts of the cations together form a sligtly waved layers parallel to the *ac* plane, while the phenyl rings stick out to the space between the layers. These layers are interconnected by the hydrogen-bonded water molecules. Moreover, there are spiral-like hydrogen bonded chains interconnecting the neighbouring cations in the direction of the *c* axis that can be described by a graph set descriptor C(4). The neighbouring cationic phenyl rings occur in two orientations offset by 75° and there is no evidence of a π-π interaction between them.

The **phbigua**(2+) cations are attached to the sulphate anions, the pure H-bond acceptors, by the N-H...O hydrogen bonds ranging from 2.647(2) Å to 2.900(2) Å. The cation – water interactions are also of the N-H...O type [2.771(2) – 3.027(2) Å]. Actually, every hydrogen atom of the biguanide part of the cation is involved in a hydrogen bond. The rich system of the hydrogen bonds pertinent to a **phbigua**(2+) cation is depicted in Fig. 10. There are also several water – anion interactions of the O-H...O type [2.755(2) – 3.061(2) Å].

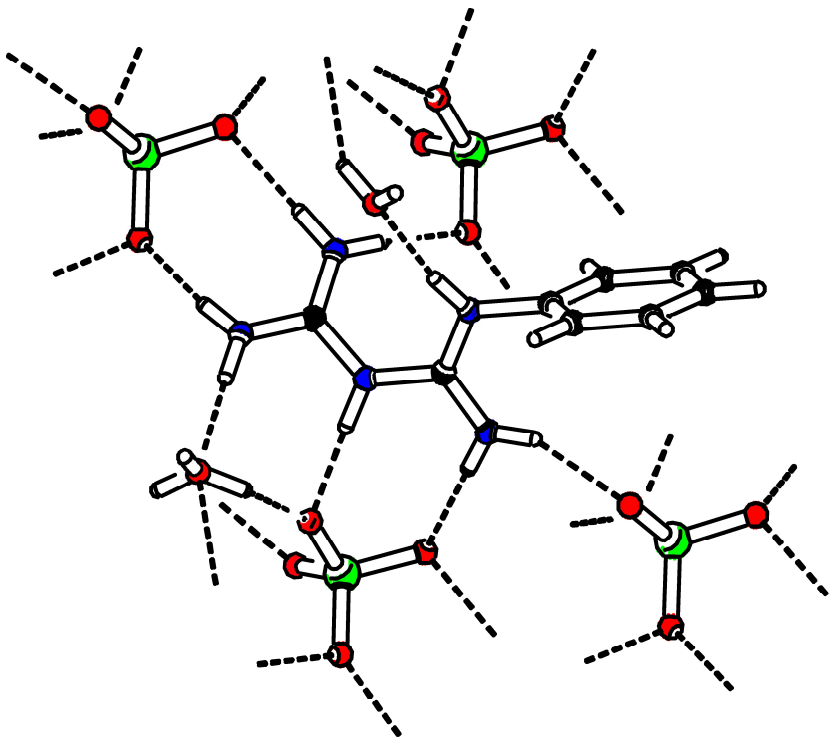

Fig. 10 The system of hydrogen bonds surrounding a **phbigua**(2+) cation in the **phbiguaSO$_4$** structure. The oxygen atoms are symbolized by red circles, nitrogen blue, carbon black, sulphur green and hydrogen atoms are colourless.

3.1.2 ***Vibrational spectra of new phbigua salts***

As the vibrational spectra of both **phbigua**(1+) and **phbigua**(2+) have been already interpreted in detail elsewhere [76, 83] including the detailed study of the **phbiguaSO$_4$** spectra [83], the recorded spectra of **phbiguaAMS** and **phbiguaHCO$_3$** are presented here only as a peaklist:

**phbiguaAMS**

IR spectrum: 495 m, 520 w, 526 w, 557 m, 590 m, 612 sh, 627 w, 696 w, 721 w, 738 w, 759 w, 791 w, 843 w, 901 w, 922 w, 965 w, 1002 w, 1045 m, 1086 m, 1110 m, 1173 m, 1193 sh, 1240 m, 1291 w, 1308 w, 1378 m, 1453 m, 1497 m, 1506 m, 1534 s, 1539 s, 1547 s, 1559 sh, 1584 m, 1604 m, 1621 sh, 1636 s, 1653 s, 1660 m, 3039 w, 3064 w, 3214 m, 3327 s, 3358 m, 3384 m, 3439 m

Raman spectrum: 208 w, 267 m, 340 w, 374 w, 393 w, 411 w, 498 w, 534 w, 555 w, 587 w, 615 w, 628 w, 680 w, 704 w, 719 w, 742 w, 966 w, 841 m, 900 w, 923 m, 963 w, 981 w, 1002 vs, 1030 m, 1047 s, 1086 w, 1165 w,1184 w, 1250 sh, 1258 m, 1295 m, 1308 sh, 1335 w, 1395 w, 1458 w, 1499 w, 1549 m, 1587 sh, 1604 s, 1624 m, 2989 w, 3040 w, 3065 m, 3204 w, 3360 w, 3437 w

**phbiguaHCO$_3$**

IR spectrum: 401 w, 411 w, 418 w, 444 m, 504 m, 545 m, 563 w, 587 w, 596 w, 630 w, 640 w, 672 m, 690 m, 751 m, 842 w, 856 m, 904 w, 941 w, 968 w, 997 w, 1014 w, 1028 w, 1045 w, 1149 w, 1176 w, 1198 w, 1256 m, 1305 m, 1345 m, 1404 m, 1453 s, 1487 s, 1497 s, 1529 m, 1560 m, 1577 m, 1601 m, 1648 m, 1656 m, 1667 m, 1702 w, 1926 w, 1972 w, 2142 w, 2573 w, 2727 m, 3014 m, 3217 s, 3293 s, 3467 m

Raman spectrum: 211 w, 249 w, 301 w, 325 w, 401 w, 413 w, 439 w, 505 w, 547 w, 614 w, 637 w, 683 w, 725 w, 749 w, 841 w, 867 w, 941 m, 999 s, 1015 m, 1029 m, 1048 w, 1068 w, 1091 w, 1159 w, 1178 m, 1200 w, 1257 m, 1301 s, 1343 w, 1454 w, 1488 w, 1502 w, 1531 w, 1557 m, 1603 vs, 1657 w, 2564 w, 3068 m, 3222 w, 3301 w, 3469 w

3.1.3 ***Second harmonic generation of selected new phbigua salts***

As two of the novel **phbigua** salts possess the noncentrosymmetric assembly, they were examined for the second harmonic generation. In the preliminary experiment with the powderized samples the **phbiguaAMS** and the **phbiguaSO$_4$** exhibited the SHG efficiency 10 times lower and 1.4 times higher than KDP, respectively. In order to determine whether the compounds can fulfill the condition for phase matching, both of them were subjected also to the measurements of the SHG efficiency in samples of a different particle size. The compounds were sieved so that the samples of distinct

particle size ranges (0-25, 25-45, 45-63, 63-75, 75-100, 100-125, 125-150 μm) were obtained. In case of the **phbiguaAMS** the smallest fraction could not be obtained as the fine powder was slightly hygroscopic. The phase-matching curves of the **phbiguaAMS** and the **phbiguaSO$_4$** are displayed at Fig. 11 and 11 respectively. None of the samples exhibited any signs of laser damage after the exposition.

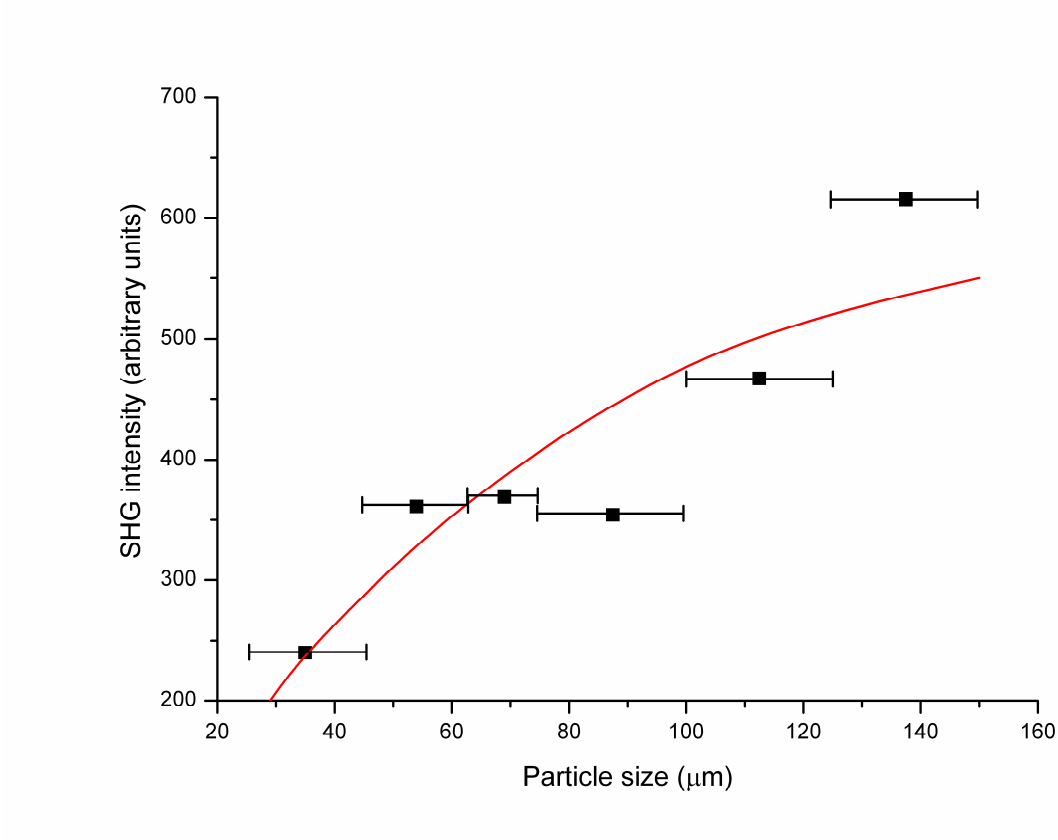


Fig. 11 The phase-matching graph of the **phbiguaAMS** (*i.e.* particle size *vs.* SHG intensity, 800 nm wavelength). The curve drawn is to guide the eye and is not a fit to the data.

The course of the **phbiguaAMS** curve indicates that the **phbiguaAMS** is a phase-matchable compound. On the contrary, interpretation of the results of the phase-matching experiments with **phbiguaSO$_4$** is more complicated. Although the observation that the SHG intensities increase in the mid-sized samples and decrease again in the samples with larger particles suggests that this compound might be a non phase-matchable one (Fig. 12), it is necessary to discuss the issue in more detail and to consider also the less obvious things. Firstly, the typical course pertinent to a non phase-matchable compound reaches its maximum of the SHG intensity very steeply at much smaller particle size than it was reached in this case and it also decreases very steeply in a relatively narrow interval of particle sizes before the slowly decreasing segment of the course is reached. Secondly, the values of the SHG intensity of the samples with the larger particle sizes can be strongly

underestimated as the number of the crystallites hit by the laser beam at once within the particular measurement necessarily decreases while the fraction of the favourably oriented ones, *i.e.* those capable of the phase-matching at the moment, stays constant. As the diameter of the laser beam in our experiment assembly can be rougly estimated to be about 300 nm, this problem becomes real and its effects have already been observed in a much more moderate intensity, *e.g.* in case of the **GUHP** (see Appendix II).

Considering this all, it can be hypothesized that the **phbiguaSO$_4$** is still a phase-matchable compound. In order to decide it definitely, several experiments with systematic search for the phase-matching angle with the cuts of the **phbiguaSO$_4$** single crystals were carried out, but the effect was not found. As the experimental assembly covered only a limited range of angles, such result did not enlighten the problem and the final decision about the **phbiguaSO$_4$** ability to fulfil the phase-matching condition could not be done.

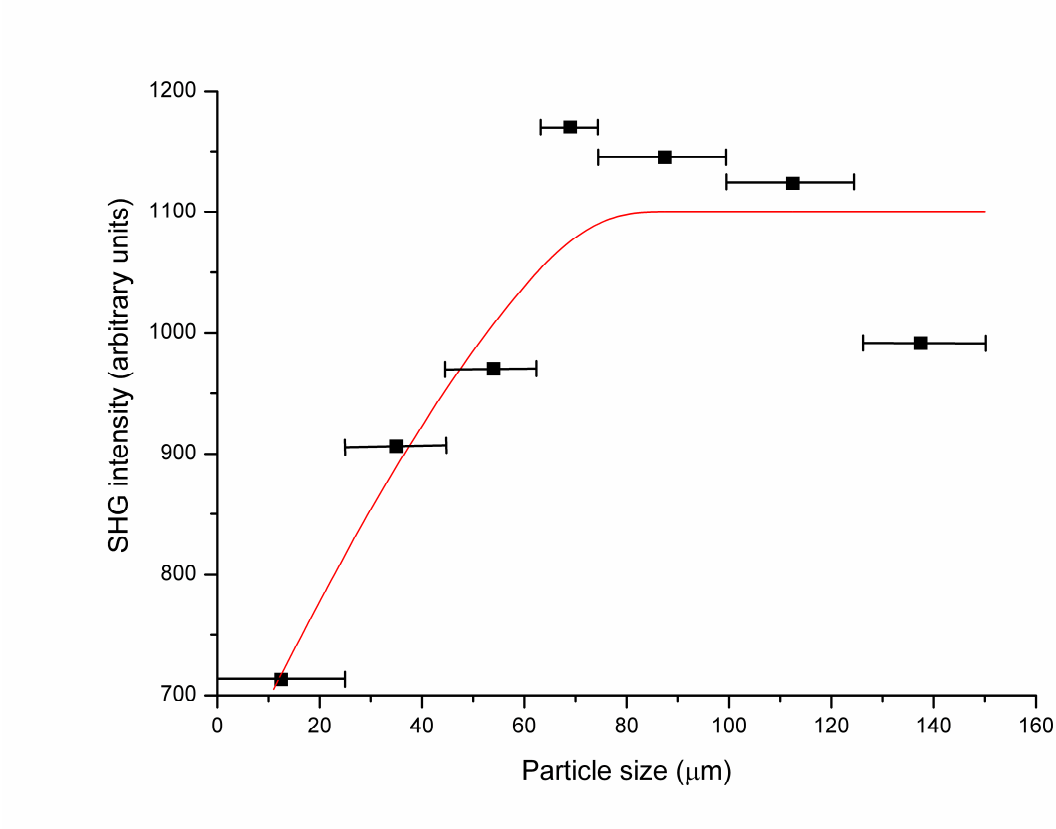


Fig. 12 The phase-matching graph of the **phbiguaSO$_4$** (*i.e.* particle size *vs.* SHG intensity, 800 nm wavelength). The curve drawn is to guide the eye and is it not a fit to the data.

### 3.1.4 *Thermal behaviour of the promising phbigua salts*

The **phbiguaAMS** is stable in air up to its melting point at 409 K. The **phbiguaSO$_4$** (melting point 429 K) exhibits a reproducible reversible anomaly both on heating (151 K) and cooling (130 K) runs with enthalpy of the transition equal to 3.0 J/g. According to the large hysteresis, this transition was identified as a first order transition.

3.1.5 ***Material properties of the promising phbigua salts***

The **phbiguaAMS** powder is quite stable and it is transparent in the interval 320 nm – 2.78 μm, but even the small crystals (with dimensions of a few mm) mostly occur in a poor quality or break spontaneously into pieces with time. Unfortunately, there were no larger crystals prepared at all. According to this and to the quite low SHG efficiency, the **phbiguaAMS** cannot be considered promising for the deeper material study.

On the other hand, the **phbigua$SO_4$** crystallizes spontaneously from its dilute aqueous solutions. Its rod like crystals in Fig. 13 crystallized spontaneously from 1.5 liter of its solution within a month. They are extremely stable in air and non-hygroscopic (there was no change observed even after a 14-month-long exposition of an uncovered crystal to the daylight including direct sunshine and the atmospheric humidity). Unfortunately, another issue greatly limits their usability for NLO. As it can be seen at the right photograph on Fig. 13, the crystals seem to have stripes on their surface. Actually these are not stripes but parallel layers appearing as deffects in the entire crystal. It can be hypothesized that these inhomogenities are formed as a result of a local loss of the water molecules of solvation [119]. Although the condition of the crystal stays constant (these deffects appear immediately after the removal of the crystals from their solution and do not worsen with time), although the material does not break along the layers and the transparency in the direction perpendicular to the layers is not tangled, either a formation of such layers presents a serious problem for a material which was intended for optical applications. The **phbigua$SO_4$** is practically transparent in the interval 320 nm to 2.78 μm. Unfortunately, the occurence of the layered deffects disqualifies it from the further NLO materials research.

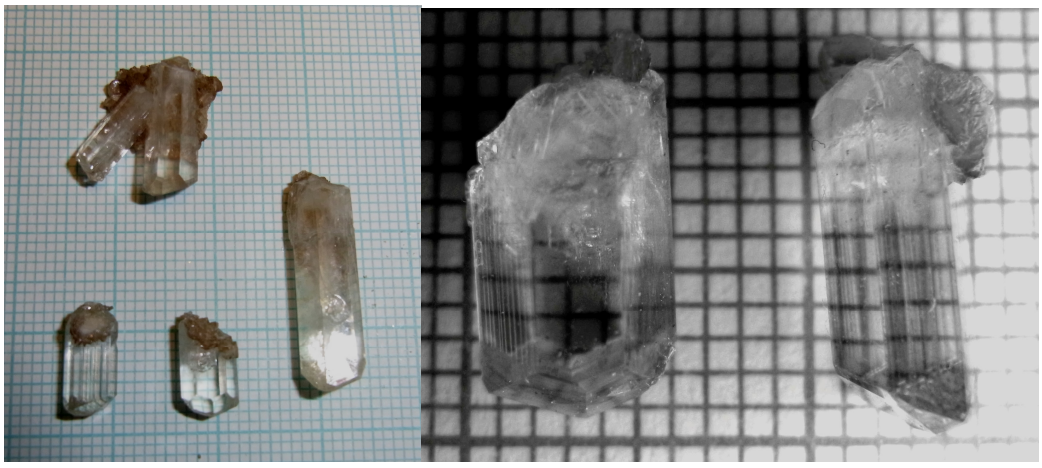

Fig. 13 The spontaneously grown crystals of **phbiguaSO4**

### 3.2 *N*,*N*-dimethylbiguanide

The (1+) and (2+) charged cations of the *N*,*N*-dimethylbiguanide (**dmbg**) exhibit a remarkable hyperpolarizability (Table 2). Although all of the previously published salts were centrosymmetric, both cationic forms possess a reasonable hyperpolarizability and so efforts were given to prepare novel **dmbg** compounds in the framework of this thesis. Unfortunately, there was only one coumpound, a nitrate, obtained as a solid phase and therefore capable of a reasonable characterization. A crystal suitable for the structure determination was first obtained after two years of crystallization of its aqueous solution.

The *N*,*N*-dimethylbiguanidium(2+) nitrate (**dmbgNO$_3$**) crystallized from the mixture of the aqueous solution of the free **dmbg** base and the stoichiometric amount of the nitric acid in the centrosymmetric assembly in the $P2_1/c$ space group. This compound is further described in a publication in Appendix I.

### 3.3 *N*-Carbamoylguanidine (guanylurea)

The guanylurea appears in the CSD mostly as a 1+ charged cation (23 structures) or in the uncharged form (2 structures). All the known guanylurea(1+) structures can be roughly divided into two groups: the simple **gu**(1+) salts and the complex compounds. In all of them, the guanylurea appears in the practically planar conformation and exhibits the so-called Y-aromaticity. Similarly to the real structures, the planar conformation of **gu**(1+) with bond lenghts corresponding to the π electrons delocalization was obtained also by the computational geometry optimization (Fig. 14; Gaussian 09W, closed shell restricted B3LYP method with 6-311G(d,p) basis set, details in Appendix II).

Comparison of bond lengths and torsion angles of **gu**(1+) in all of the known salts structures, where the guanylurea often assists the formation of a layered structure, is given in Tables 8 and 9 together with the same data pertinent to the uncharged **gu** in an adduct with ethanole. The most noticeable difference between the uncharged **gu** and its cation is that the N3 of **gu** acts as a hydrogen bond acceptor in the O-H...N interaction, while the N3-H3 in the **gu**(1+) takes part in the hydrogen bonds in role of a H-bond donor, forming often N-H...O bonds, or, rarely, also N-H...Cl bonds (CCDC code JODZOR, Table 5). The most distorted **gu**(1+) cations are present in a dicyanamide and in a chloride (CCDC codes DAWDAH and AGUSAX, respectively; Table 5).

Table 8. Bond lengths of guanylurea moieties in selected structures. For compounds with multiple guanylurea(1+) cations in the asymmetric unit, the bond lengths of all of them are listed.

| CCDC code | Space group | Abbreviation | C1-N1 | C1-N2 | C1-N3 | C2-N3 | C2-N4 | C2-O1 |
|---|---|---|---|---|---|---|---|---|
| DIVVAF | $P2_12_12_1$ | gu(0).EtOH | 1.339(4) | 1.324(4) | 1.347(4) | 1.355(4) | 1.358(4) | 1.252(4) |
| AGUSEB | $P2_1/c$ | $guN_3.H_2O$ | 1.319(1) | 1.314(2) | 1.361(1) | 1.401(1) | 1.333(2) | 1.228(1) |
| - - - | $P2_1/c$ | $guBF_4$ | 1.316(1) | 1.311(1) | 1.363(1) | 1.394(1) | 1.331(2) | 1.229(1) |
| AGUSAX | $P2_1/c$ | guCl | 1.324(2) | 1.313(2) | 1.357(2) | 1.398(2) | 1.331(2) | 1.235(2) |
| JODZOR | $P2_1/n$ | $guCl.1/2H_2O$ | 1.322(3) | 1.313(3) | 1.356(3) | 1.395(3) | 1.326(3) | 1.221(3) |
| | | | 1.318(2) | 1.304(3) | 1.356(3) | 1.394(2) | 1.319(3) | 1.225(3) |
| DAWDAH | $C2/c$ | $guC_2N_3$ | 1.324(2) | 1.314(2) | 1.363(2) | 1.404(2) | 1.333(2) | 1.227(2) |
| QIRGIH | $Pna2_1$ | $guN_3O_4$ | 1.331(2) | 1.323(2) | 1.371(2) | 1.415(2) | 1.336(2) | 1.236(2) |
| CUYZEC | $Cc$ | $guH_2PO_3$ | 1.318(3) | 1.313(3) | 1.355(3) | 1.395(2) | 1.328(3) | 1.226(3) |
| GADQAE | $P2_1/c$ | $gu(CH_3HPO_3).H_2O$ | 1.309(3) | 1.319(3) | 1.349(3) | 1.402(3) | 1.324(3) | 1.224(3) |
| DUNHID | $P$-1 | $guH_2PO_4$ | 1.320(1) | 1.320(1) | 1.358(1) | 1.399(1) | 1.329(1) | 1.217(1) |
| EKIBAB | $P$-1 | $guHSeO_3$ | 1.323(3) | 1.308(3) | 1.359(3) | 1.396(3) | 1.328(3) | 1.227(3) |
| DIVVEJ01 | $P2_1/c$ | $guClO_4$ | 1.319(2) | 1.318(2) | 1.357(2) | 1.398(2) | 1.330(2) | 1.233(2) |
| NOJKIH | $P$-1 | $guHSO_4$ | 1.322(2) | 1.315(2) | 1.367(2) | 1.406(2) | 1.355(2) | 1.227(2) |
| - - - | $P$-1 | $gu_2SO_4.2H_2O$ | 1.313(2) | 1.322(2) | 1.364(2) | 1.397(2) | 1.345(2) | 1.222(2) |
| | | | 1.312(2) | 1.318(2) | 1.367(2) | 1.399(2) | 1.331(2) | 1.232(2) |
| - - - | $P$-1 | $gu_4(HSO_4)_2SO_4$ | 1.313(2) | 1.321(2) | 1.360(2) | 1.402(2) | 1.327(2) | 1.228(2) |
| | | | 1.314(2) | 1.325(2) | 1.361(2) | 1.403(2) | 1.330(2) | 1.230(2) |
| | | | 1.317(2) | 1.321(2) | 1.356(2) | 1.406(2) | 1.327(2) | 1.230(2) |
| | | | 1.314(2) | 1.325(2) | 1.362(2) | 1.409(2) | 1.328(2) | 1.227(2) |
| NAZBOG | $C2/c$ | $gu_2SO_4.2H_2O$ | 1.323(2) | 1.312(2) | 1.358(2) | 1.403(2) | 1.334(2) | 1.220(2) |
| | | | 1.314(2) | 1.312(2) | 1.364(2) | 1.396(2) | 1.333(2) | 1.232(2) |
| | | | 1.323(2) | 1.305(2) | 1.367(2) | 1.394(2) | 1.329(2) | 1.228(2) |
| - - - | $P2_1/c$ | guHox | 1.319(2) | 1.311(2) | 1.369(1) | 1.393(1) | 1.336(2) | 1.230(1) |
| - - - | $P$-1 | $guan_2Cl_3$ | 1.321(2) | 1.312(2) | 1.361(2) | 1.396(2) | 1.336(2) | 1.227(2) |
| - - - | $Cc$ | $guHPO_3F$ | 1.324(7) | 1.301(7) | 1.348(7) | 1.396(7) | 1.325(7) | 1.229(7) |
| - - - | $Pnma$ | $gu_2PO_3F$ | 1.306(2) | 1.323(2) | 1.361(2) | 1.391(1) | 1.334(2) | 1.230(2) |
| - - - | $Pbca$ | $gu_2PO_3F$ | 1.305(9) | 1.318(8) | 1.370(7) | 1.414(8) | 1.322(9) | 1.221(8) |
| | | | 1.301(9) | 1.312(7) | 1.386(6) | 1.384(8) | 1.330(8) | 1.236(8) |
| - - - | $P1$ | $gu_2(HPO_3F)(PO_3F)$ | 1.316(3) | 1.311(3) | 1.355(3) | 1.396(3) | 1.335(4) | 1.225(3) |
| | | | 1.310(3) | 1.304(3) | 1.359(3) | 1.390(3) | 1.329(3) | 1.218(3) |
| | | | 1.317(3) | 1.302(3) | 1.361(3) | 1.402(3) | 1.324(3) | 1.225(3) |
| AGUSIF | $P2_1$ | $guCH_2N_5$ | 1.314(2) | 1.318(2) | 1.359(2) | 1.391(2) | 1.343(2) | 1.227(2) |
| - - - | $P2_12_12_1$ | guHtart | 1.327(2) | 1.306(2) | 1.367(2) | 1.408(2) | 1.331(2) | 1.223(2) |

Table 9 Torsion angles of guanylurea moieties in selected structures. For compounds with multiple guanylurea(1+) cations in the asymmetric unit, the torsion angles of all of them are listed. All of the angles are listed in the absolute value.

| CCDC code | Space group | Abbreviation | N1-C1-N3-C2 | N2-C1-N3-C2 | O1-C2-N3-C1 | N4-C2-N3-C1 |
|---|---|---|---|---|---|---|
| DIVVAF | $P2_12_12_1$ | gu(0).EtOH | 177.5(3) | 3.7(5) | 6.6(4) | 176.3(3) |
| AGUSEB | $P2_1/c$ | $guN_3.H_2O$ | 176.5(1) | 4.4(2) | 2.4(2) | 178.4(1) |
| - - - | $P2_1/c$ | $guBF_4$ | 179.1(1) | 0.4(2) | 2.7(2) | 177.2(1) |
| AGUSAX | $P2_1/c$ | guCl | 178.8(1) | 0.6(2) | 15.2(2) | 166.3(1) |
| JODZOR | $P2_1/n$ | $guCl.1/2H_2O$ | 178.9(2) | 1.0(3) | 5.0(3) | 175.9(2) |
| | | | 178.9(2) | 1.2(3) | 0.3(3) | 179.7(2) |
| DAWDAH | $C2/c$ | $guC_2N_3$ | 169.6(1) | 13.3(2) | 10.5(2) | 169.8(1) |
| QIRGIH | $Pna2_1$ | $guN_3O_4$ | 178.2(5) | 1.8(8) | 2.9(8) | 177.8(5) |
| CUYZEC | $Cc$ | $guH_2PO_3$ | 178.7(2) | 0.7(3) | 7.6(3) | 172.6(2) |
| GADQAE | $P2_1/c$ | $gu(CH_3HPO_3).H_2O$ | 178.5(2) | 1.6(3) | 3.9(3) | 175.8(2) |
| DUNHID | $P$-1 | $guH_2PO_4$ | 179.6(2) | 1.3(2) | 4.8(2) | 175.0(2) |
| EKIBAB | $P$-1 | $guHSeO_3$ | 175.5(2) | 5.8(4) | 2.1(4) | 179.4(2) |
| DIVVEJ01 | $P2_1/c$ | $guClO_4$ | 179.2(2) | 0.7(3) | 3.7(2) | 176.3(2) |
| NOJKIH | $P$-1 | $guHSO_4$ | 178.1(2) | 1.8(2) | 1.3(2) | 178.0(2) |
| - - - | $P$-1 | $gu_2SO_4.2H_2O$ | 2.3(2) | 176.9(1) | 8.5(2) | 172.9(1) |
| | | | 1.3(2) | 178.9(1) | 2.3(2) | 178.6(1) |
| - - - | $P$-1 | $gu_4(HSO_4)_2SO_4$ | 7.3(2) | 172.2(1) | 1.4(2) | 177.8(1) |
| | | | 6.1(2) | 174.2(1) | 3.8(2) | 176.4(1) |
| | | | 4.6(2) | 174.9(1) | 9.0(2) | 171.1(1) |
| | | | 6.6(2) | 174.3(1) | 3.1(2) | 177.0(1) |
| NAZBOG | $C2/c$ | $gu_2SO_4.2H_2O$ | 179.1(2) | 0.9(2) | 3.4(2) | 177.4(2) |
| | | | 178.6(2) | 1.8(3) | 1.7(2) | 179.2(2) |
| | | | 175.2(2) | 5.3(2) | 1.1(3) | 178.7(2) |
| - - - | $P2_1/c$ | guHox | 175.7(1) | 4.2(2) | 0.7(2) | 178.9(1) |
| - - - | $P$-1 | $guan_2Cl_3$ | 175.8(1) | 3.7(2) | 2.6(2) | 177.6(1) |
| - - - | $Cc$ | $guHPO_3F$ | 175.2(4) | 5.9(8) | 11.2(8) | 170.1(5) |
| - - - | $Pnma$ | $gu_2PO_3F$ | 176.4(1) | 5.0(2) | 5.0(2) | 176.1(1) |
| - - - | $Pbca$ | $gu_2PO_3F$ | 179.1(7) | 2.9(9) | 0.3(9) | 179.3(8) |
| | | | 178.7(8) | 4.0(9) | 1.0(9) | 179.5(9) |
| - - - | $P1$ | $gu_2(HPO_3F)(PO_3F)$ | 178.2(2) | 3.2(3) | 1.7(3) | 179.8(2) |
| | | | 179.5(2) | 1.1(3) | 0.5(3) | 179.2(2) |
| | | | 179.1(2) | 0.9(3) | 1.3(3) | 179.7(2) |
| AGUSIF | $P2_1$ | $guCH_2N_5$ | 177.9(2) | 1.9(3) | 6.0(3) | 175.7(2) |
| | $P2_12_12_1$ | guHtart | 173.1(1) | 6.1(2) | 7.2(2) | 173.9(1) |

The new **gu** salts prepared in the framework of this thesis are listed in Table 10. Five of them are to be described in this text, namely two sulphates, a tartrate, an oxalate and a mixed chloride of **gu**(1+) and anilinium(1+), others have already been published and are presented in Appendices.

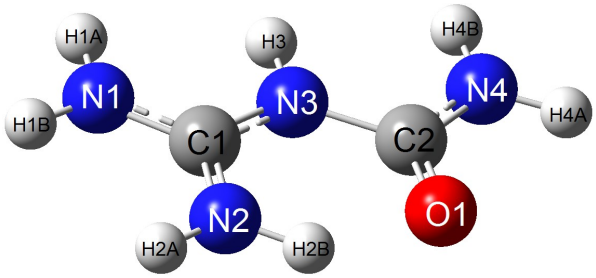


Fig. 14 The optimized geometry of guanylurea(1+) with atom numbering

Table 10: New salts of **guanylurea**

| Abbreviation | Chemical name | Crystal system | Space group | Z | R factor (Temp.) | CCDC No./Code |
|---|---|---|---|---|---|---|
| **$guBF_4$** | guanylurea(1+) tetrafluoroborate | monoclinic | $P2_1/c$ | 4 | 0.0242 120 K | |
| **$guH_2PO_3$ (GUHP)** | guanylurea(1+) hydrogen phosphite | monoclinic | $Cc$ | 4 | 0.0276 293 K | 752254 CUYZEC |
| **$gu_4(HSO_4)_2SO_4$** | guanylurea(1+) bis(hydrogen sulphate) sulphate | triclinic | $P$-1 | 4 | 0.0280 150 K | 880724 |
| **$gu_2SO_4$** | guanylurea(1+) sulphate dihydrate | triclinic | $P$-1 | 2 | 0.0339 150 K | 880723 |
| **guHtart** | guanylurea(1+) hydrogen L-tartrate | orthorhombic | $P2_12_12_1$ | 2 | 0.0256 150 K | 880722 |
| **guHox** | guanylurea(1+) oxalate monohydrate | monoclinic | $P2_1/c$ | 4 | 0.0256 120 K | |
| **$guan_2Cl_3$** | bis(anilinium(1+)) guanylurea(1+) chloride dihydrate | triclinic | $P$-1 | 2 | 0.0274 150 K | |
| **$guHPO_3F$** | guanylurea(1+) hydrogen flurophosphate | monoclinic | $Cc$ | 4 | 0.0491 120 K | |
| **$gu(HPO_3F)_{0.76}(H_2PO_3)_{0.24}$** | mixed crystals of guanylurea(1+) hydrogen fluorophosphate and guanylurea(1+) hydrogen phosphite | monoclinic | $Pn$ | 4 | 0.0503 120 K | |
| **$gu(HPO_3F)_{0.115}(H_2PO_3)_{0.885}$** | | monoclinic | $Pn$ | 4 | 0.0191 120 K | |
| **$gu(HPO_3F)_{0.184}(H_2PO_3)_{0.816}$** | | monoclinic | $Pn$ | 4 | 0.0225 120 K | |
| **$gu_2PO_3F$** | guanylurea(1+) fluorophosphate dihydrate | orthorhombic | $Pnma$ | 4 | 0.0335 120 K | |
| **$gu_2PO_3F$** | guanylurea(1+) fluorophosphate dihydrate | orthorhombic | $Pbca$ | 8 | 0.0698 120 K | |
| **$gu_3(HPO_3F)(PO_3F)$** | guanylurea(1+) hydrogen fluorophosphate fluorophosphate | triclinic | $P1$ | 1 | 0.0303 297 K | |

All of the new salts will be discussed here and a special attention will be paid to an exceptionally interesting compound, the guanylurea hydrogen phosphite, **GUHP**.

The guanylurea(1+) bis(hydrogen sulphate) sulphate, **$gu_4(HSO_4)_2SO_4$**, and the guanylurea(1+) sulphate dihydrate, **$gu_2SO_4$**, crystallized from the 10% aqueous solutions of dicyandiamide and an equimolar ratio of 1 M sulphuric acid. The guanylurea(1+) hydrogen tartrate, **guHtart,** and the guanylurea(1+) hydrogen oxalate monohydrate, **guHox**, were prepared from a 10% aqueous solution of **gu** hydroxide (see Experimental) and equimolar ratio of 0.4 M solution of the L-tartaric or oxalic acid, respectively. The bis(anilinium(1+)) guanylurea(1+) chloride dihydrate, **$guan_2Cl_3$**, was obtained as a by-product of the reaction between aniline and dicyandiamide in diluted HCl, which was carried out to prepare the N-phenylbiguanide. This compound formed when the reaction was carried out at pH 4-5 and this finding is in accordance with the literature [85].

### 3.3.1 *The structure of new gu salts*

The structures of **$guBF_4$** and **$guH_2PO_3$** (**GUHP**) are described in publications in Appendix VI and Appendix II, respectively. All of the **gu** fluorophosphates are discussed in Appendix VII, Appendix VIII and Appendix IX.

The **$gu_2SO_4$** crystallizes as needle-shaped crystals in the triclinic crystal system in the space group *P*-1. Its asymmetric unit consists of two **gu**(1+) cations, one sulphate anion and two water molecules of solvation. The alternating cations, anions and water molecules form hydrogen-bonded layers parallel to *bc* plane (Fig. 15). The connection between these layers is mediated by the hydrogen bonds connecting water molecules and the tetrahedral anions sticking out of the layers. These hydrogen bonds are of type O-H...O [2.694(2) – 3.003(2) Å] and they take part in the most noticeable motif of the structure, the large hydrogen-bonded rings, which can be described by a graph set descriptor $R_4^4(16)$.

The **$gu_4(HSO_4)_2SO_4$** crystallizes as large prisms in the centrosymmetric assembly in the triclinic crystal system, space group *P*-1. Its asymmetric units consist of four **gu**(1+) cations, two hydrogen sulphate anions and one sulphate anion. The chains of anions parallel to the *b* axis form layers situated parallelly to the *ab* plane, while the **gu**(1+) cations connect these layers so that the hydrogen-bonded rings corresponding to the graph set descriptors $R_2^2(8)$ and $R_2^3(6)$ are formed. Every individual **gu**(1+) from the asymmetric unit is deflected in a different way (Table 9) and the **gu**(1+) cations slightly deviate from the parallel assembly in the structure (Fig. 16).

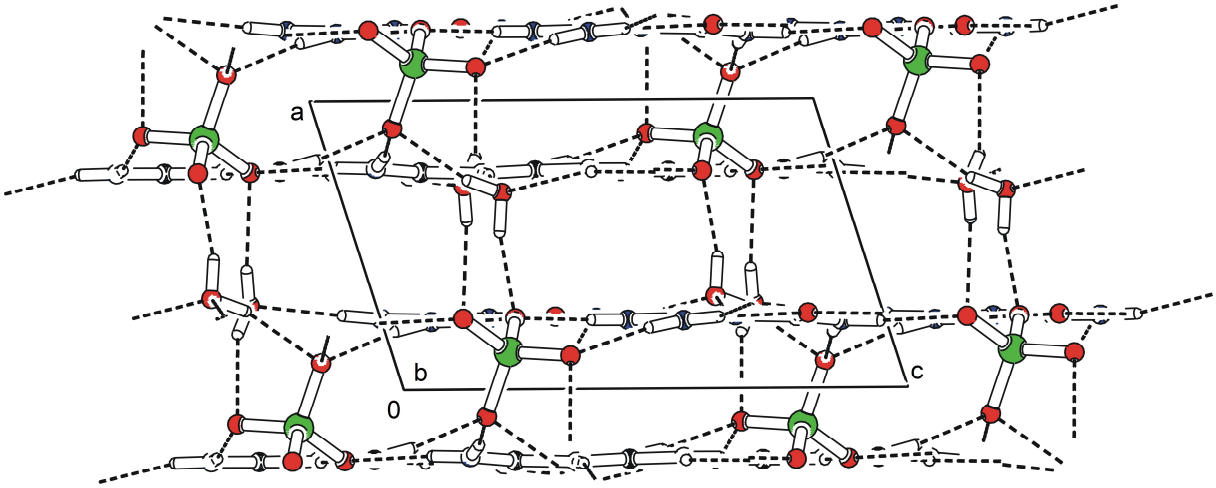


Fig. 15 The packing of the **gu$_2$SO$_4$** structure viewed along the *b* axial direction. Hydrogen bonds are symbolized by dashes. The practically planar **gu** cations are all situated parallelly to *bc* plane. The oxygen atoms are symbolized by red circles, nitrogen blue, carbon black, sulphur green and hydrogen atoms are colourless.

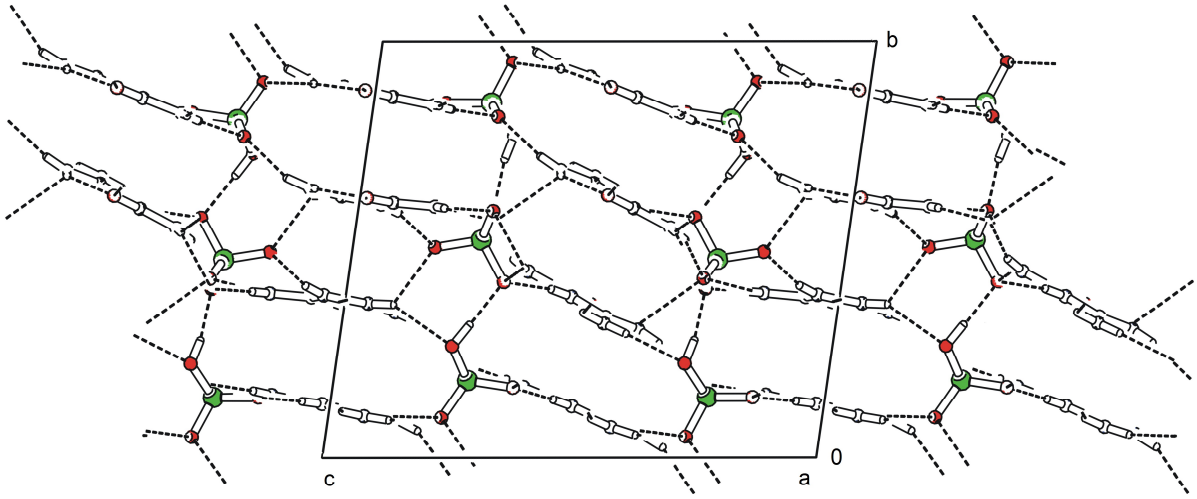


Fig. 16 The packing of the **gu$_4$(HSO$_4$)$_2$SO$_4$** structure viewed down the *a* axial direction. The anionic layers are oriented parallelly to the *ab* plane, the **gu**(1+) cations interconnect them. Hydrogen bonds are symbolized by dashes. The oxygen atoms are symbolized by red circles, nitrogen blue, carbon black, sulphure green and hydrogens are colourless.

The **guHtart** crystallizes as tiny colourless rod-like crystals in the noncentrosymmetric space group $P2_12_12_1$. Its asymmetric unit contains one **gu**(1+) cation and one hydrogen tartrate anion. The cations and anions form a hydrogen-bonded common network that is organised so that alternating cationic and anionic layers lie parallelly to the *ab* plane (Fig. 17). As H-bond donors, the **gu**(1+) cations are attached to the hydrogen tartrate anions by the N-H...O hydrogen bonds [2.858(2) – 2.964(2) Å]

forming patterns that can be described by the graph set descriptor $R_4^4(15)$. On the contrary, there is also an interaction of O-H...O type [2.805(1) Å], where the cation appears in the H-bond acceptor role. There is an intramolecular hydrogen bond of N-H...O type [donor...acceptor distance 2.683(2) Å] in the **gu**(1+) cations while the anions are interconnected by a system of O-H...O hydrogen bonds [2.515(1) – 2.917(1) Å].

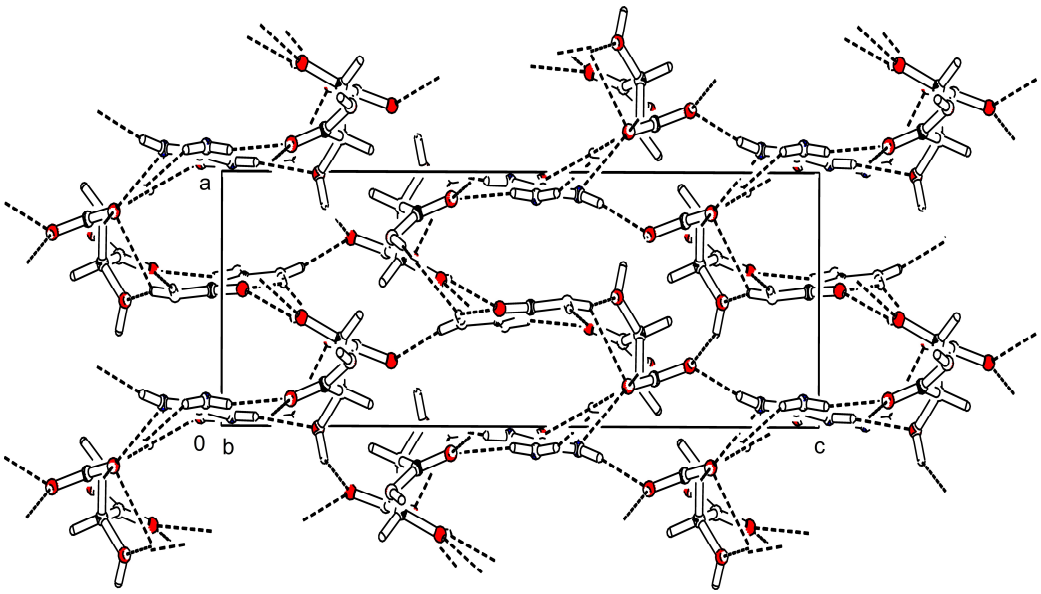


Fig. 17 The packing of the **guHtart** viewed down the *b* axial direction. The **gu**(1+) cations are perpendicular to the projection, hydrogen bonds are symbolized by dashes. The red circles symbolize the oxygen atoms, blue those of nitrogen, black carbon atoms and hydrogens are colourless.

The **guHox** crystallizes as small needle-shaped colourless crystals in the centrosymmetric assembly in the space group $P2_1/c$. Its asymmetric unit consists of one **gu**(1+) cation, one hydrogen oxalate anion and one water molecule of solvation. The **guHox** structure is a common network formed by alternating cations, anions and water molecules. Its noticeable feature is the pairwise assembly of **gu**(1+) cations mediated by a N-H...O hydrogen bond [2.961(1) Å] situated respectively so that both of the cations are the H-bond donors and acceptors at a the same time. These **gu**(1+) pairs appear in the structure in two orientations offset by 44°. The connection between cations and anions is mediated by numerous hydrogen bonds of N-H...O type [2.789(1) – 2.979(1) Å]. The water molecules are attached by an interaction of O-H...O type to the **gu**(1+) [2.914(1) Å] and to the oxalate anions [2.729(1) – 3.080(1) Å]. In these hydrogen bonds, the water molecules served as H-bond donors, while there is also an interaction of O-H...O type [2.604(1) Å] between $H_2O$ and the hydrogen oxalate anion, where the water molecule appears as a H-bond acceptor.

The **guan$_2$Cl$_3$** crystallizes in form of pink prisms in the space group *P*-1. Its asymmetric unit consists of two anilinium(1+) cations, one **gu**(1+) cation, three chloride anions and two water molecules of solvation. The main feature of the structure are the parallelly assembled hydrogen-bonded chains involving chloride anions, water molecules, protonated amino groups of the anilinium(1+) and the amino groups of the guanidine part of **gu**(1+) (Fig. 18) that can be described by the graph set descriptor $C_6^3(14)$. The phenyl rings of the anilinium(1+) and the **gu**(1+) cations stick out of the chains and they are placed practically parallelly to each other. As the neighbouring phenyl rings and the Y-aromatic **gu**(1+) cations are situated over each other in the distance about 3.5 – 3.7 Å, their π-π interaction can be expected.

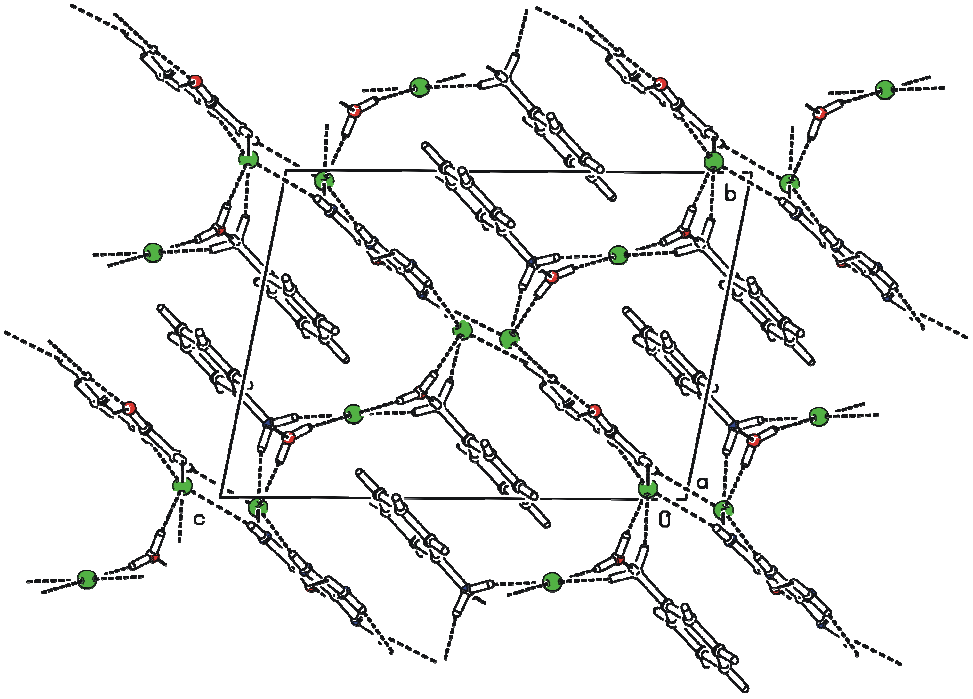


Fig. 18 The packing of the **guan$_2$Cl$_3$** viewed down the *a* axis, hydrogen bonds are symbolized by dashes. The **gu**(1+) cations are perpendicular to the projection, interconnecting the chains. The red circles symbolize the oxygen atoms, blue nitrogen atoms, black carbon atoms, green chlorine atoms and hydrogens are colourless.

### 3.3.2 *Vibrational spectra of new gu salts*

As the vibrational spectra of the **gu**(1+) cation have been studied in a publication in Appendix V, they are not further discussed in this text. The recorded maxima of new compounds are presented as peaklists as a further characterization of the prepared materials.

**$gu_4(HSO_4)_2SO_4$**:

IR spectrum: 131 m, 146 m, 221 w, 280 w, 435 s, 446 s, 501 m, 578 s, 585 s, 708 m, 879 m, 929 m, 976 m, 1015 m, 1088 m, 1166 m, 1206 m, 1352 m, 1463 w, 1505 w, 1543 w, 1590 m, 1634 m, 1690 m, 1739 m, 1771 w, 3034 m, 3211 m, 3337 m

Raman spectrum:

176 m, 280 m, 418 m, 436 s, 449 vs, 562 m, 582 w, 614 w, 709 m, 891 m, 929 m, 977 s, 1010 m, 1050 s, 1081 sh, 1132 m, 1214 w, 1350 w, 1462 m, 1545 w, 1599 m, 1633 w, 1701 w,1718 w, 1747 m, 3250 w, 3317 w

**$gu_2SO_4$**:

IR spectrum :

123w, 148w, 179m, 206w, 287w, 443m, 553m, 619 s, 666 m, 710 m, 734 m, 791 w, 879 w, 932 w, 976 w, 1082 s, 1358 m, 1463 m, 1548 m, 1601 m, 1635 m, 1694 m, 1726 m, 1843 w, 2062 w, 3149 m, 3196 s, 3310 s, 3338 s

Raman spectrum:

165 w, 197 w, 288 w, 441 m, 455 s, 568 w, 607 w, 623 w, 714 m, 940 m, 978 vs, 1059 sh, 1069 m, 1126 m, 1357 w, 1465 w, 1534 w, 1600 w, 1629 w, 1701 w, 1745 w, 3233 w, 3305 w, 3371w

**guHtart**:

IR spectrum:

419 w, 443 w, 483 sh, 531 m, 602 m, 687 m, 721 m, 838 m, 888 m, 995 m, 1074 s, 1125 s, 1349 s, 1540 m, 1591 m, 1653 m, 1696 w, 1757 w, 3210 w, 3328 m, 3408 m, 3438 m

Raman spectrum:

113 m, 138 s, 182 m, 274 m, 445 w, 520 w, 640 w, 706 w, 789 m, 838 w, 888 m, 931 w, 989 w, 1079 m, 1147 w, 1223 w, 1335 w, 140 6w, 1458 w, 1686 w, 1726 w, 2958 vs, 3232 brs

**guHox**:

IR spectrum:

117 w, 190 w, 263 w, 297 w, 365 m, 444 m, 481 m, 563 m, 609 m, 660 m, 705 m, 717 m, 747 m, 801 w, 872 w, 948 w, 1037 w, 1121 w, 1229 s, 1265 m, 1370 m, 1396 m, 1465 m, 1187 m, 1603 m, 1637 s, 1673 m, 1709 s, 1732 s, 2570 m, 3139 m, 3198 m, 3338 m, 3392 m, 3436 m, 3535 w

Raman spectrum:

125 m, 197 m, 282 w, 396 w, 441 m, 453 m, 490 vs, 567 m, 719 m, 741 m, 853 w, 877 s, 948 s, 1089 m, 1118 m, 1164 w, 1266 w, 1372 m, 1463 m, 1488 sh, 1535 w, 1578 w, 1668 m, 1694 m, 1721 m, 1759 w, 3210 br, 3340 br

**$guan_2Cl$**:

IR spectrum:

434 m, 451 m, 478 s, 527 m, 560 m, 616 m, 683 s, 730 s, 750 m, 791 w, 836 w, 910 w, 976 w, 1005 w, 1033 m, 1066 m, 1111 m, 1196 m, 1342 m, 1464 m, 1496 s, 1530 s, 1583 s, 1613 m, 1643 m, 1698 m, 1732 m, 2586 m, 2621 m, 2888 s, 2946 s, 2979 s, 3154 s, 3293 m, 3317 m, 3353 m, 3401 m, 3447 m

Raman spectrum:

111 s, 451 m, 616 w, 792 s, 927 w, 1005 vs, 1032 m, 1075 m, 1185 s, 1199 m, 1471 w, 1605 m, 1738 m, 3210 br, 3340 br

**$guBF_4$**:

IR spectrum:

434 m, 520 s, 560 s, 598 sh, 668 m, 721 m, 767 m, 791 w, 984 brs, 1291 w, 1533 w, 1589 m, 1618 w, 1666 m, 1709 m, 2727 w, 3220 br, 3315 m, 3405 m, 3452 m, 3371 m, 3507 m

Raman spectrum:

132 s, 268 m, 354 w, 436 s, 552 w, 630 m, 707 m, 768 vs, 884 w, 940 m, 994 w, 1013 w, 1084 m, 1124 m, 1354 w, 1470 m, 1536 w, 1581 w, 1629 m, 1702 w, 1729 m, 3411 s, 3453 m, 3479 m, 3508 w

### 3.3.3 *Second harmonic generation of new gu salts*

The noncentrosymmetric **gu** salts were examined for the second harmonic generation. The **$guH_2PO_3$ (GUHP)** exhibited SHG efficiency comparable to the urea standard and it was proven to be a phase matchable compound (Appendix II). As the SHG efficiency comparable to urea was exceptional within the whole family of compounds examined in this thesis, a detailed study of the optical properties of **GUHP** was carried out (Appendix III and IV).

The **guHtart** exhibited the SHG efficiency 10 times lower than KDP.

The **$guHPO_3F$** isostructural with the **GUHP** and the mixed crystals of these two compounds also exhibited a noticeable SHG efficiency (Appendix VIII), but none of them reached the value obtained for the pure **GUHP**.

### 3.3.4 *Thermal behaviour of the interesting gu salts*

The DSC measurements revealed no effects in case of **$guH_2PO_3$** (**GUHP**), **$gu_2SO_4$** and **guHtart** from 93 K up to their melting points at 452 K, 467 K and 428 K, respectively. The **$gu_4(HSO_4)_2SO_4$** exhibited a reversible glass transition at 353 K and melting at 438 K. The **$guBF_4$** was stable until beginning of the decomposition process at 463 K. The **guHox**

underwent complicated decomposition processes already when heated above the room temperature.

### 3.3.5 *Material properties of the promising gu salts*

The **gu$H_2PO_3$** (**GUHP**) easily crystallizes in cluster-formed planar crystals that are transparent in the 275 nm – 2.82 μm interval. According to the noticeable SHG efficiency of **GUHP**, the refractive indices, birefringency, SHG refractive indices and also NLO coefficients of this compound were determined (Appendix III). This compound was found exceptionally interesting as it also exhibited an unusual effect, the noncollinear SHG (Appendix IV), and the very rare SHG conical refraction [120]. It can be concluded, that **GUHP** deserves preparation of large single crystals for the deeper study of its optical properties.

The **guHtart** crystallizes in form of thin rod-like crystals which are transparent in the 235 nm – 2.86 μm interval. Unfortunately, its crystallization is very slow and the aqueous solution of **guHtart** has a tendency to oversaturating with the result of viscous, yellowish solution that does not crystallize at all.

The **gu**(1+) (hydrogen) fluorophosphates (Appendix VII, VIII and IX) are generally unstable compounds. Except the mixed crystals with the majority of **GUHP**, all of them are hygroscopic. No crystals larger than a few mm were obtained from any of them. Unfortunately, the **guHP$O_3$F**, a compound isostructural with **GUHP**, did not bring any improvement neither to the SHG efficiency, nor to the material properties when the mixed crystals were prepared. The (hydrogen) fluorophosphates cannot be considered as a promising group in search for the desired NLO optical properties.

### 3.3.6 *Preparation of large single crystals of the gu$H_2PO_3$ (GUHP)*

According to the interesting properties of **GUHP**, efforts were given to prepare large single crystals in optical quality that would enable more detailed study of optical properties, *e.g.* a more accurate determination of the refractive indices. The basic preparation was carried out by the 'universal crystal breeding method' [121]. It means, at least 500 ml of the saturated aqueous solution of **GUHP** (solubility given in Table 11) with an excess of the solid phase at the bottom was placed into a thermostated box. When the equilibrium between the solid phase and the solution at the given temperature established, the solid was filtered off, the perfect small single crystals were hung into the solution as crystal seeds and the system was left to crystallize at the constant temperature for several months. The scheme of a crystallization aparature is given at Fig. 19.

Table 11 The solubility of the **GUHP** at considerable crystallization temperatures (listed as g **GUHP** per 100 g $H_2O$)

| Temperature [°C] | 3 | 10 | 20 | 30 | 40 | 50 | 60 | 70 | 75 | 80 |
|---|---|---|---|---|---|---|---|---|---|---|
| Solubility [g/100 g $H_2O$] | 7.4 | 8.9 | 12.9 | 19.4 | 27.0 | 32.8 | 51.1 | 62.1 | 74.8 | 88.3 |

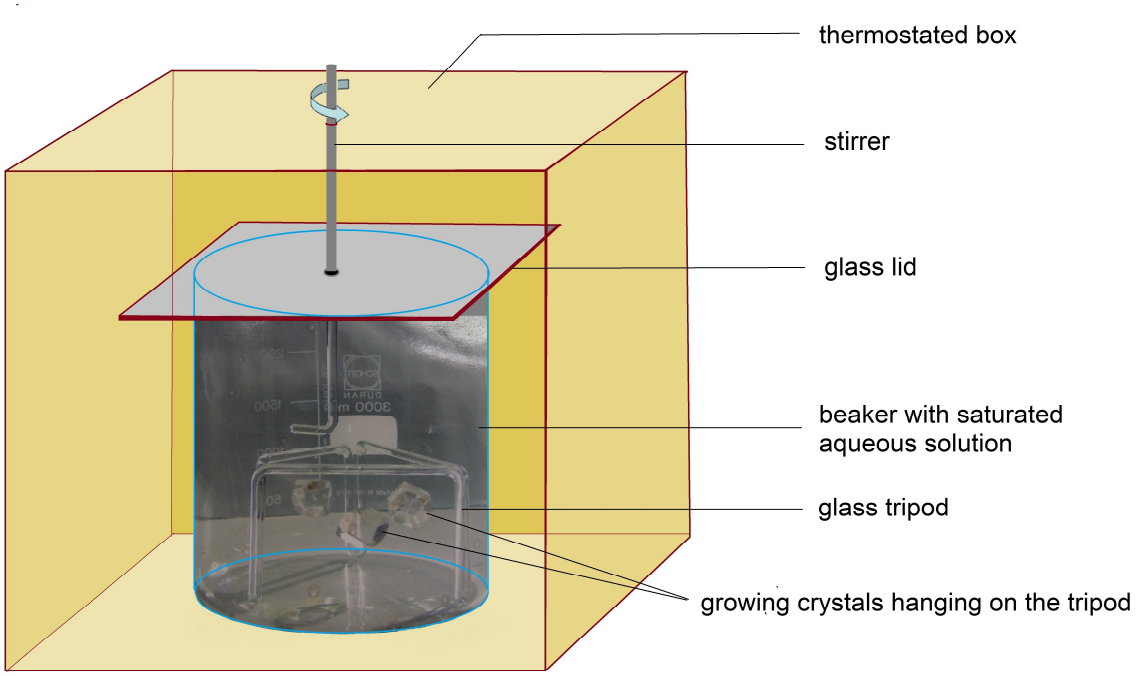


Fig. 19 The schematized assembly of a crystallization aparature for breeding of large single crystals

A variety of experiments with crystallization at different constant temperatures was carried out and the temperature range 35 – 40°C was found to be optimal – at that temperature range, enough of the material is dissolved, but the compound is not at danger of a damage by the prolonged heating. Another method with the temperature gradually sinking led to excessive formation of parasitic crystals at the bottom of the vessel. Unfortunately, the tendency of **GUHP** to crystal growth in clusters persisted at any temperature and the crystal breeding never led to an individual well developed single crystal – instead, the originally single crystalline seed split during the growth and the clusters of thin (0 0 1) platelets were obtained (Fig. 20). The beginning of this effect was observed at the microscopic level as tiny scales deviating from the rest of the crystal for about a few degrees appeared during the growth on the surface of the crystal seed (Fig. 20). Finally, the large but thin platelets of **GUHP** in optical quality were prepared (Fig. 21). The biggest crystal obtained from an aqueous solution was about 7 mm thick (Fig. 21).

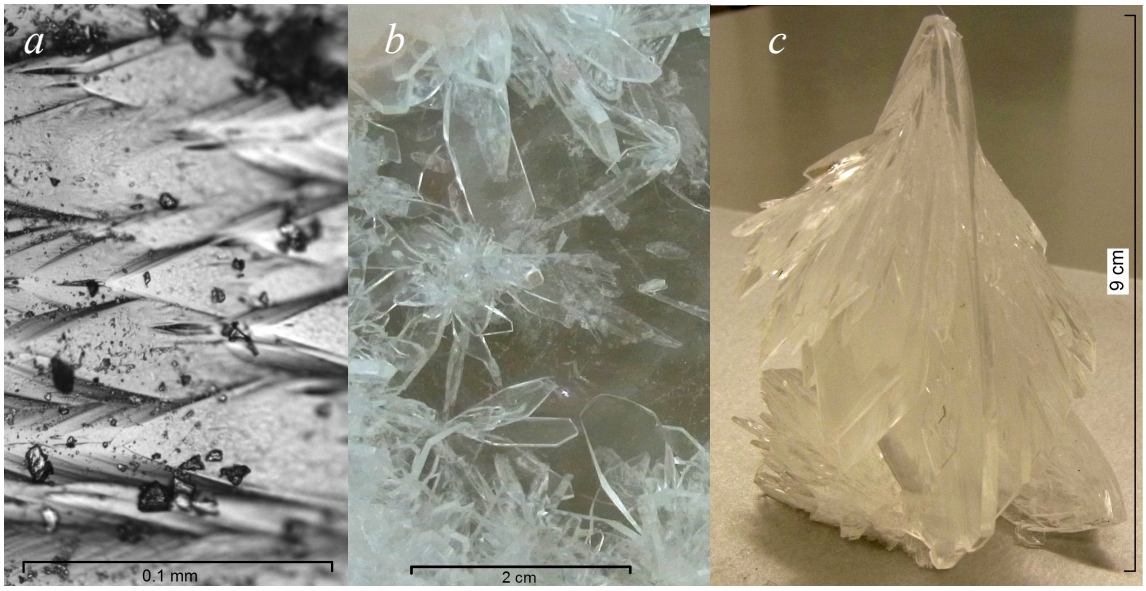


Fig. 20 Crystallization of **GUHP**: *a* – formation of scales at the surface of a crystal seed during the growth - the origin of splitting of the single crystal, *b* – spontaneously grown clusters of parasitic crystals of **GUHP** at the bottom of a crystallization vessel, *c* – a cluster of platy crystals of **GUHP** grown on a single crystal seed

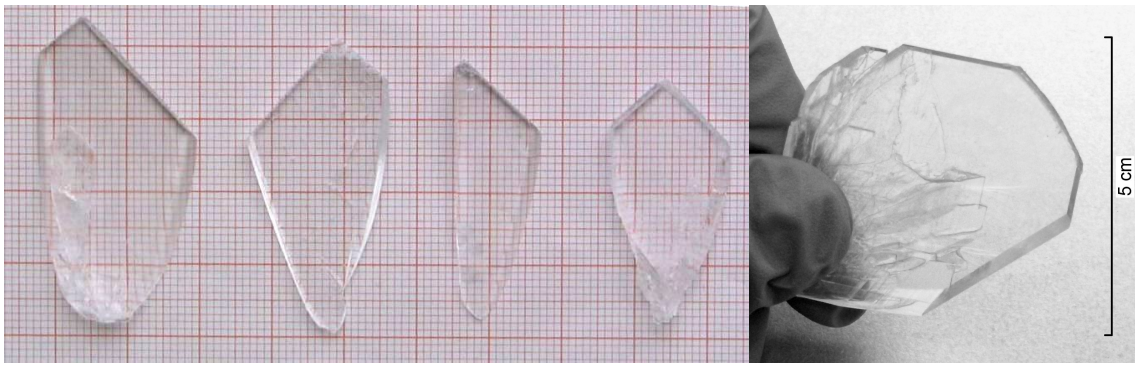


Fig. 21 Large single crystals of **GUHP** in optical quality separated from the clusters

Efforts were given to find an alternative condition of crystals preparation that would enable coming over the problem of thin crystals clusters formation. As the temperature did not exhibit any significant effect on the clustering, a set of experiments with modified composition of the solvent was carried out. The mixtures of water and methanole, ethanole, propanole and isopropanole ranging from (3:1) to (1:3) volume ratios were tested respectively as solvents. The mixtures of water with ethanole (1:1) and water with isopropanole (2:1) gave thicker, less aggregating well developed crystals in the preliminary experiments, but the long term crystal breeding was accompanied by occurence of many parasitic crystals at the bottom of the vessels and it was complicated

by the unequal evaporation of the used solvents. In the end, no sufficiently large crystals were obtained by this method.

Although several well developed single crystals in quality sufficient for the further characterizations was obtained, it can be concluded that the preparation of large single crystals of **GUHP** still remains challenging.

### 3.3.7 *Further characterizations of GUHP*

The preparation of the large single crystals of **GUHP** enabled the use of the relatively large samples with a minimum of defects. Besides the optical characterizations of the material, such samples made the study of thermal expansion of **GUHP** possible as well [122]. The study of the thermal expansion of a material is a classical but very sensitive method for the examination of its behaviour depending on temperature. In fact, such a study can be very useful for a detailed examination of a compound considered as a promising NLO material while revealing of any anomaly in the temperature dependent behaviour might indicate a slight change in the structure, too tiny to be uncovered by other methods, but potentially important.

The thermal expansion measurements were executed in the temperature range 140 - 350 K. Two intervals in which the **GUHP** exhibits a standard behaviour as it gradually contracts with the decreasing temperature were found. In these intervals, the dependence of the deformation on the temperature was practically linear. Between these intervals, *i.e.* between 210 and 270 K, an anomaly with a conspicuously nonlinear development of the monitored lengths was observed. In order to understand this anomaly, a detailed DSC measurement was repeatedly carried out, but it did not reveal any effects [122].

In order to further investigate the observed effect, an additional X-ray structure determination of **GUHP** at the temperature lying safely under the temperature region in which the anomaly occurs, particularly at 150 K, was carried out. The comparison of the structure parameters, bond lengths and angles and hydrogen bonds at 293 K and 150 K, *i.e.* above and under the anomaly, is given in Tables 12, 13 and 14, respectively.

Generally, the structures at 150 K and 293 K do not differ much. The most noticeable change was the shortening of the crystal cell lengths which was not proportional. While the *b* and *c* significantly shortened in the low temperature, the *a* stayed almost without change. An important change was the significant decrease of the Flack parameter, which was high in the 297 K structure and witnessed for presence of a small reversely oriented areas inside the crystal. In the 150 K, there is no evidence of such domains according to the Flack parameter.

Table 12 Comparison of the structure data of **GUHP** at 150 K and 293 K

| | **150 K** | **293 K** |
|---|---|---|
| *a* (Å) | 6.6852(2) | 6.6990(3) |
| *b* (Å) | 6.7778(2) | 6.8420(2) |
| *c* (Å) | 16.2758(5) | 16.3540(1) |
| *β* (°) | 96.504(1) | 96.514(3) |
| Volume (Å$^3$) | 732.73(4) | 744.74(6) |
| Flack parameter | 0.02(4) | 0.0(3) |
| R factor | 1.69 | 2.76 |

Concerning the bond lengths, there was no significant change. An additional hydrogen bond appeared in the low temperature structure in the Platon software, but this is apparently more the question of the selected criteria for the decision about hydrogen bonds than a significant change of the structure. For this reason, the lengths that would correspond to the respective hydrogen bond at 293 K are listed in the Table 13 as well. Still, such a minor difference in a hydrogen bond which leads to the excess from the selected criteria can be understood as the effect of a slight difference in the electron distribution between the 150 K and 293 K structures as well.

Similarly, the slight differences between the bond lengths, especially between the carbon and nitrogen atoms in the skeleton of the cation, influence the hydrogen bonds and therefore the whole structure. The overall appearance of the differences between the 150 K and 293 K structures witnesses for a number of subtle changes concerning the whole structure assembly and definitely, it is not possible to assign the changes only to a particular building block of the structure.

Table 13 Comparison of hydrogen bonds in **GUHP** at 150 and 293 K

| | 150 K | 293 K | 150 K | 293 K | 150 K | 293 K | 150 K | 293 K |
|---|---|---|---|---|---|---|---|---|
| D-H...A | d(D-H) [Å] | | d(H...A)[Å] | | d(D...A)[Å] | | DHA[°] | |
| N1-H1A...O1$^{i}$ | 0.80(2) | 0.77(3) | 2.16(1) | 2.19(3) | 2.696(1) | 2.714(2) | 124(1) | 126(3) |
| N1-H1B...O4$^{ii}$ | 0.90(2) | 1.01(3) | 2.04(2) | 1.96(3) | 2.929(1) | 2.950(3) | 170(1) | 168(3) |
| N2-H2A...O3$^{iii}$ | 0.84(2) | 0.95(3) | 2.098(2) | 1.99(3) | 2.940(1) | 2.937(3) | 180(2) | 173(3) |
| N2-H2B...O1 | 0.81(1) | 0.78(3) | 2.03(1) | 2.02(3) | 2.640(1) | 2.646(3) | 132(1) | 138(3) |
| N3-H3...O2 | 0.90(1) | 0.94(3) | 1.88(1) | 1.84(3) | 2.768(1) | 2.776(2) | 173(1) | 173(2) |
| O4-H4...O3$^{iv}$ | 0.87(1) | 0.88(4) | 1.72(1) | 1.73(4) | 2.575(1) | 2.591(2) | 167(1) | 165(4) |
| N4-H4A...O2$^{v}$ | 0.80(2) | 0.87(4) | 2.21(2) | 2.17(4) | 3.013(1) | 3.037(2) | 174(2) | 174(3) |
| N4-H4B...O3 | 0.81(1) | 0.77(3) | 2.24(1) | 2.31(3) | 3.045(1) | 3.078(3) | 174(1) | 176(3) |
| N1-H1A...O2 | 0.80(2) | 0.77(3) | 2.58(2) | 2.61(3) | 3.220(1) | 3.222(3) | 139(1) | 138(2) |

(i) -1+x,y,z; (ii) x,1-y,1/2+z; (iii) x,1-y,1/2+z; (iv) -1/2+x,1/2+y,z; (v) 1+x,y,z

Table 14 Comparison of bond lengths, angles and torsion angles in **GUHP** at 150 K and 293 K

| Bond length [Å] | 293 K | 150 K | Bond angle [°] | 293 K | 150 K |
|---|---|---|---|---|---|
| N1-C1 | 1.318(3) | 1.324(1) | O1-C2-N4 | 123.9(2) | 123.7(1) |
| N2-C1 | 1.313(3) | 1.318(1) | C1-N1-H1A | 123(2) | 121(1) |
| N3-C1 | 1.355(3) | 1.359(1) | C1-N1-H1B | 122(2) | 123.1(9) |
| N3-C2 | 1.395(2) | 1.397(1) | H1A-N1-H1B | 116(3) | 115(1) |
| N4-C2 | 1.328(3) | 1.335(1) | C1-N2-H2A | 121(2) | 117(1) |
| O1-C2 | 1.226(3) | 1.230(1) | C1-N2-H2B | 114(2) | 118(1) |
| N1-H1A | 0.77(3) | 0.80(2) | H2A-N2-H2B | 125(3) | 124(1) |
| N1-H1B | 1.01(3) | 0.90(2) | C1-N3-H3 | 113(2) | 113.3(9) |
| N2-H2A | 0.95(3) | 0.84(2) | C2-N3-H3 | 122(2) | 122.2(9) |
| N2-H2B | 0.78(3) | 0.81(1) | C2-N4-H4A | 110(2) | 115(1) |
| N3-H3 | 0.94(3) | 0.90(1) | C2-N4-H4B | 125(3) | 124(1) |
| N4-H4A | 0.87(4) | 0.80(2) | H4A-N4-H4B | 126(3) | 121(2) |
| N4-H4B | 0.77(3) | 0.81(1) | O2-P1-O3 | 117.5(1) | 117.4(1) |
| P1-O2 | 1.489(2) | 1.497(1) | O2-P1-O4 | 112.3(1) | 112.0(1) |
| P1-O3 | 1.504(1) | 1.511(1) | O3-P1-O4 | 107.2(1) | 107.4(1) |
| P1-O4 | 1.572(2) | 1.582(1) | O2-P1-H1 | 107(1) | 107(1) |
| P1-H1 | 1.27(2) | 1.30(1) | O3-P1-H1 | 113(1) | 109(1) |
| O4-H4 | 0.88(4) | 0.87(1) | O4-P1-H1 | 100(1) | 104(1) |
| Bond angle [°] | | | P1-O4-H4 | 120(2) | 117(1) |
| N1-C1-N2 | 120.6(2) | 120.8(1) | Torsion angle [°] | | |
| N2-C1-N3 | 122.5(2) | 122.4(1) | N1-C1-N3-C2 | -178.7(2) | -178.7(1) |
| N1-C1-N3 | 116.9(2) | 116.8(1) | N2-C1-N3-C2 | 0.7(3) | 0.9(1) |
| C1-N3-C2 | 124.9(2) | 124.4(1) | O1-C2-N3-C1 | -7.6(3) | -7.5(1) |
| N3-C2-N4 | 114.5(2) | 114.4(1) | N4-C2-N3-C1 | 172.6(2) | 172.4(1) |
| O1-C2-N3 | 121.7(2) | 121.9(1) | | | |

In order to enlighten the observed effect in a more subtle way, the temperature dependent vibrational spectra of **GUHP** were recorded and interpreted. The MID (Fig. 22) and FAR IR spectra and Raman spectra of **GUHP** have been measured in the interval from 77 K to 310 K with a step of 20 K or 10 K in the 77 – 200 K and 200 – 310 K intervals, respectively. Most of the recorded maxima did not exhibit any change with the temperature, but the detailed analysis of the spectra showed that several peaks shifted noticeably, while others split or diminished with temperature. The maxima exhibiting any change at all (*i.e.* 9 in the MID IR, 6 in the FAR IR and 7 in the Raman spectrum) were examined in order to reveal the possible trends of the changes. The graphical depiction of the development of these changes is given in Fig. 23.

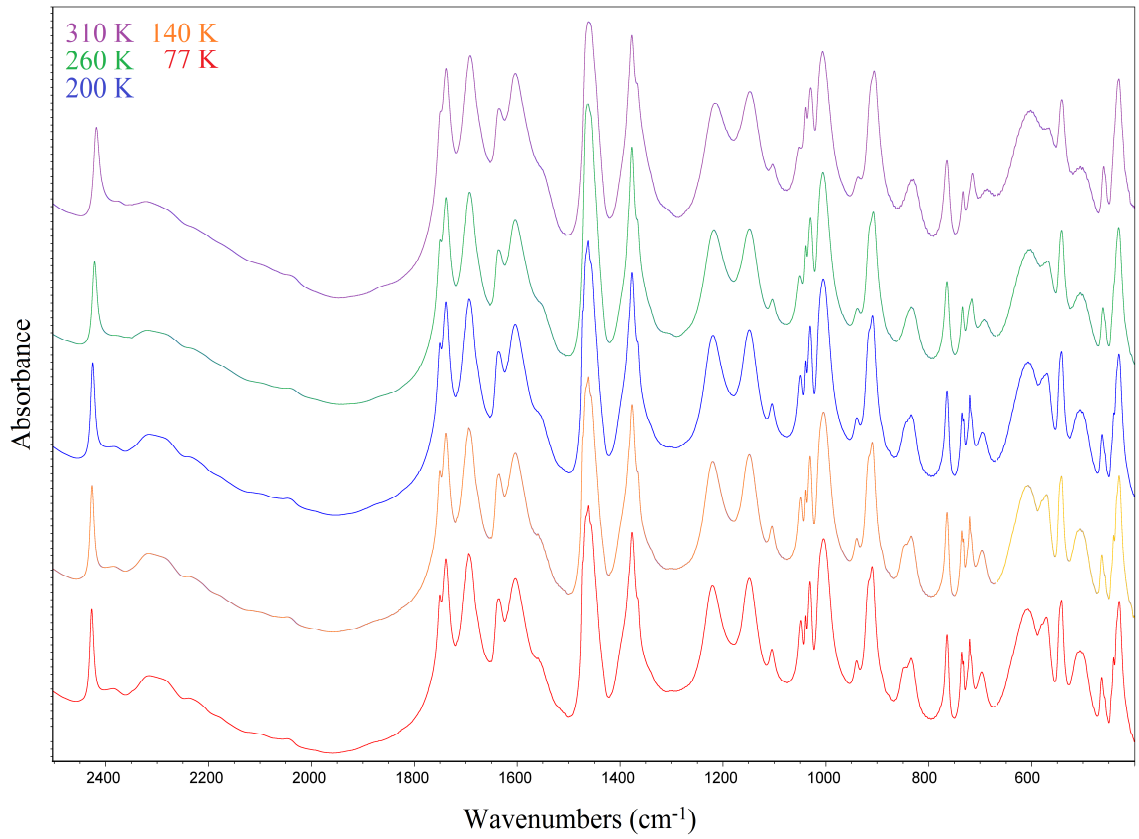


Fig. 22 Selected temperature dependent MID IR spectra of **GUHP** in the 400 – 2600 $cm^{-1}$ region

Most of the maxima undergoing the changes did not exhibit any special trends and their wavelengths rose or sunk in an almost linear manner as expectable, but eight of them in the MID IR spectrum exhibited a significant deviation from the linear course. Although even these selected changes in the MID IR spectra were relatively subtle and they almost cannot be seen in Fig. 22, the detailed analysis of them revealed an interesting trend.

The graphical depiction of the typical development of such an observed anomal course of the wavelength shift is given in Fig. 24. In all eight cases, the data could be fitted by two straight lines. The intersection of the lines lies in interval 202 – 228 K. The temperatures pertinent to the intersection of the lines are given with the assignment of the particular vibrational maximum (taken from assignment in Appendix V) in Table 15.

As all of these effects occured only in the MID IR spectral region, they can be considered as manifestations of vibrations of the polar groups in the **GUHP**. The spectroscopic observation that some of the noticeable shifts of the vibrational maxima correspond to the $NH_2$ groups serving as the hydrogen bond donors, which are targeted by the slight rearrangement of the structure, corresponds well to the finding of a slight difference in the hydrogen bonds between the 150 K and 293 K structures.

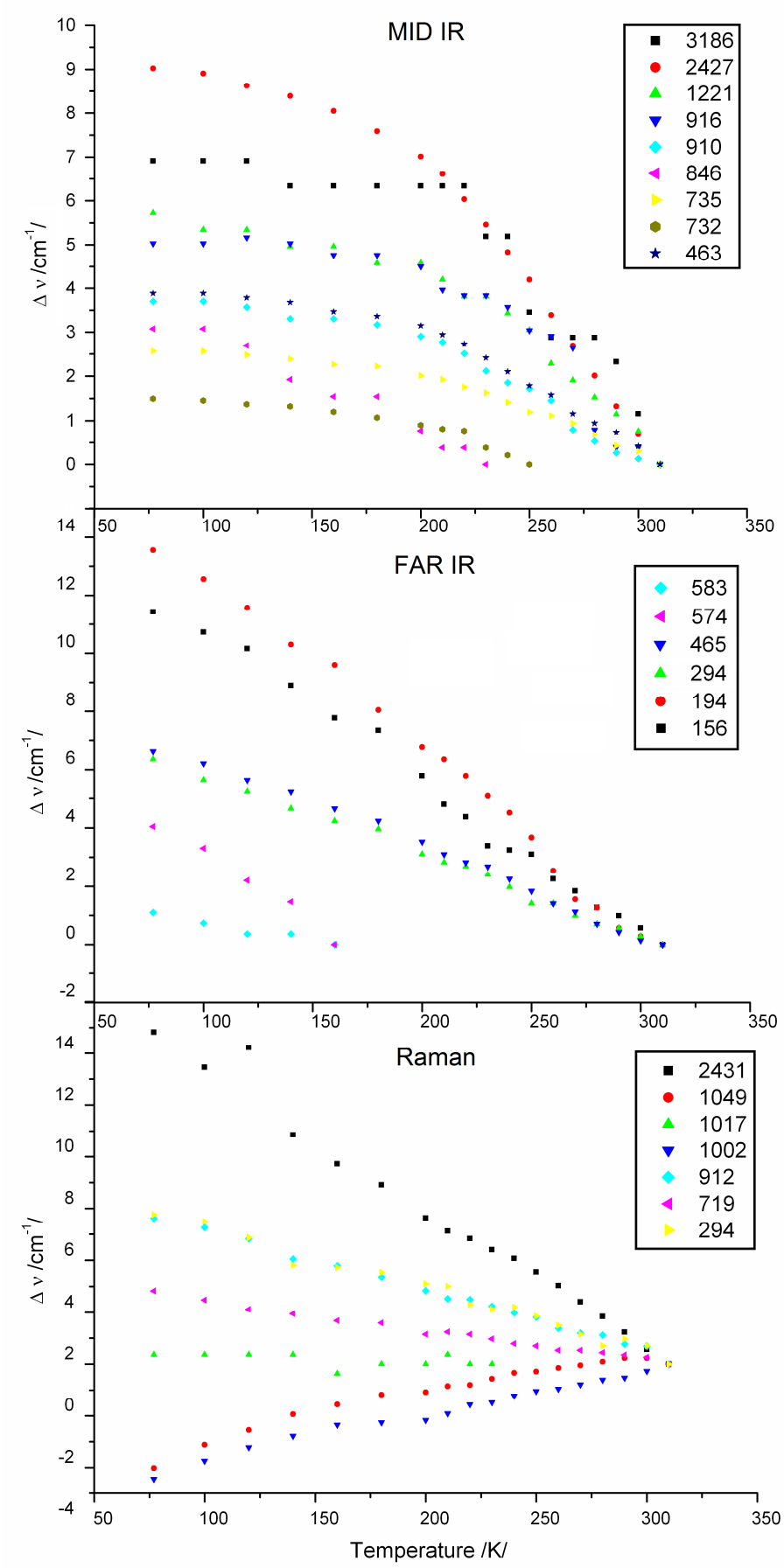


Fig. 23 Temperature dependent absolute changes of the frequency of selected peaks of **GUHP**, wavelengths pertinent to the individual datasets are presented in the legend in $cm^{-1}$.

Similarly, also the shifts of the maxima corresponding to the manifestations of the anions occur, as their oxygen atoms playing the role of the hydrogen bond acceptors and their O-H groups serving as the hydrogen bond donors are targeted by the moderate rearrangement of the structure and the hydrogen bonds. Although the P-H group is not involved in the hydrogen bonds system directly, its bond length and accordingly also its manifestation is influenced by the changes of the electron distribution affecting the neighbouring atoms as well.

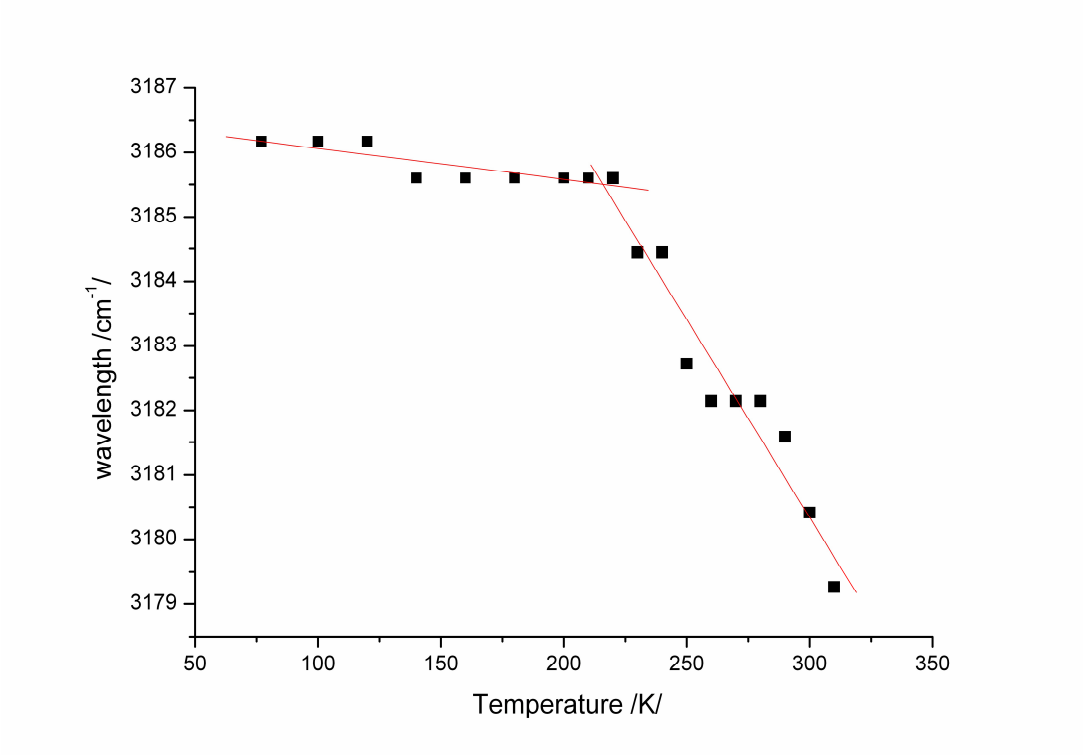


Fig. 24 Example of the anomaly in the temperature dependent change of the selected peak in the MID IR spectrum of **GUHP**

Table 15 Temperatures of the intersection of the two straight lines fitted to the data of selected anomally developing shifts of the wavelengths in the MID IR spectrum of **GUHP** and the assignment of the given maxima

| Intersection temperature /K/ | Corresponding wavelength /$cm^{-1}$/ | Assignment |
|---|---|---|
| 216 | 3186 | ν N-H(...O) |
| 202 | 2426 | ν PH |
| 228 | 1219 | δ (P)OH |
| 206 | 916 | ν PO(H) ? |
| 205 | 909 | ν PO(H) |
| 211 | 735 | τ $NH_2$, π $N_2CO$, π $CN_3$ |
| 216 | 732 | τ $NH_2$, π $N_2CO$, π $CN_3$ |
| 205 | 463 | δ NCN, δ NCO |

The analysis of the recorded temperature dependent spectra indicated a moderate change of the **GUHP** structure about 210 K, which is in good agreement with the anomaly onset found by the thermal expansion measurements. In fact, the observations from the thermal expansion experiments, the temperature dependent vibrational spectra and the comparison of the X-ray structure analyses carried out at 150 K and 293 K correspond well to each other. It can be concluded from our findings that **GUHP** undergoes between the 210 and 270 K a process consisting of small changes affecting the structure most at about 210 K.

All of our findings from the above mentioned analyses indicate that the observed anomaly corresponds to a subtle rearrangement of the structure of **GUHP**, a process which consumes such a small amount of energy that it cannot be revealed by the DSC measurements. As the original space group is maintained, this process can be classified as an isostructural transition. Such transitions have been observed in the salts of guanidine derivatives only rarely [123, 76]. In fact, documenting of such effects lies near the limits of the characterization methods. As there are no substantial changes of the structure during the observed transition, this process could be discovered and further described at all only because of the very sensitive methods that were applied in combination. The main result of this investigation is that the **GUHP** undergoes a complex but very moderate change of the structure in a wide temperature range under 170 K, while above this temperature it is stable enough for the practical applications at least up to 350 K.

Besides the investigation of the thermal behaviour of **GUHP**, also the study of its NLO properties could be further developed as several sufficiently large samples in optical quality were prepared. Recently, interesting results were achieved in the study of stimulated Raman scattering and cascaded NLO processes in **GUHP** and these results are to be published soon [124].

Concerning all of the known facts about **GUHP**, it can be concluded that it is a very interesting compound worth further investigation. With no doubt, from the NLO point of view, it can be considered as the most interesting compound of **gu** ever described. According to the relatively broad transparency window of **GUHP**, its high birefringence and mechanical stability, to the fact that it is not hygroscopic at all and that it exhibits a resistence to the optical damage comparable to the best commercially used materials (Appendix III), it can be concluded that **GUHP** has a real potential for becoming a NLO material of practical use. The challenging issue to be overcome is the difficulty in obtaining sufficiently thick single crystals (*i.e.* above 10 mm in the shortest dimension) in the controlled crystal growth experiments.

### 3.4 *N*,*N*′,*N*″-triphenylguanidine

The *N*,*N*′,*N*″-triphenylguanidine (**tphgua**) appears in the complex compounds as an uncharged or anionic ligand, but its most interesting form is a 1+ charged cation posessing a π delocalization and theoretically capable of a trigonal symmetry. Although the trigonal symmetry seems to be sterically advantageous, there is no evidence of maintenance of the trigonality in any known **tphgua**(1+) compound. There are several **tphgua**(1+) salts with a noncentrosymmetric assembly and paralelly to the preparation of this thesis, new interesting studies of the noticeable NLO properties of some of them were published by a research group from Portugal [110].

Considering all this, efforts were given to prepare new noncentrosymmetric **tphgua**(1+) compounds with regard to the possible preparation of an octupolar compound analogous to the known guanidinium tartrate [73]. Attempts were given to prepare salts of inorganic and also chiral and achiral organic anions. Unfortunately, only two compounds were prepared in a defined enough state so that their crystal structure (Table 16) and overall characteristics could be determined at all.

The **tphgua**(1+) hydrogen phosphite (**tphgua$H_2PO_3$**) was prepared by mixing the powderized **tphgua** base with an equimolar amount of the 0.4M aqueous solution of $H_3PO_3$. The product was obtained immediately as a white precipitate. The same compound was obtained also in an alternative process, when the 10% solution of the base in acetone was mixed with the 2M aqueous solution of the acid, but this time it first appeared after a week in a form of needle-shaped shiny colourless crystals.

The **tphgua**(1+) hydrogen sulphate (**tphgua$HSO_4$**) was prepared by mixing the powderized free base with an equimolar amount of the 1M aqueous solution of sulphuric acid. The product started to crystallize in a few hours and after a week appeared also small platy colourless monocrystals suitable for the structure determination. The alternative preparation using the acetone as a solvent of the **tphgua** base led to the same results, but the crystallization lasted longer and the platy crystals were less developed.

Table 16: New salts of **tphgua**

| Abbreviation | Chemical name | Crystal system | Space group | Z | R factor (Temp.) | CCDC No./Code |
|---|---|---|---|---|---|---|
| **tphgua$H_2PO_3$** | *N*,*N*′,*N*″-triphenylguanidium(1+) hydrogen phosphite | monoclinic | $P2_1/n$ | 4 | 0.0385 (150 K) | 880725 |
| **tphgua$HSO_4$** | *N*,*N*′,*N*″-triphenylguanidium(1+) hydrogen sulphate | monoclinic | $P2_1/n$ | 4 | 0.0431 (150 K) | 880726 |

3.4.1 ***The structure of the new tphgua salts***

The **tphguaH$_2$PO$_3$** crystallizes in a centrosymmetric space group $P2_1/n$. Its asymmetric unit consists of one **tphgua**(1+) cation (Fig. 25) and one hydrogen phosphite anion. A noticeable motif of **tphguaH$_2$PO$_3$** structure is the pairwise assembly of the hydrogen phosphite anions, forming hydrogen-bonded rings, that can be described by a graph set descriptor $R_2^2(8)$. These rings are mediated by an alternating O-H...O type hydrogen bond [2.557(2) Å]. Another important motif consists of two anions and two cations connected by the hydrogen bonds of N-H...O type [2.795(2) – 2.917(2) Å] forming a large ring corresponding to the $R_4^4(16)$. These two motifs are arranged in chains parallel to the *b* axis (Fig. 26).

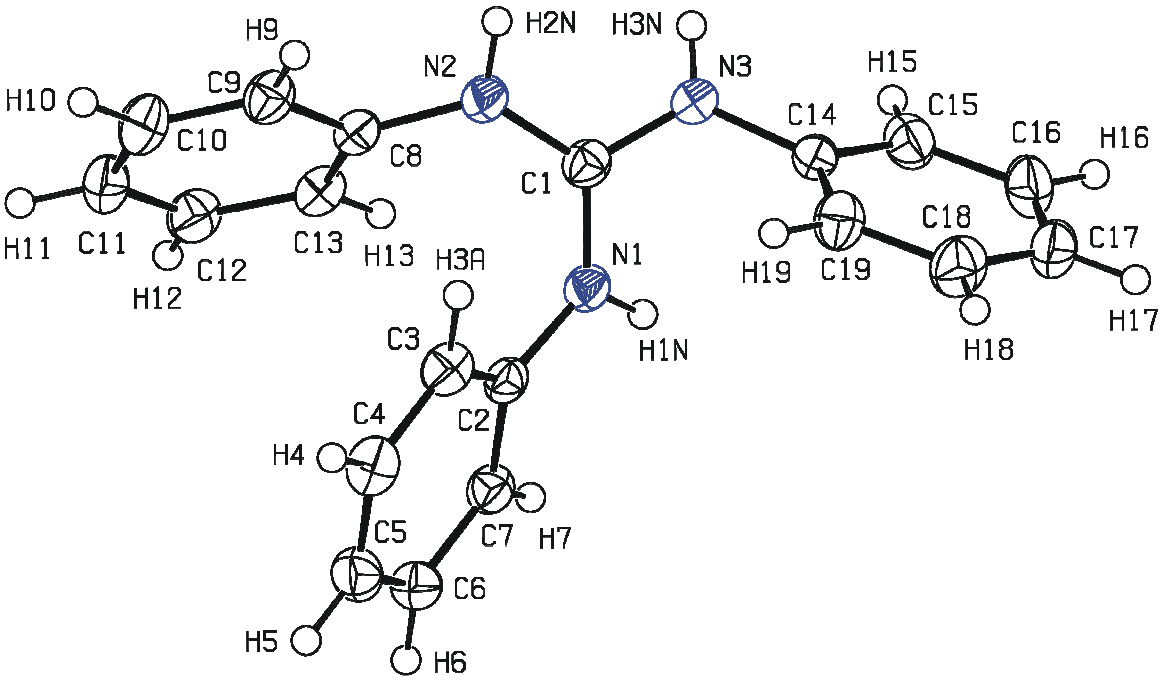


Fig. 25 Numbering of the **tphgua**(1+) cation in **tphguaH$_2$PO$_3$**. The displacement parameters are drawn at the 50% probability level

The **tphguaHSO$_4$** also crystallizes in a centrosymmetric space group $P2_1/n$. Organization of its structure is similar to the previously described **tphguaH$_2$PO$_3$**: the main feature of the structure are the hydrogen-bonded chains parallel to the *b* axis, formed by the alternating pairwise assembled cations and the motifs formed by two cations and two anions which can be described by the $R_2^2(8)$ and $R_4^4(16)$ graph set descriptors, respectively

(Fig. 27). The hydrogen bond between the anions is mediated by an alternating O-H...O bond [2.668(2) Å], the cations are attached to the anions by the N-H...O hydrogen bonds [2.747(2) – 2.900(2) Å].

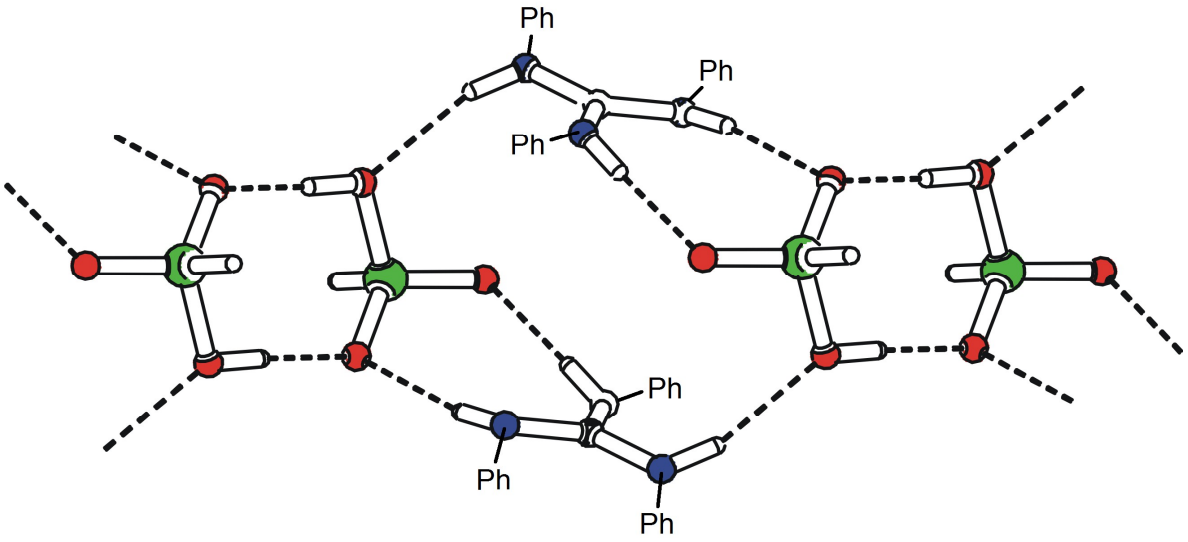


Fig. 26 The detail of the **tphguaH$_2$PO$_3$** structure – a chain parallel to the *b* axis, formed by the alternating hydrogen-bonded anionic pairs and the systems of two anions and two cations, that can be described by the $R_2^2(8)$ and $R_4^4(16)$ graph set descriptors, respectively. The phenyls in the **tphgua** cations were schematized as **Ph** for clarity, hydrogen bonds are symbolized by dashes, the red circles symbolize the oxygen atoms, blue nitrogen atoms, black carbon atoms, green phosphorus and hydrogens are colourless.

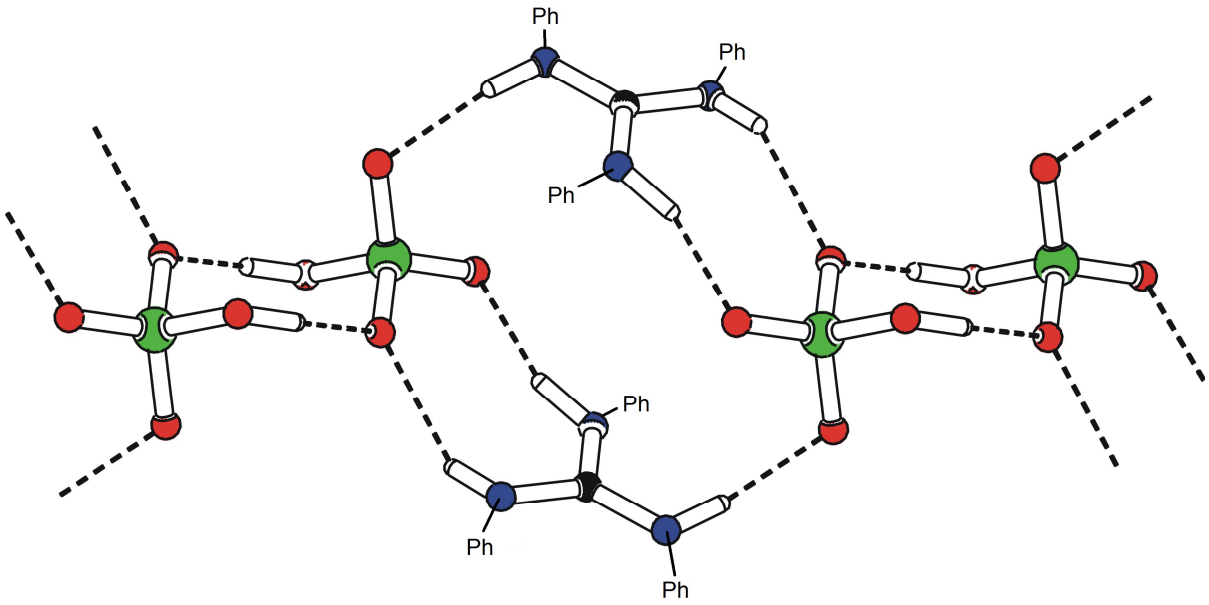


Fig. 27 The detail of the **tphguaHSO$_4$** structure – a chain parallel to the *b* axis, formed by the alternating hydrogen-bonded anionic pairs and the systems of two anions and two cations, that can be described by the $R_2^2(8)$ and $R_4^4(16)$ graph set descriptors, respectively. The phenyls in the **tphgua** cations were schematized as **Ph** for clarity, hydrogen bonds are symbolized by dashes, the red circles symbolize the oxygen atoms, blue nitrogen atoms, black carbon atoms, green sulphur and hydrogens are colourless.

Both structures of the new **tphgua** salts contain the motif of the pairwise assembled anions and the parallel chains formed by both anions and cations. Similar assembly is known in another structure of a **tphgua** hydrogen sulphate (code XIBZUE in CSD), other **tphgua** salts possess a common network of periodically alternating cations and anions. The conformation of the cations in both structures is very far from the once considered trigonal symmetry.

### 3.4.2 *Vibrational spectra of the new tphgua salts*

As the vibrational spectra of the **tphgua**(1+) cation have been studied in detail elsewhere [82], they are not further discussed in this work. The recorded maxima are presented as peaklists as a further characterization of the prepared materials.

**tphgua$H_2PO_3$**:

IR spectrum: 107 w, 145 w, 307 w, 345 w, 458 m, 475 m, 508 m, 541 w, 693 m, 727 m, 754 m, 1218 w, 1259 w, 1301 w, 1377 s, 1444 s, 1462 s, 1487 m, 1496 m, 1540 w, 1586 m, 1597 m, 1617 w, 1653 m, 2368 m, 2726 w, 3053 w

Raman spectrum: 136 w, 175 w, 215 w, 256 w, 308 w, 361 w, 416 w, 474 w, 499 w, 545 w, 617 m, 683 w, 726 m, 753 w, 826 w, 861 w, 891 m, 1002 s, 1041 m, 1156 m, 1183 m, 1266 s, 1302 s, 1505 m, 1543 w, 1605 s, 2370 w, 3069 vs

**tphgua$HSO_4$**:

IR spectrum: 116 w, 161 w, 290 w, 338 w, 349 w, 417 w, 441 w, 462 w, 480 w, 490 w, 504 m, 534 w, 576 m, 593 guHtartm, 634 w, 693 w, 740 m, 762 s, 835 w, 859 w, 870 m, 1617 m, 1653 s, 2937 s, 2990 s, 3053 s, 3099 m, 3284 w

Raman spectrum: 218 w, 164 m, 292 w, 417 w, 515 w, 577 w, 617 w, 636 w, 734 m, 768 w, 835 w, 867 m, 998 vs, 1030 m, 1043 m, 1081 w, 1165 w, 1181 m, 1211 w, 1263 s, 1303 s, 1463 w, 1496 m, 1539 w, 1587 m, 1600 s, 2983 w, 3069 s, 3195 w

### 3.4.3 *Thermal behaviour of the new tphgua salts*

Although the **tphgua$H_2PO_3$** and **tphgua$HSO_4$** macroscopically appeared to be stable up to the melting at 494 K and 464 K, respectively, the DSC revealed a cascade of complicated decomposition processes with onsets already about 440 K and 375 K, respectively.

# 4. **CONCLUSIONS**

This thesis is focused on preparation of novel compounds suitable for NLO. In particular, the target property was the second harmonic generation. At first, the promising group of compounds was selected, namely the salts of organic bases with delocalized π electrons, derived from guanidine. As a preestimation of the NLO potential, the static hyperpolarizabilities of cations of selected bases were computed and their values were found promising. The particular bases studied were the *N*-phenylbiguanide, the *N*,*N*-dimethylbiguanide, the *N*-carbamoylguanidine (guanylurea) and the *N*,*N*′,*N*″-triphenylguanidine, first two of them capable of forming the (1+) and (2+) charged cations, the other two only of (1+) cations. Two of the bases were synthesized in the framework of this thesis, the other two were commercially available. The counterions to these bases originated from strong inorganic acids as the sulphuric, nitric or phosphoric acid, weaker inorganic acids as the phosphorous and the amidosulphuric acid, the weak ones as the carbonic acid, or from the achiral organic acids as oxalic acid or the chiral ones as tartaric acid. The choice of the particular strong or weaker acid was used as means for influencing the protonization of the selected cation. Also the tendency to form a particular hydrogen bonded systems of the anions (*e.g.* hydrogen phosphite chains) noticeably influenced the final structure assemblies. On the contrary, the chiral organic anions directly caused the noncentrosymmetry of the final structures.

The general reaction environment were the aqueous solutions. The crystallizations were usually set at all considerable stoichiometric ratios. Although there were many solids obtained, only the well defined compounds, *i.e.* the compounds for which the single crystal XRD analysis was solved, were taken in account for further experiments.

The ***N*-phenylbiguanide** gave origin to three new salts. All of them possessed a layered structure – the anions together with the guanidine parts of the cations formed layers while the phenyl rings stuck out into the space between the layers, which is a quite common organization of **phbigua** salts structures. Two of the new compounds were assembled noncentrosymmetrically. One of them, the **phbiguaAMS** exhibited an SHG efficiency about 10% KDP, while the other, the **phbigua$SO_4$**, was much more interesting – it was a first ever analyzed structure containing the phbigua(2+) cations and it exhibited an SHG efficiency comparable to urea. Moreover, its crystals grew spontaneously to remarkable dimensions but unfortunately, their quality was tangled by the parallelly assembled layers of deffects in the whole volume which were hypothesized to be areas that lose the water of solvation. Although these deffects did not worsen with time and they

did not affect the transparency or the firmness of the crystals, they disqualified the compound from the further NLO materials research.

The both noncetrosymmetric **phbigua** salts can also be understood as an excellent example of the cation protonization directed by the nature of the acids used as sources of the anions – while the weak amidosulphuric acid manages to protonize the **phbigua** only to a (1+) state, the sulphuric acid is capable of directing the occurence of both (1+) and (2+) charged cations. In the diluted solutions of the sulphuric acid, the (1+) charged **phbigua** cation formed an anhydrous sulphate which was previously published elsewhere [76], while the more drastic conditions led even to formation of the (2+) charged cation with a higher hyperpolarizability in comparison to the **phbigua**(1+). It can be summarized that both **phbigua**(1+) and **phbigua**(2+) are the prospective building blocks for NLO.

There was only one salt of the ***N*,*N*-dimethylbiguanide** prepared in this thesis and that was a nitrate of the (2+) charged **dmbg** cation. Its crystallization dured extremely long and the crystallization solutions often ended as a viscous thick matter. The finally prepared crystals had the centrosymmetric assembly and their parameters were only sufficient for the structure analysis. According to this and to the data known from the literature, it can be concluded that the ***N*,*N*-dimethylbiguanide** is, contrary to its relatively high hyperpolarizability, a not favourable compound for NLO.

The total number of the prepared ***N*-carbamoylguanidine** (guanylurea) salts was 13 and one of the compounds appeared in two polymorphs. The most common motif in the structures were the parallelly oriented **gu**(1+) cations, often forming a layered assembly. Most of the compounds crystallized easily. Nine of the new structures were noncentrosymmetric, but only the **guHtart** and **gu$H_2PO_3$** (**GUHP**) exhibited a reasonable material properties necessary for the considered NLO applications together with a noticeable SHG efficiency: the SHG efficiency of **guHtart** was about 10% KDP while the efficiency of **GUHP** was comparable to urea. The **GUHP** was found to be an ideal candidate for a deeper examination – it could be prepared in a large amount, it crystallized easily, it was phase-matchable, it exhibited a high birefringence, extreme resistence to optical damage and many interesting and even rare NLO properties (Appendix II, III, IV and [120]). Though, the controlled preparation of large monocrystals was attempted and further optical characterizations of this interesting material were carried out. Its only problem is the tendency to split during the crystal growth which may be overcome by modifying the crystallization conditions. Another interesting result in the research of the **gu** salts is the preparation of a fluorophosphate isostructural to the **GUHP** and the cocrystallization of the two compounds in various ratios. Although the utilitary target

of the fluorophospates preparation, (*i.e.* improvement of the **GUHP** properties with a special accent to counteract the splitting during the crystal growth) was not fulfilled, the sole existence of such compounds was very interesting and contributed significantly to a small number of known isostructural couples of hydrogen phosphite – fluorophosphate salts.

It can be concluded, that the planar **gu**(1+) is a promising building block for NLO and that, above all, the **GUHP** is the most interesting compound investigated in this work and it can be seriously considered as a material with the potential for practical use in the NLO applications.

The ***N*,*N*′,*N*″-triphenylguanidine** gave origin to two new compounds containing the motif of chains formed by regularly alternating cations and anions. Both of them were centrosymmetric. The theoretically considered trigonal symmetry was not observed at all. Although there are some **tphgua**(1+) salts known as interesting from the NLO point of view [82, 110 and 73], the compounds prepared in this work are of no importance for second order NLO effects.

Some of the results have already been published and are present in Appendices of this thesis, the unpublished results which are presented in the main text are intended to be published too. All of the new crystal structures were either published or deposited with the CCDC.

It can be concluded that the aim of the thesis was fulfilled since a prospective field of possible new NLO materials was investigated and a fair number of new compounds was described including the first structure proof of a (2+) charged **phbigua** cation. Moreover, a compound with a potential for the practical use as a NLO material was investigated in detail.

Considering the whole findings in this thesis, the further directioning of the research should be oriented on the most prospective salts of *N*-phenylbiguanide and *N*-carbamoylguanidine (guanylurea). In particular, the attention concerning the *N*-phenylbiguanide should be paid to preparing of further salts of the interesting (2+) charged **phbigua** cations. Concerning the **gu** salts, there are two main outlooks of the research. Firstly, the possible isostructural transition of the **GUHP** should be examined in detail and the preparation of large **GUHP** single crystals should be optimized so that the-crystal splitting be avoided. Secondly, a search for another gu compound with NLO properties comparable to **GUHP** should be intensely continued.

## 5. SUMMARY

This thesis was focused on preparation of novel compounds suitable for nonlinear optics (NLO). In particular, the target property was the second harmonic generation (SHG) and the group of interest were the salts of the cations with delocalized π electrons derived from guanidine, which can serve as carriers of the NLO properties. Four guanidine derivatives, namely the *N*-phenylbiguanide, the *N*,*N*-dimethylbiguanide, the *N*-carbamoylguanidine (guanylurea) and the *N*,*N*′,*N*″-triphenylguanidine, were selected and their NLO potential was proven by quantum chemical computations.

In total, twenty new structures were described and those with the noncentrosymmetric structure assembly, fulfilling the basic condition for the $\chi^{(2)}$ nonlinear effects, were examined for the second harmonic generation (SHG). Four of the prepared compounds exhibited a noticeable SHG efficiency, the SHG of two of them was even comparable to urea. The most promising compound, the guanylurea hydrogen phosphite (**GUHP**), was deeper examined while many interesting NLO properties were revealed. Another important result of the thesis is the proof that the *N*-phenylbiguanide can appear also as a (2+) charged cation while this finding opens a new chapter of the study of this prospective base.

All of the structures were either published or deposited with the CCDC. There are ten publications in the Appendix of this thesis, nine of them have already been published, the last one is in an advanced stage of the refereeing process right now. The author of this thesis is the first author of six of the publications.

## REFERENCES

[1] "single crystal." Encyclopædia Britannica Online. Encyclopædia Britannica Inc., 2012. Web. 17 Jan. 2012, http://www.britannica.com/EBchecked/topic/545924/single-crystal.

[2] D. Shechtman, I. Blech, D. Gratias, J.W. Cahn, Phys. Rev. Lett. 53 (1984) 1951.

[3] International Union of Crystallography, Report of the Executive Committee for 1991, Acta Crystallogr. A48 (1992) 922.

[4] M. Baake, D. Frettlöh, Z. Kristallogr. 222 (2007) 312.

[5] W. Steurer, Z. Kristallogr. 222 (2007) 308.

[6] D. Lifshitz, Z. Kristallogr. 222 (2007) 313.

[7] J. D. Dunitz, Pure Appl. Chem. 63 (1991) 177.

[8] J. M. Lehn, Pure Appl. Chem. 50 (1978) 871.

[9] J. M. Lehn, Supramolecular Chemistry: Concepts and Perspectives, Wiley VCH, Weinheim, 1995.

[10] G. M. J. Schmidt, Pure Appl. Chem. 27 (1971) 647.

[11] G. R. Desiraju, Crystal Engineering: The Design of Organic Solids, Elsevier, Amsterdam, 1989.

[12] M. J. Zaworotko. B. Moulton, Chem Rev. 101 (2001) 1629.

[13] G. R. Desiraju, Angew. Chem. 34 (1995) 2311.

[14] A. Gavezzotti in D. Braga and F. Grepioni (Eds.), Making Crystals by Design, Wiley VCH, Weinheim, 2007.

[15] J. W. Steed, J. L. Atwood, Supramolecular Chemistry, John Wiley & Sons, Chichester 2002.

[16] H.-J. Schneider, A. Yatsimirski, Principles and Methods in Supramolecular Chemistry, John Wiley & Sons, Chichester 2000.

[17] M. C. Etter, J. Phys. Chem. 95 (1991) 4601.

[18] M. C. Etter, Acc. Chem. Res. 23 (1990) 120.

[19] G. M. Day in E. Tiekink, J. Vittal and M. Zaworotko (Eds.), Organic Crystal engineering: frontiers in crystal engineering, John Wiley & Sons, Chichester, 2010.

[20] W. C. McCrone in D. Fox, M. M. Labes and A. Weissberger (Eds.), Physics and Chemistry of the Organic Solid State, part 2, Interscience, New York 1965.

[21] G. M. Day, A. V. Trask, W. D. S. Motherwell, W. Jones, Chem. Commun. 42 (2006) 54.

[22] P. Becker, Adv. Mater. 10 (1998) 979.

[23] F. H. Allen, Acta Crystallogr. B58 (2002) 380.

[24] Inorganic Crystal Structure Database, Version 2012-1, Fachinformationszentrum Karlsruhe & U.S. Department of Commerce.

[25] S. K. Kurtz, T. T. Perry, J. Appl. Phys. 39 (1968) 3798.

[26] M. V. Hobden, J. Appl. Phys. 38 (1967) 4365.

[27] D. S. Chemla, J. Zyss, Nonlinear Optical Properties of Organic Molecules and Crystals, Academic Press, Orlando 1987.

[28] S. K. Park, J. Y. Do, J. J. Ju, S. Park, M.-S. Kim, M.-H. Lee, Mater. Lett. 59 (2005) 2872.

[29] J. Zyss, J. F. Nicoud, Curr. Opin. Solid State Mater. Sci. 1 (1996) 354.

[30] H. Ratajczak, J. Baran, J. Barycki, S. Debrus, M. May, A. Pietraszko, H. M. Ratajczak, A. Tramer and J. Venturini, J. Mol. Struct. 555 (2000) 149.

[31] Y. Uesu, H. Yokota, S. Kawado, N. Kato, J. Korean Phys. Soc. 51 (2007) 804.

[32] G. Liu, T. Xie, L. Yu, J. Su, I. V. Tomov, Q. Wang, B. Rao, J. Zhang, Z. Chen in G. J. Tearney and T. D. Wang (Eds.), Proceedings of SPIE 7172: Endoscopic Microscopy IV, San Jose, USA, 25-26 January 2009, http://dx.doi.org/10.1117/12.825133.

[33] J. Zyss, Molecular Nonlinear Optics: Materials, Physics and Devices, Academic Press, Boston, 1994.

[34] C. H. Lee, R. K. Chang, N. Bloembergen, Phys. Rev. Lett. 18 (1967) 167.

[35] C. Bosshard, G. Knopfle, P. Prêtre, P. Günter, J. Appl. Crystallogr. 71 (1991) 1594.

[36] K. Clays, A. Persoons, Phys. Rev. Lett. 66 (1991) 2980.

[37] L. M. Hayden, S. T. Kowel, M. P. Srinivasan, Opt. Commun. 61 (1987) 351.

[38] P. D. Maker, R. W. Terhune, M. Nisenoff, C. M. Savage, Phys. Rev. Lett. 8 (1962) 21.

[39] R. J. Gehr, A. V. Smith, J. Opt. Soc. Am. B: Opt. Phys. 15 (1998) 2298.

[40] I. Matulková, I. Němec, P. Němec, Československý časopis pro fyziku 61 (2011) 76.

[41] C. B. Aakeröy, P. B. Hitchcock, B. D. Moyle, K. R. Seddon, J. Chem. Soc. Chem. Comm. 23 (1989) 1856.

[42] H. Hellwig, J. Liebertz, L. Bohatý, Solid State Commun. 109 (1999) 249.

[43] G. D. Boyd, K. Nassau, R. C. Miller, W. L. Bond, A. Savage, Appl. Phys. Lett. 11 (1964) 234.

[44] P. H. Davies, M. V. Hobden, K. F. Hulme, O. Jones, W. Pomeroy, J. Warner, IEEE J. Quantum Elect. QE4 (1968) 393.

[45] J. Baran, S. Debrus, M. May, H. Ratajczak, B. Pol. Acad. Sci.-Chem. 48 (2000) 113.

[46] T. N. Guru Row, Coord. Chem. Rev. 183 (1999) 81.

[47] H. Nobutoki, H. Koezuka, J. Phys. Chem. A101 (1997) 3762.

[48] R. Hierle, J. Badan, J. Zyss, J. Cryst. Growth 69 (1984) 545.

[49] S. R. Marder, J. W. Perry, C. P. Yakymyshyn, Chem. Mater. 6 (1994) 1137.

[50] W. H. Thompson, M. Blanchard-Desce, V. Alain, J. Muller, A. Fort, M. Barzoukas, J. T. Hynes, J. Phys. Chem. A103 (1999) 3766.

[51] D. Xue, S. Zhang, J. Phys. Chem. A101 (1997) 5547.

[52] J. Heck, S. Dabek, T. Meyer-Friedrichsen, H. Wong, Coord. Chem. Rev. 190-192 (1999) 1217.

[53] J. L. Hoard, E. W. Silverto, J. V. Silverto, J. Am. Chem. Soc. 90 (1968) 2300.

[54] C. B. Aakeröy, K. R. Seddon, Chem. Soc. Rev. 22 (1993) 397.

[55] K. Aoki, K. Nagano, Y. Iitaka, Acta Crystallogr. B27 (1971) 11.

[56] T. Baraniraj, P. Philominathan, Spectrochim. Acta A75 (2010) 74-76.

[57] D. Sankar, V. R. Menon, P. Sagayraj, J. Madhavan, Physica B405 (2010) 192.

[58] J. Zyss, J. Chem. Phys. 98 (1993) 6583.

[59] I. Matulková, I. Němec, I. Císařová, P. Němec, Z. Mička, J. Mol. Struct. 886 (2008) 103.

[60] A. Suvitha, P. Murugakoothan, Spectrochimica Acta A86 (2012) 266.

[61] I. Matulková, I. Němec, I. Císařová, P. Němec, P. Vaněk, J. Mol. Struct. 966 (2010) 23.

[62] A. Gobbi, G. Frenking, J. Am. Chem. Soc. 115 (1993) 2362.

[63] P. Holý, Supramolekulární chemie 1, ÚOCHB AVČR, Prague 2004.

[64] S. Miyata and X. T. Tao, Synthetic Met. 81 (1996) 99.

[65] C. B. Aakeröy, A. M. Beatty, B. A. Helfrich, Angew. Chem. Int. Ed. Engl. 40 (2001) 3240.

[66] K. S. Thanthiriwatte, K. M. Nalin de Silva, Theochem - J. Mol. Struct. 617 (2002) 169.

[67] G. R. Desiraju, J. Mol. Struct. 656 (2003) 5.

[68] A. Nangia, G. R. Desiraju, Top. Curr. Chem. 98 (1998) 57.

[69] A. Nangia in E. Tiekink, J. Vittal and M. Zaworotko (Eds.), Organic Crystal engineering: frontiers in crystal engineering, p. 151, John Wiley & Sons, Chichester, 2010.

[70] G. M. Frankenbach, M. C. Etter, Chem. Mater. 4 (1992) 272.

[71] G. M. Espallargas, L. Brammer in D. Braga and F. Grepioni (Eds.), Making Crystals by Design, Wiley VCH, Weinheim, 2007.

[72] Ladislav Bohatý, Institut für Kristallographie, Cologne, Germany, personal communication, 2010.

[73] J. Zyss, J. Pecaut, J. P. Levy, R. Masse, Acta Crystallogr. B49 (1993) 334.

[74] V. A. Russel, M. C. Etter, M. D. Ward, J. Am. Chem. Soc. 116 (1994) 1941.

[75] J. Zyss, J. Chem. Phys. 109 (1998) 659.

[76] I. Matulková, PhD Thesis, Charles University in Prague, Faculty of Science, Dept. of Inorganic Chemistry, Prague, 2007.

[77] L. Fabbrizzi, M. Micheloni. P. Paoletti, G. Schwarzenbach, J. Am. Chem. Soc. 99 (1977) 5574.

[78] J. Sterne, Therapie 13 (1958) 650.

[79] Y. Cohen, O. Costerousse, Med. Hyg. 4 (1961) 145.

[80] A. Ostrogovich, Gazz. Chim. Ital. 39 (1911) 540.

[81] M. Fridrichová, Diploma thesis, Charles University in Prague, Faculty of Science, Dept. of Inorganic Chemistry, Prague, 2007.

[82] C. Cardoso, P. S. P. Silva, M. R. Silva, A. M. Beja, J. A. Paixao, F. Nogueira, A. J. F. N. Sobral, J. Mol. Struct., 878 (2008) 169.

[83] I. Matulková, I. Němec, I. Císařová, R. Czaplicki, P. Němec, M. Fridrichová, B. Sahraoui, Crystal engineering of novel semiorganic NLO materials based on N-phenylbiguanide – a family of novel compounds with an exceptional representative (Article in preparation).

[84] G. Kohn, J. Prakt. Chem. 84 (1912) 394.

[85] L.-P. Guo, X.-D. Du, J.-H. Lei, J.-X. Zhao, Yingyong Huaxue Journal 25 (2008) 1082.

[86] A. J. Thompson, S. C. R. Lummis, Curr. Pharm. Design 12 (2006) 3615.

[87] S. Kanoo, S. B. Deshpande, Neurosci. Lett. 440 (2008) 242.

[88] F. Brugger, H. Gempeler, Double Liaison - Chimie des Peintures 22 (1975), 171.

[89] I. Matulková, I. Císařová. I. Němec, Acta Crystallogr. E66 (2010) o3187.

[90] I. Matulková, I. Císařová, I. Němec, Acta Crystallogr. E67 (2011) o118.

[91] J. Supniewski, T. Chrusciel, B. Pol. Acad. Sci. 2 (1954) 29.

[92] B. Viollet, B. Guigas, N. S. Garcia, J. Leclerc, M. Foretz, F. Andreelli, Clin. Sci. 122 (2012) 253.

[93] N. F. Wiernsperger, Diabetes Technol. The. 2 (2000) 259.

[94] G. Taubes, Science 335 (2012) 286.

[95] M. L. Zhu, L. P. Lu, P. Yang, X. L. Jin, Acta Crystallogr. E58 (2002) m272.

[96] J. Haag, Liebigs Ann. Chem. 122 (1862) 22.

[97] T. M. Klapötke, C. M. Sabaté, Z. Anorg. Allg. Chem. 636 (2010) 163.

[98] V. S. Sastri, M. Elboujdaini, J. R. Perumareddi, Corrosion, 64 (2008) 657.

[99] K. Izran, A. Zaidon, G. Beyer, A. M. A. Rashid, F. Abood, S. Rahim, J. Trop. For. Sci. 22 (2010) 175.

[100] G. Ronca, Biochim. Biophys. Acta 132 (1967) 214.

[101] R. K. Graupner, J. D. Hultine, J. A. Van Vechten, PCT Int. Appl., 2005, application WO 2005108289 A2 20051117.

[102] I. V. Mendenhall, PCT Int. Appl., 2002, application WO 2002040430 A2 20020523.

[103] M. Scoponi, E. Polo, V. Bertolasi, V. Carassiti, G. Bertelli, J. Chem. Soc. Perkin. Trans. 2 (1991) 1619.

[104] V. Merz, W. Weith, Ber. Dtsch. Chem. Ges. 2 (1869) 621.

[105] K. D. Nagiev, D. G. Gambarov, P. R. Mamedov, F. M. Chyragov, J. Anal. Chem. 60 (2005) 409.

[106] J. Kapko, J. Polym. Sci. Pol. Lett. 21 (1983) 731.

[107] P. J. Bailey, K. J. Grant, S. Pace, S. Parsons, L. J. Stewart, J. Chem. Soc. Dalton 22 (1997) 4263.

[108] K. T. Holman, S. D. Robinson, A. Sahajpal, J. W. Steed, J. Chem. Soc. Dalton 1 (1999) 15.

[109] P. J. Bailey, A. J. Blake, M. Kryszczuk, S. Parsons, D. Reed, J. Chem. Soc. Chem. Comm. 16 (1995) 1647.

[110] P. S. P. Silva, C. Cardoso, M. R. Silva, J. A. Paixao, A. M. Beja, M. H. Garcia, N. Lopes, J. Phys. Chem. A114 (2010) 2607.

[111] I. Georgieva, N. Mintcheva, N. Trendafilova, M. Mitewa, Vib. Spectrosc. 27 (2001) 153.

[112] M. S. Wickleder, Z. Kristallogr. 220 (2005) 192.

[113] M. S. Wickleder, Z. Anorg. Allg. Chem. 627 (2001) 1675.

[114] P. Muthusubramanian, A. Sundara Raj, Can J. Chem. 61 (1983) 2048.

[115] A. Altomare, M. C. Burla, M. Camalli, G. Cascarano, C. Giacovazzo, A. Guagliardi, G. Polidori, J. Appl. Crystallogr. 27 (1994) 435.

[116] G. M. Sheldrick, Acta Crystallogr. A64 (2008) 112.

[117] A. L. Spek, Acta Crystallogr. D65 (2009) 148.

[118]Gaussian 09, Revision A.02, M. J. Frisch, G. W. Trucks, H. B. Schlegel, G. E. Scuseria, M. A. Robb, J. R. Cheeseman, G. Scalmani, V. Barone, B. Mennucci, G. A. Petersson, H. Nakatsuji, M. Caricato, X. Li, H. P. Hratchian, A. F. Izmaylov, J. Bloino, G. Zheng, J. L. Sonnenberg, M. Hada, M. Ehara, K. Toyota, R. Fukuda, J. Hasegawa, M. Ishida, T. Nakajima, Y. Honda, O. Kitao, H. Nakai, T. Vreven, J. A. Montgomery, Jr., J. E. Peralta, F. Ogliaro, M. Bearpark, J. J. Heyd, E. Brothers, K. N. Kudin, V. N. Staroverov, R. Kobayashi, J. Normand, K. Raghavachari, A. Rendell, J. C. Burant, S. S. Iyengar, J. Tomasi, M. Cossi, N. Rega, J. M. Millam, M. Klene, J. E. Knox, J. B. Cross, V. Bakken, C. Adamo, J. Jaramillo, R. Gomperts, R. E. Stratmann, O. Yazyev, A. J. Austin, R. Cammi, C. Pomelli, J. W. Ochterski, R. L. Martin, K. Morokuma, V. G. Zakrzewski, G. A. Voth, P. Salvador, J. J. Dannenberg, S. Dapprich, A. D. Daniels, O. Farkas, J. B. Foresman, J. V. Ortiz, J. Cioslowski, D. J. Fox, Gaussian, Inc., Wallingford CT, 2009.

[119] Prof. Dr. Ladislav Bohatý, Institut für Kristallographie, Cologne, Germany, personal communication, 2012.

[120] J. Kroupa, J. Opt. 12 (2010) 045706.

[121] Prof. Dr. Ladislav Bohatý, Institut für Kristallographie, Cologne, Germany, personal communication, 2010.

[122] Prof. Dr. Ladislav Bohatý, Institut für Kristallographie, Cologne, Germany, personal communication, 2012.

[123] RNDr. Irena Matulková, PhD., personal communication, 2012.

[124] L. Bohatý, A. Kaminskii, M. Fridrichová, Stimulated Raman scattering of the prospective NLO semi-organic GUHP (Article in preparation).

# Appendices

## List of Appendices

**I** M. Fridrichová, I. Císařová, I. Němec, **1,1-Dimethylbiguanidium(2+) dinitrate**, Acta Crystallogr. E68 (2012) o18.

**II** M. Fridrichová, I. Němec, I. Císařová, P. Němec, **Guanylurea(1+) hydrogen phosphite: a novel promising phase-matchable material for second harmonic generation.** CrystEngComm 12 (2010) 2054.

**III** M. Fridrichová, J. Kroupa, I. Němec, I. Císařová, D. Chvostová, **Guanylurea(1+) hydrogen phosphite: study of linear and nonlinear optical properties,** Phase Trans. 83 (2010) 761.

**IV** J. Kroupa, M. Fridrichová, **Spontaneous noncollinear second harmonic generation in GUHP**, J. Opt. 13 (2011) 035204.

**V** M. Fridrichová, I. Němec, I. Matulková, R. Gyepes, F. Borodavka, J. Kroupa, J. Hlinka, I. Gregora, **Vibrational spectra of guanylurea(1+) hydrogen phosphite - novel remarkable material for nonlinear optics**, Vib. Spectrosc. 2012 (Manuscript in refereeing process).

**VI** M. Fridrichová, J. Fábry, K. Fejfarová, R. Krupková, P. Vaněk, **N-[Amino(imino)methyl]uronium tetrafluoroborate**, Acta Crystallogr. E68 (2012) o1114.

**VII** J. Fábry, M. Fridrichová, M. Dušek, K. Fejfarová, R. Krupková, **Two polymorphs of bis(2-carbamoylguanidinium) fluorophosphonate dihydrate**, Acta Crystallogr. C68 (2012) o71.

**VIII** J. Fábry, M. Fridrichová, M. Dušek, K. Fejfarová, R. Krupková, **Mixed crystals of 2-carbamoylguanidinium with hydrogen fluorophosphonate and hydrogen phosphite in the ratios 1:0, 0.76(2):0.24(2) and 0.115(7):0,885(7)**, Acta Crystallogr. C68 (2012) o76.

**IX** J. Fábry, M. Fridrichová, M. Dušek, K. Fejfarová, R. Krupková, **Tris(2-carbamoylguanidinium) hydrogen fluorophosphonate fluorophosphonate monohydrate**, Acta Crystallogr. E68 (2012) o47.

**X** Fridrichová M., Němec I., Císařová I., Tesařová N., Němec P., Karakaş A., Kahraman N., Taşer M., **Novel salts of 2,4-diaminoquinazoline - searching for materials for second harmonic generation based on a promising polarizable cation**, J. Chem. Crystallogr. 42 (2012) 809.